Hodgkin lymphoma secreted factors determine macrophage polarization and function

Doctoral Thesis

In partial fulfillment of the requirements for the degree
"Doctor rerum naturalium (Dr. rer. nat.)"
in the Molecular Medicine Study Program
at the Georg-August University Göttingen

submitted by Annekatrin Arlt

born in Riesa

Göttingen, 2018

Members of the thesis committee

Prof. Dr. Dieter Kube (Supervisor)

University Medical Center Göttingen
Clinic for Hematology and Medical Oncology
Robert-Koch-Straße 40
37075 Göttingen
dieter.kube@med.uni-goettingen.de

Prof. Dr. Jörg Wilting

University Medical Center Göttingen
Institute of Anatomy and Cell Biology
Kreuzbergring 36
37075 Göttingen
joerg.wilting@med.uni-goettingen.de

Prof. Dr. Ralf Dressel

University Medical Center Göttingen
Institute for Cellular and Molecular Immunology
Humboldtallee 34
37073 Göttingen
rdresse@gwdg.de

Date of Disputation:

Affidavit

By this I declare that I independently authored the presented thesis

"Hodgkin lymphoma secreted factors determine macrophage polarization and function "

and that I did not use other auxiliary means than indicated. Paragraphs that are taken from other publications, by wording or by sense, are marked in every case with a specification of the literary source.

Furthermore, I declare that I carried out the scientific experiments following the principles of Good Scientific Practice according to the valid "Richtlinien der Georg-August-Universität Göttingen zur Sicherung guter wissenschaftlicher Praxis".

Annekatrin Arlt

Abstract

Hodgkin lymphoma (HL) is a unique entity where the fraction of malignant cells accounts for only 1 % of the tumor. The cells are embedded in a complex background of non-neoplastic immune infiltrates. Profound interactions of the malignant cells with neighboring cells are a requisite to sustain their survival and allow tumor development. Among the cell types commonly found in the HL tumor mass are macrophages whose presence has been associated with poor prognosis. Macrophages are innate immune cells and critical regulators of immune responses and tissue remodeling. They are known to occur in all cancer types where they exhibit various functions to promote tumor growth and metastasis. This study aims to gain a deeper insight into the interplay of HL cells with macrophages.

Herein, we show that HL cells actively recruit macrophages. Using Boyden chamber assays we found that monocytes and macrophages migrate toward HL conditioned medium (CM). Applying CM directly on the cells further revealed that factors in the CM support the differentiation of monocytes into macrophages and macrophage repolarization. By the analyses of selected markers via flow cytometry and qRT-PCR we found that these macrophages expose an M2-like phenotype. A characteristic feature was their high CD206 expression. Investigations into the functional consequence of high CD206 expression included endocytosis assays and revealed an enhanced uptake of CD206 specific targets. Alongside we found that macrophages secret high amounts of MMP-9 and alter the tumor formation of HL cells in a chorion allantois membrane assay. By applying selected factors on monocytes we found that the increased CD206 expression in HL derived macrophages could be a result of IL-13 produced by HL cells. Further analysis of the phenotype of HL derived macrophages included RNA sequencing and revealed an enrichment of upregulated genes involved in antigen presentation and as well co-stimulation and -inhibition.

Taken together, these findings support a model in which HL cells secret factors to attract and generate macrophage with a specific M2-like activation state. Analyses of their phenotype and features indicate that these cells serve functions in tissue remodeling and T cell interaction.

Contents

List of figures

List of tables

Abbreviations

ABVD	chemotherapy regimen of doxorubicin, bleomycin, vinblastine, and dacarbazine
ADAM	a disintegrin and metalloproteinase
Arg1	arginase 1
APC	allophycocyanin
BAFF	B cell activating factor
BEACOPP	chemotherapy regimen of bleomycin, etoposide, doxorubicin, cyclophosphamide, vincristine, procarbazine and prednisone
bFGF	basic fibroblast growth factor
CAM	chorion allantois membrane
CCL	chemokine (C-C motif) ligand
CCR	chemokine (C-C motif) receptor
CD	cluster of differentiation
CD1a$^+$	CD1a positive (cell)
CD4$^+$	CD4 positive (cell)
CD8$^+$	CD8 positive (cell)
CD14$^+$	CD14 positive (cell)
CD206$^+$	CD206 positive (cell)
cHL	classical Hodgkin lymphoma
CLEC	C-type lectin-like domain containing protein
CM	conditioned medium
CR	cysteine-rich (domain)
CTLD	C-type lectin-like domain
ctrl	control
CX3CL1	chemokine (C-X3-C motif) ligand 1
CX3CR1	chemokine (C-X3-C motif) receptor 1
CXCL	chemokine (C-X-C motif) ligand
DC	dendritic cell
DLBCL	diffuse large B cell lymphoma
EMT	epithelial to mesenchymal transition
FCS	fetal calf serum

FcγR	Fcγ receptor
FITC	fluorescein isothiocyanate
FNII	fibronectin type II (domain)
fwd	forward
GalNAc	*N*-acetylgalactosamine
GlcNAc	*N*-acetylglucosamine
GM-CSF	granulocyte-macrophage colony-stimulating factor
HL	Hodgkin lymphoma
HLA	human leukocyte antigen
HRS	Hodgkin-Reed-Sternberg (cell)
IFN-γ	interferon-γ
IL	interleukin
iNOS	inducible nitric oxide synthase
JAK	Janus kinase
KO	knock out
M-CSF	macrophage colony-stimulating factor
M-CSF-R	macrophage colony-stimulating factor receptor
MHC	major histocompatibility complex
MICA	MHC class I polypeptide-related sequence A
MMP	matrix metalloproteinase
NK	natural killer (cell)
NKG2D	natural killer group 2D
NLPHL	nodular lymphocyte-predominant Hodgkin lymphoma
OS	overall survival
PD-1	programmed cell death protein 1
PD-L1	programmed cell death 1 ligand 1
PE	phycoerythrin
PFS	progression free survival
PLA2	phospholipase A2
PLA2R	phospholipase A2 receptor
PPARγ	peroxisome proliferator-activated receptor γ
RBP-J	recombining binding protein suppressor of hairless

rev	reverse
RNA-Seq	RNA sequencing
SAA3	serum amyloid A3
STAT	signal transducer and activator of transcription
TAM	tumor associated macrophage
TGF-β	transforming growth factor β
T_H	T helper (cell)
TME	tumor microenvironment
TNF-α	tumor necrosis factor α
T_{Reg}	regulatory T cell
TYK2	tyrosine kinase 2
uPAR	urokinase-type plasminogen activator receptor
VEGF	vascular endothelial growth factor

1 Introduction

For several decades tumor research was mainly based on identifying the genetically aberrant, malignant cells and their tumorigenic potential. However, in the past twenty years the view has shifted from cancer being a collection of mutated cells toward a systemic understanding of the disease. Otherwise healthy but malfunctioning cells built up a complex structure with the malignant cells to support tumor establishment, growth and progression. Together with extracellular matrix and soluble factors this is referred to as the tumor microenvironment (TME) (Egeblad et al. 2010).

The TME plays an active role in tumor development generally by providing a tumor supportive milieu thereby promoting tumor growth and progression (Wang et al. 2017). The cellular components consist of a variety of immune cell infiltrates such as T cells, B cells, natural killer (NK) cells, neutrophils, mast cells, dendritic cells (DC) and macrophages (Kerkar & Restifo 2012). Under physiological conditions the immune system provides an anti-tumor response to genetically and phenotypically aberrant cells, however, within the TME the cells are functionally defect. The immune cells are unable to act against the malignant cells either due to exhaustion or because they are manipulated to actively support cancer cells by suppressing immune responses or by supplying growth factors and other stimulants (Albini et al. 2015; Pauken & Wherry 2015). Beside the cellular compartment also extracellular matrix components are altered in the tumor tissue and themselves possess tumorigenic properties (Wang et al. 2017; Afik et al. 2016). The composition of soluble factors is partly a result of the neoplastic cells secretome as well as of the recruited benign cells. Taken together these factors form with the neoplastic cells a complex structure that in its whole built up the tumor (Egeblad et al. 2010). More recent clinical studies have focused on the TME and found that the composition of the TME is connected to disease progression, prognosis and influence treatment response (Pagès et al. 2010). Hence, analysis of TME-cancer cell interactions have increased rapidly in the last two decades to reveal mechanisms by which cancer cells establish their own immune suppressive and tumor promoting structures and how to address this therapeutically.

1.1 Macrophages

Macrophages have been found in tumors of literally every origin and localization. Commonly their presence has been associated with poor prognosis, early relapse and treatment failure (Shabo et al. 2008; Atanasov et al. 2015; Steidl et al. 2010; Deau et al. 2013).

Macrophages are part of the innate immune system and characterized by professional phagocytosis (Cavaillon 2011). They are common in all tissues and play an important role in tissue homeostasis by patrolling the environment for foreign cells and particles or damaged and dead body cells. Upon encountering potential pathogens macrophages can promote an inflammatory response whereas the clearance of apoptotic cells requires immune suppression to allow tissue regeneration. Thus, they also have the ability to dampen inflammatory reactions. Because of their ability to fulfill these opposing functions alongside with the ability to encourage tissue repair and wound healing macrophages are viewed as key regulators in the immune system which has become of special interest in the context of the TME.

1.1.1 Macrophage origin and development

Macrophages are present throughout the body in relatively constant numbers. The first known route of macrophage to occur was by differentiation from monocytes. Monocytes recruited from the blood stream into a tissue can further develop into macrophages (Varol et al. 2009). However, it was later found that the pool of tissue resident macrophages does not require per se monocyte recruitment. Analysis of knock out (KO) mice where differentiation of monocytes to macrophages was inhibited showed that the number of macrophages are stable in healthy individuals and not reduced compared to wild type mice (Bigley et al. 2011). Consequently, it was also shown that tissue resident macrophages can maintain themselves by self-renewal and that colonization of the body during embryogenesis does not require monocytes (Ajami et al. 2007; Aziz et al. 2009; Schulz et al. 2012). Macrophages colonize the body in two waves during embryogenic development which has been studied in detail in mice. They first appear during yolk sac hematopoiesis at day 7 of development (Palis et al. 1999). Myeloid progenitor cells differentiate directly into macrophages which spread from the yolk sac into the body. The second wave occurs during fetal liver hematopoiesis at day 10. In this stage fetal monocytes disseminate from the fetal liver into the body and further differentiate in the tissues to macrophages (Naito et al. 1990; Hoeffel et al. 2012). Thus, most tissue macrophages originate prior to birth. The tissue resident macrophages were shown to be

self-renewal, hence, recruitment from monocytes is not required. However, if recruitment or recolonization is necessary for example during or after infections, macrophages can be derived from circulating monocytes that originate from the bone marrow.

Upon colonizing of a tissue or encountering changes within their tissue macrophages adapt their phenotype accordingly. As a result of multiple surrounding factors, such as soluble molecules, direct cell-cell interactions as well as chemical and physical properties of the extracellular matrix macrophages change their state, hence, giving rise to multiple tissue specific phenotypes (Varol et al. 2015). It has been shown that this specification is not an end point and cells can adapt their phenotype further in response to changes in their environment. One example for changes in the microenvironment can be the infiltration of pathogens. Macrophages are able to detect foreign material in the tissue and in such a case they will get activated toward a so called M1 type and induce an immune reaction.

1.1.2 Macrophage activation: The M1-M2 axis

Due to their high plasticity that is maintained throughout their lifespan macrophages are not classified into subtypes. Since they commonly show similar phenotypes within a specific niche macrophages can be categorized by their localization (section 1.1.1) but more common is the description of the activational state. Roughly, macrophages promoting immune responses as a result of danger signals are referred to as M1 activated whereas cells suppressing immune actions to support wound healing are referred to as M2 activated (Mills et al. 2000; Gordon 2003). The nomenclature comes from their function in this context to promote T cells to either produce T helper (T_H) 1 cytokines or T_H2 cytokines which in turn activate more macrophages toward an M1 or M2 type, respectively. In mice it was found that M1 macrophages preferably produce inducible nitric oxide synthase (iNOS) to generate NO from arginine. The NO is further metabolized to reactive nitrogen species leading to an oxidative burst and elimination of invading microorganisms. M2 cells were found to produce ornithine from arginine by arginase 1 (Arg1) which is the substrate for polyamine and proline syntheses, important molecules for cellular proliferation and tissue repair (Mills & Ley 2014). This clear distinction of macrophage activation by arginine metabolism, however, seems to be invalid in humans (Weinberg et al. 1995; Raes et al. 2005; Martinez et al. 2006). In *in vitro* studies usually a panel of surface markers and secreted cytokines is analyzed to determine the activation state. These include tumor necrosis factor (TNF)-α, interleukin (IL)-12, IL-23, chemokine (C-C Motif) receptor (CCR)7 and cluster of differentiation (CD)40 for M1 activated cells and

CD163, CD206, chemokine (C-C Motif) ligand (CCL)17, CCL18 and transforming growth factor (TGF)-β for M2 activated cells (Murray et al. 2014). In histological analysis of tumor sections the presence of M2 macrophages is usually demonstrated by staining of CD163 or CD206. To distinguish M1 activation transcription factors such as phosphorylated signal transducer and activator of transcription 1 (pSTAT1) and recombining binding protein suppressor of hairless (RBP-J) are used (Barros et al. 2013). Detailed analysis of macrophage phenotypes, however, revealed that they possess a broader activation spectrum than initially defined by the M1-M2 dichotomy. Comprehensive transcriptome analysis of responses toward different stimuli and stimuli combinations showed that several M1- and M2-like state exist that are not detected by previously defined markers (Xue et al. 2014). Broadly it has been concluded from this and other studies that rather than an M1-M2 axis with roughly opposing states there is a whole landscape of activation states macrophages can switch to (Mosser & Edwards 2008). Reconstruction of the macrophage polarizations in the TME have supported this view (Kiss et al. 2018).

1.1.3 Tumor associated macrophages

Macrophages are referred to as tumor associated when they reside within or in close proximity to the tumor. Macrophages are common in all tissue and can regulate immune reaction and tissue homeostasis. Almost consequently macrophages can be found within tumors of any origin and localization. Analyses across different entities showed that the percentage of macrophages usually ranges from 5 % to 50 % (Gentles et al. 2015). According to the classification into activational states tumor associated macrophages (TAM) roughly resemble M2 macrophages or are described as M2-like as they are often detected by CD163 or CD206 expression in tumor sections (Heusinkveld & van der Burg 2011; Zhang et al. 2012). Using these markers, however, leads to a bias since they are characteristic for M2 activated cells. Analysis of intratumoral macrophages by single cell RNA sequencing or mass spectrometry revealed a high heterogeneity in this population with phenotypes that are not covered by the bimodal description of M1-M2 activation (Chevrier et al. 2017; Lavin et al. 2017). This suggests a highly dynamic regulation of macrophages in the TME. Since *in vitro* generated cells normally do not show the same degree of heterogeneity the functional relevance of these subsets and thereby the whole regulatory potential of TAMs remain unclear.

Irrespective of their specific phenotype within the tumor macrophages have been shown to fulfill several pro-tumoral functions e.g. by promoting angiogenesis, encouraging metastasis

4

and preventing immune responses best described by suppressing cytotoxic T cell activity (Figure 1). Studies found that TAMs promote angiogenesis by secretion of vascular endothelial growth factor (VEGF), tumor necrosis factor α (TNF-α), IL-1β, IL-8, and basic fibroblast growth factor (bFGF) (Mantovani et al. 2002; De Palma & Lewis 2013). Besides by secretion of matrix metalloproteinases (MMP) and other matrix modulating enzymes such as urokinase-type plasminogen activator receptor (uPAR) they can promote vessel formation (Coussens et al. 2000; Hildenbrand et al. 1999). Correlation studies have furthermore shown that the macrophage content is linked to the microvessel density supporting the view that TAMs expose pro-angiogenic functions (Badawi et al. 2015; Zhang et al. 2011). Aside from promoting angiogenesis the matrix remodeling activity of macrophages supports metastasis. TAMs are a major source of proteolytic enzymes apart from MMPs these include e.g. cathepsins and a disintegrin and metalloproteinases (ADAM) which accounts for matrix degradation in the TME (Mason & Joyce 2011). The altered stroma architecture leads to enhanced tumor cell invasion and metastasis by removing the physical barriers but also by releasing growth factors stored in the extracellular matrix (Liguori et al. 2011). Metastasis is furthermore promoted by macrophages present in the premetastatic niches. These macrophages have been primed by tumor cell derived factors, e.g. tumor exosomes, or by TAM derived factors such as serum amyloid A3 (SAA3) and TNF-α and supported extravasation, establishment and growth of the tumor cells which was observed in mouse models of melanoma and lung metastasis (Peinado et al. 2012; Tomita et al. 2011; Qian et al. 2009). An important aspect in promoting metastasis in solid cancers is that macrophages can support the epithelial to mesenchymal transition (EMT) e.g. by secretion of transforming growth factor β (TGF-β) which is a critical step for neoplastic epithelial cells to gain migratory and invasive properties (Gao et al. 2012). Another well described and important function of TAMs is the establishment of an immune suppressive environment among other mechanisms by inhibiting the cytotoxic activity of T cells. One example is the expression of programmed cell death protein 1 ligand 1 (PD-L1) on their cell surface and the direct interaction with T cells expressing the inhibitory receptor programmed cell death protein 1 (PD-1) (Carey et al. 2017). Additionally, they can carry other co-inhibitory ligands such as B7-H4 or secrete immune suppressive stimuli such as IL-10 (Kryczek et al. 2006; Ruffell et al. 2014). Aside from direct interaction TAMs can recruit regulatory T cells (T_{Reg}) through the secretion of CCL17 and CCL22, which in turn mediate the inhibition of cytotoxic T cells (Kryczek et al. 2006).
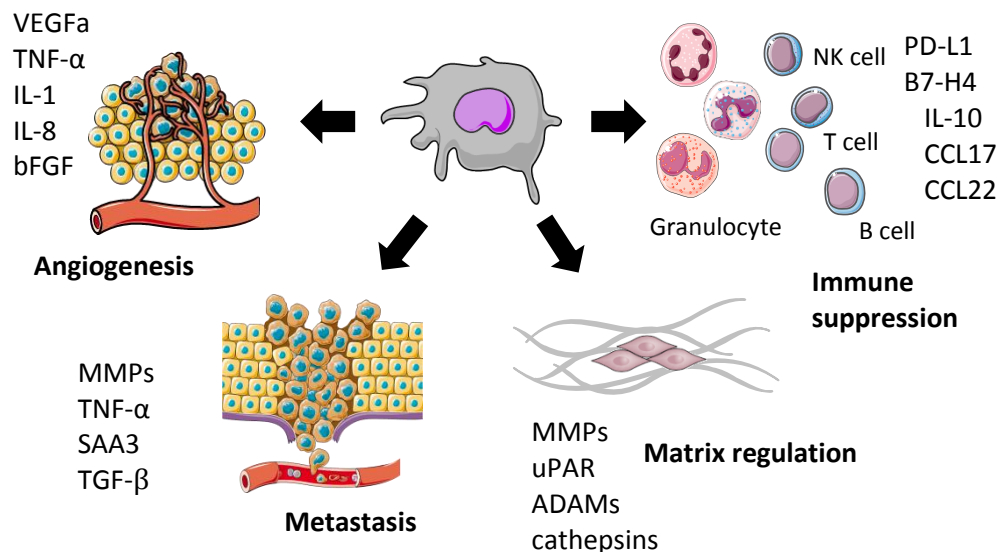
Figure 1: TAM mediated functions in the TME.

TAMs can promote angiogenesis and metastasis, regulate matrix organization and suppress immune responses. Mediating factors are depicted next to each function, references are given in the text (section 1.1.3).

The clinical relevance of TAMs has long been discussed. There are now various studies that have correlated the frequency of TAMs with a poor overall survival (OS) or progression free survival (PFS). On the contrary there are also a notable numbers of reports that have found no such correlation (Heusinkveld & van der Burg 2011; Kridel et al. 2015; Guo et al. 2016). It has to be noted that detection methods and the applied thresholds for macrophage contents vary broadly between different studies. However, the increasing number of reports that have found a negative correlation of OS and PFS with the amount of macrophages present in the tumor is indicating that macrophages indeed might play an important role in tumor progression but the prognostic impact is still controversial. Aside from the prognostic value there is evidence that macrophages can modulate the outcome of anti-cancer therapy. In mice experiments it was shown that macrophages interfere with chemo- and radiotherapy. In a mouse model of prostate cancer macrophages were recruited to the tumor site shortly after radiotherapy to stimulate tumor regrowth (Xu et al. 2013). Additionally, macrophages were mobilized to the tumor site in breast cancer models after applying chemotherapeutic agents and protected cancer cells from chemotherapeutic induced death (DeNardo et al. 2011; Shree et al. 2011). Macrophages can also interfere with antibody based therapies via their Fcγ receptors (FcγR). Binding of Fc fragments of the antibodies was shown to induce antibody dependent cellular

cytotoxicity or phagocytosis in macrophages thereby enhancing the efficiency of antibody therapies (Clynes et al. 2000; Minard-Colin et al. 2008). However, it was also shown that immunosuppressive, pro-angiogenic, and pro-tumoral effector functions can be activated upon FcγR-antibody binding (Grugan et al. 2012; Andreu et al. 2010; Pander et al. 2011). Another, therapeutically exploitable functional aspect of TAMs is their immune suppressive behavior especially the inhibition of cytotoxic CD8$^+$ T cells. Hence, depletion of macrophages to allow anti-tumor T cell cytotoxicity was introduced as a new therapeutic strategy. A study in cervical cancer showed that depletion of macrophages enhanced infiltration of CD8$^+$ T cells (Lepique et al. 2009). However, macrophage depletion might lead to compensatory effects such as recruitment of granulocytes to the tumor site as seen in a mouse model of melanoma (Kumar et al. 2017). Another idea is to reprogram macrophages toward a M1 phenotype which then expose anti-tumor activity or activate T cells. This has been shown a promising approach in bladder cancer and pancreatic cancer models (Beatty et al. 2011; Luo & Knudson 2010).

In conclusion, macrophages exhibit a plethora of phenotypes and functions. This includes angiogenesis, metastasis, immune suppression and interference with antitumor treatments. The recent findings on macrophage behavior in the TME have led to a variety of new therapeutic strategies. However, there is still the need to learn more about the mechanism of their manipulation and their actions especially in context of treatment strategies to fully exploit their potential in therapeutic concepts.

1.2 The mannose receptor CD206

The mannose receptor, also known as CD206 or macrophage mannose receptor, is a C-type lectin and part and eponym of the mannose receptor family. These receptors are described as being involved in the endocytosis of exogenous and endogenous substrates accounting for functions in host defense and tissue remodeling. Clinically CD206 became relevant as a marker for M2 activated macrophages in the TME.

1.2.1 The mannose receptor family

The mannose receptor family is a family of structurally related proteins consisting of four members in mammals, i.e. mannose receptor (CD206), Endo180 (CD280), phospholipase A2 receptor (PLA2R) and Dec-205 (CD205). Each family member is built up by five elements: a

short C-terminal cytoplasmic domain, a transmembrane region, 8-10 C-type lectin-like domains (CTLD), a fibronectin type II domain (FNII) and N-terminal a cysteine-rich (CR) domain (see Figure 2 for the structure of CD206). The cytoplasmic tail of the proteins has no known functions while the transmembrane domain anchors the protein in the cell membrane. The three extracellular domains can bind to specific targets and mediate their internalization.
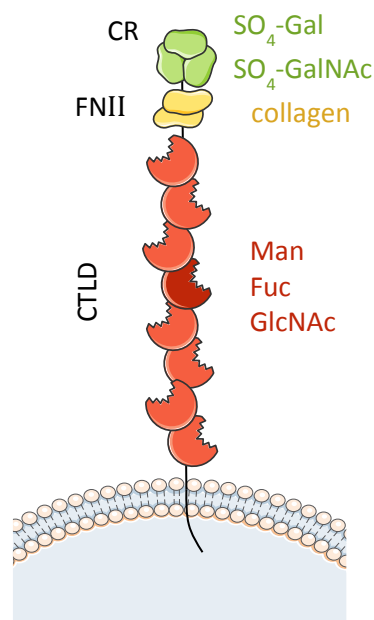
Figure 2: Structural properties of CD206.

Schematic of the structure of CD206 in an extended conformation. CTLD (red), FN II (yellow) and CR (green) domains are shown. CTLD4 (dark red) mediates sugar binding. Ligands of each domain are given in the corresponding color (Man–mannose, Fuc–fucose, Gal–galactose) (Taylor et al. 2005).

The CTLDs bind to terminal mannose, fucose and *N*-acetylglucosamine (GlcNAc) residues, the FNII domain was shown to bind collagens and the CR domain binds to sulfated galactose and sulfated *N*-acetylgalactosamine (GalNAc) (Fiete et al. 1998; Martinez-Pomares et al. 2006). Not all domains have been shown to be functional in each protein. The binding of residual mannose, fucose and GlcNAc is mediated by only one CTLD, this is CTLD4 in CD206, CTLD2 in Endo180 and CTLD5 in PLA2R (Llorca 2008). For DEC-205 no carbohydrate binding was demonstrated so far. The FNII domain has been shown to bind collagens in all protein family members, however, with varying affinity to different collagen types (Martinez-Pomares 2012). The CR domain has only been shown to be functional in CD206 (Leteux et al. 2000). Despite their functionality in substrate binding the domains also account for the conformation of the

proteins. Analysis of the structure revealed that proteins of this family can either exist in an elongated or bent form (Napper et al. 2001; Boskovic et al. 2006). In this bent conformation the sugar binding CTLD and the collagen binding FNII domain come into close proximity which might account for ligand specificity of the receptors (Llorca 2008). Additionally, multimerization is required for the functioning of the receptors. As it was shown for isolated CD206 and Endo180, these receptors are unable to bind collagen as monomers but substrate binding was seen after crosslinking (Martinez-Pomares et al. 2006). The substrate uptake is clathrin dependent (Howard & Isacke 2002; Martinez-Pomares 2012). After internalization into the early endosome the receptors can be retrieved and transported back to the cell membrane. Thus, the receptors cycle constantly between the plasma membrane and intracellular compartments, only about 15 % of the receptors are present at the cell surface (Howard & Isacke 2002; Taylor et al. 2005).

1.2.2 Expression and functions of CD206

CD206 is expressed by macrophages, DCs and endothelial cells. The tissue distribution is well studied in mouse and CD206 positive cells can be found in most tissues (Martinez-Pomares 2012). Various exogenous and endogenous ligands have been described for the mannose receptor, implicating several functions of the receptor in inflammation and homeostasis. First descriptions of CD206 have placed it as a clearance system for circulating lysosomal hydrolases (Lee et al. 2002). In the following more endogenous substrates have been identified, e.g. lutropin, and cells expressing CD206 were shown to clear these substrates from the system (Leteux et al. 2000). Other endogenous molecules that can be bound and internalized by CD206 are collagens (Martinez-Pomares et al. 2006). The collagen uptake might indicate a role for the receptor in tissue reorganization such as during developmental processes. However, CD206 KO mice showed no disruption of tissue development (Martinez-Pomares et al. 2006). Among the exogenous binding partners of CD206 are several microbes including bacterial pathogens such as *Mycobacterium tuberculosis* and fungi like *Candida albicans* (Lee et al. 2003). It is suggested that via binding to CD206 an enhanced phagocytosis and pathogen clearance is achieved. However, again in KO mice no inferior immune defense was observed after fungal infection (Swain et al. 2003; Lee et al. 2003). Therefore, the involvement of the receptor in inflammatory reactions remains unclear. It has to be considered that loss of CD206 might be compensated by upregulation of other mannose receptor family

Introduction

members or other cell types resume CD206 mediated functions, e.g. fibroblasts expressing Endo180 (Martinez-Pomares et al. 2006; Bianchetti et al. 2012).

In DCs it was shown that internalization of substrates via CD206 led to presentation of the according peptides and glycolipids in major histocompatibility complex (MHC) class II or CD1b molecules, respectively (Tan et al. 1997; Prigozy et al. 1997). This links the endocytic functions of the receptor to immune responses in inflammatory processes though direct contribution via pathogen uptake could not be proven. Interestingly, CD206 expressed on DCs can also bind directly to T cells via CD45. A study showed that this direct interaction in combination with antigen crosspresentation via MHC I reduced the cytotoxic activity of CD8^{+} T cells (Schuette et al. 2016).

In conclusion, many possible ligands and mechanisms of action have been described for CD206 by *in vitro* studies. In infection the receptor might contribute to inflammatory responses by enhancing the antigen presentation of DCs. Besides through the direct DC-T cell interaction the receptor might play a role in immune tolerance. Whether these functions can be exhibited in macrophages remains unclear. For macrophages specifically it was shown that expression of the receptor by murine bone marrow resident cells mediated collagen uptake, thus, indicating a role aside from inflammatory reactions to tissue homeostasis or remodeling. However, fibroblasts were shown to fulfill the same function via Endo180. Taken together, the impact and relevance of the proposed functions found *in vitro* in physiological conditions still needs to be evaluated.

1.3 Hodgkin lymphoma

1.3.1 Clinical and molecular features of Hodgkin lymphoma

Hodgkin lymphoma (HL) is a rare hematological malignancy. In Germany, HL accounts for 14 % of lymphoma cases and an estimate of 2510 cases will be diagnosed in 2018. In nearly 4 % of cases patients will be children (below 15 years) (Robert Koch-Institut, 2017). HL is categorizes into two main subgroups, the classical Hodgkin lymphoma (cHL), which represents about 95 % of cases, and the nodular lymphocyte-predominant HL (NLPHL). Based on histological features cHL is further divided into four subtypes: nodular sclerosis (60 %), mixed cellularity (30 %), lymphocyte-rich and lymphocyte-depleted subtype (Swerdlow et al. 2008).

10

The standard treatment in cHL is chemotherapy using a combination of doxorubicin, bleomycin, vinblastine and dacarbazine (ABVD) followed by radiation. Another common chemotherapy regimen includes BEACOPP (bleomycin, etoposide, doxorubicin, cyclophosphamide, vincristine, procarbazine and prednisone) (Engert 2016). The prognosis of cHL is relatively good with 80 % curation rate using this combinational approach of chemo- and radiation therapy. The remaining 20 % account for cases of relapsed or refractory disease. The standard regimens for these patients is high-dose chemotherapy followed by autologous stem cell transplant, which leads to a curation rate of about 50 % in these cases (Hoppe et al. 2017) . Hence, there are about one fifth of cases which are not cured by standard therapy and initial treatment failure or relapsed disease is accompanied by a drop in prognosis. Besides patients that have been successfully treated can have long-term side effects as a result of chemotherapy that diminish their life quality. Especially patients treated with radiation therapy have an increased risk to develop secondary malignancies. Also cardiac diseases occur in about 15 % of patients within the first five years after treatment (Hoppe et al. 2017). Thus, improving the therapy of cHL aims toward a reduction of toxicities and better therapy options for patients with initial treatment failure or relapsed disease.

The malignant cells in cHL consist of mononuclear Hodgkin and bi- or polynuclear Reed-Sternberg cells (HRS). The phenotype of HRS cells is highly variable and shows feature of several lymphatic and myeloid lineages such as expression of CD3, granzyme B, CD20, macrophage colony stimulating factor receptor (M-CSF-R) and CD15 while the common leukocyte marker CD45 is absent. Present on all HRS cells is CD30, a receptor of activated B and T cells, which is also used for diagnosis of cHL (Schmitz et al. 2009). Similarly deregulated and non-lineage specific is the cytokine expression profile of HRS cells. A wide spectrum of T_H cell cytokines can be expressed by HRS cells, such as the T_H2 cytokines IL-2, IL-5, IL-6, IL-9, IL-10, IL-13, and T_H1 cytokines IL-12 and interferon (IFN)-γ as well as other cytokines like IL-1, TGF-β, IL-7, IL-8 and B cell activating factor (BAFF) (Skinnider et al. 2002; Aldinucci et al. 2016). Because of this lineage diversity the origins of HRS cells were discussed for years until their B cell origin was clarified by the detection of clonal and somatically mutated immunoglobulin heavy- and light-chain gene rearrangements (Küppers et al. 1994; Kanzler et al. 1996; Marafioti et al. 2000).

1.3.2 The microenvironment of classical Hodgkin lymphoma

Characteristic for cHL is the small portion of malignant cells in the tumor that is outnumbered by the vast and rich cellular fraction of the TME. The malignant cells only account for 0.2-2 % of the cellular compartment within the tumor mass. They are embedded in a complex environment of non-neoplastic cells mainly consisting of immune infiltrates. Predominant in the TME are T cells with the occurrence of NK cells, mast cells, neutrophils, eosinophils, DCs and macrophages (Aldinucci et al. 2016). The immune infiltrates establish a reactive background for the malignant cells and support tumor progression. The cells show no further anti-tumor activity which they expose under healthy conditions. Analysis on how exactly HRS cells escape immune surveillance in the inflammatory milieu and built up their environment has been studied for years identifying multiple mechanisms. A well described mechanism for immune escape is the downregulation of MHC I on HRS cells which is correlated with inferior prognosis (Reichel et al. 2015; Roemer, Advani, Redd, et al. 2016). However, the absence of self-molecules on cells normally leads to the activation of NK cells. Thus, further mechanisms for immune suppression are developed in cHL. It was shown that HRS cells secret factors that can shed MHC class I polypeptide-related sequence A (MICA) from their cell surface which is the ligand for natural killer group 2D (NKG2D) a signal of damaged cells to become destroyed by immune cells. The soluble ligand binds to its receptor on NK and $CD8^+$ T cells leading to receptor internalization thereby disrupting the immune defense against abnormal cells (Chiu et al. 2018). Despite mechanisms of immune evasion exhibited by HRS cells themselves, immune suppression in cHL is also outsourced to $CD4^+$ T cells such as T_{Regs} as well as to mast cells and macrophages. In clinical studies it was found that especially $CD4^+$ T cells or T_{Regs} are associated with a worse prognosis whereas $CD8^+$ cell count correlates with a better prognosis (Koreishi et al. 2010; Hollander et al. 2018; Alonso-Álvarez et al. 2017). Additionally, studies reported that mast cells and macrophages correlate with worse prognosis (Glimelius et al. 2005; Canioni et al. 2009; Guo et al. 2016). This indicates that an environment of regulatory immune cells that can mediate the escape from immune surveillance is advantageous for disease progression. Accordingly, HRS cells were found to produce large amounts of CCL17 which recruits CCR4 positive T_{Regs}, CCL5 to attract mast cells and CCL2 which is detected by monocytes (Aldinucci et al. 2008; Fischer et al. 2003; Niens et al. 2008; Luciani et al. 1998). Additionally, the number of macrophages is correlated with the number T_{Regs} which might indicate that environmental cells are involved in the recruitment of each other as well (Barros et al. 2012; Barros et al. 2015).

Another well-known direct mechanism of HRS cells to silence CD8^{+} T cells is the PD-1-PD-L1 interaction. HRS cells have genetic aberrations in the *CD274* (PD-L1) gene locus leading to an increased expression of the protein on the cell surface (Roemer et al. 2016; Green et al. 2010). Besides a recent study described that macrophages within the TME express PD-L1 as well and are surrounded by CD8^{+} T cell presumably to mediate PD-L1 dependent inhibition of T cell cytotoxic activity (Carey et al. 2017). In 2012 two agent targeting the PD-1-PD-L1 axis were approved in Europe for treatment of relapsed cHL, nivolumab, and pembrolizumab, both inhibitory antibodies of PD-1.

In conclusion, cHL is cancer entity with the distinguished and unique feature of a rich and complex TME where the non-neoplastic cells outnumber the malignant cells. HRS cells and the TME exhibit several functions to suppress immune responses thereby allowing tumor progression. The findings of defective PD-L1 expression on HRS cells led to the approval of immune therapeutic agents for relapsed cHL. Thus, further studies on the interaction of HRS cells with the TME might prove valuable for new therapeutic options.

Aims of this study

Mutual interactions of HRS cells with non-transformed cells of the TME are a hallmark of cHL. There is growing evidence that the presence of macrophages in cHL is associated with poor prognosis. Studies in other entities have revealed that macrophages are critical regulators of a tumor supporting, immune suppressive microenvironment. How tumor cells built up their environment and which factors contribute to the recruitment and manipulation of bystander cells is still under investigation. In cHL the mechanisms by which macrophages enter the tumor and the functions they fulfill are likewise not completely understood.

Thus, in this study we aim to gain a deeper insight into how HRS cells reprogram monocytes and macrophages, thereby answering the following questions:

1. Can monocytes or macrophages be recruited by lymphoma derived factors?
2. Can monocytes be differentiated into macrophages by lymphoma derived factors?
3. How does lymphoma derived factors shape the macrophage phenotype and functional properties?
4. Which lymphoma derived factors are involved in the process of macrophage polarization?

In order to answer these questions migration of primary human monocytes and monocyte derived macrophages toward lymphoma secreted factors was investigated. Furthermore, lymphoma conditioned medium (CM) was used to differentiate monocytes into macrophages. The macrophages were characterized concerning their gene expression and protein surface expression. Identifying high CD206 expression as a specific marker of cHL derived macrophages functional aspects of the cells were further analyzed using different endocytosis assays. Tumor formation of cHL cells with macrophages was additionally observed in a chorion allantois membrane (CAM) assay. Lastly, IL-13 and macrophage colony stimulating factor (M-CSF), factors produced by cHL CM, were analyzed for their effects on CD206 gene and surface expression in monocytes and macrophages.

2   Material and Methods

2.1   Material, recipes and equipment

2.1.1   Cell lines

Cell lines used in the present study are listed in Table 1.

Table 1: Cell lines

Cell line	Source	Reference
HBL-1	Diffuse Large B Cell Lymphoma (EBV-)	(Nozawa et al, 1988)
HDLM-2	Hodgkin Lymphoma (EBV-)	(Drexler et al, 1986)
KM-H2	Hodgkin Lymphoma (EBV-)	(Kamesaki et al, 1986)
L-1236	Hodgkin Lymphoma (EBV-)	(Wolf et al, 1996)
L-428	Hodgkin Lymphoma (EBV-)	(Schaadt et al, 1979)
L-540	Hodgkin Lymphoma (EBV-)	(Diehl et al, 1981)
OCI-LY3	Diffuse Large B Cell Lymphoma (EBV-)	(Tweeddale et al, 1987)

2.1.2   Primary material

Outdated Fresh Frozen Plasma bags from donors with blood group AB+ were kindly provided by the Department of Transfusion Medicine, University Medical Center Göttingen.

Cell enriched fractions of whole human blood, so called buffy coats, were as well obtained from the Department of Transfusion Medicine, University Medical Center Göttingen.

2.1.3   Chemicals, solutions and consumable supplies

Chemicals, solutions and consumables used for this study are presented in Table 2 and Table 3.

Table 2: Chemicals and solutions

Chemical or solution	Manufacturer
10x DPBS	Sigma-Aldrich, Munich, D
Accutase solution	Capricorn scientific, Ebsdorfergrund, D
Acetic acid	Roth, Karlsruhe, D

Chemical or solution	Manufacturer
Acid fuchsin	Sigma-Aldrich, Munich, D
Acrylamide/bisacrylamide 30 %	Roth, Karlsruhe, D
Acrylamide/bisacrylamide 40 %	BioRad, Munich, D
Ammonium persulfate (APS)	Sigma-Aldrich, Munich, D
Biocoll separating solution	Biochrom, Berlin, D
Bovine serum albumin (BSA)	Serva, Heidelberg, D
Bromophenol blue	Sigma-Aldrich, Munich, D
Calcium chloride (CaCl$_2$)	Merck Millipore, Billerica, USA
Chicken eggs	Valo BioMedia GmbH, Osterholz-Scharmbeck, D
Collagen (type-I)	Trevigen, Gaithersburg, USA
Crystal violet	Sigma-Aldrich, Munich, D
Deoxyribonucleoside triphosphates (dATP, dCTP, dGTP, dTTP)	PrimeTech LTD, Minsk, BY
Dimethyl sulfoxide (DMSO)	Sigma-Aldrich, Munich, D
DPBS pH 7.4 (cell culture grade)	PAN-Biotech GmbH, Aidenbach, D
Eosin	Roth, Karlsruhe, D
Ethanol (100 %)	J.T. Baker, Deventer, NL
Ethylenediaminetetraacetic acid (EDTA)	Riedel-de Haën, Seelze, D
Full Range Rainbow Molecular Weight Marker	GE Healthcare, Munich, D
Gelatin	Merck KGaA, Darmstadt, D
Glutaraldehyde	Roth, Karlsruhe, D
Glycerol	Roth, Karlsruhe, D
Glycine	Roth, Karlsruhe, D
Goat serum	Sigma-Aldrich, Munich, D
Hematoxylin	Sigma-Aldrich, Munich, D
HEPES	Sigma-Aldrich, Munich, D
Hot FIREpol DNA polymerase	PrimeTech LTD, Minsk, BY
Hydrochloric acid (HCl) 37 %	Sigma-Aldrich, Munich, D
Hydrogen peroxide (H$_2$O$_2$)	Sigma-Aldrich, Munich, D

Chemical or solution	Manufacturer
Iron(III) chloride (FeCl$_3$)	Sigma-Aldrich, Munich, D
Isopropanol	Sigma-Aldrich, Munich, D
Lightgreen SF	Sigma-Aldrich, Munich, D
Magnesium chloride (MgCl$_2$)	PrimeTech LTD, Minsk, BY
Mannose	Roth, Karlsruhe, D
Matrigel	BD Biosciences, Franklin Lakes, USA
Mayer's hemalum solution	Roth, Karlsruhe, D
Methanol 100 % (p.a.)	J.T. Baker, Deventer, NL
Orange G	Sigma-Aldrich, Munich, D
Paraffin	Roth, Karlsruhe, D
Paraformaldehyde	Roth, Karlsruhe, D
Penicillin-Streptomycin	Lonza, Basel, CH
Percoll	GE Healthcare, Freiburg, D
Phosphotungstic acid (H$_3$PW$_{12}$O$_{40}$)	Sigma-Aldrich, Munich, D
Ponceau S	Sigma-Aldrich, Munich, D
Potassium dihydrogen phosphate (KH$_2$PO$_4$)	Roth, Karlsruhe, D
Roti-Histokitt II	Roth, Karlsruhe, D
RPMI-1640 with L-glutamine	Lonza, Basel, CH
RPMI-1640 with L-glutamine, no phenol red	Thermo Fisher Scientific, Waltham, USA
Sodium azide (NaN$_3$)	Sigma-Aldrich, Munich, D
Sodium bicarbonate (NaHCO$_3$)	Sigma-Aldrich, Munich, D
Sodium chloride (NaCl)	Merck KGaA, Darmstadt, D
Sodium dihydrogen phosphate (Na$_2$HPO$_4$)	Roth, Karlsruhe, D
Sodium dodecyl sulfate (SDS)	Merck KGaA, Darmstadt, D
Sodium phosphate dibasic (NaH$_2$PO$_4$)	Sigma-Aldrich, Munich, D
SYBR Green I Nucleic Acid Gel Stain	Roche, Mannheim, D
Trehalose	Roth, Karlsruhe, D
Tetramethylethylenediamine (TEMED)	Sigma-Aldrich, Munich, D
Tris-base	Sigma-Aldrich, Munich, D
Tris HCL	Sigma-Aldrich, Munich, D
TritonX-100	Roth, Karlsruhe, D

Chemical or solution	Manufacturer
Trypan blue 0.4 % in PBS	Life Technologies, Carlsbad, USA
Trypsin/EDTA (cell culture grade)	Biochrom AG, Berlin, D
Xylol	Roth, Karlsruhe, D

Table 3: Consumables

Consumable	Manufacturer
384-well clear optical reaction plate	Applied Biosystems, Foster City, USA
Cell culture flasks T25, T75, T175	Sarstedt, Nümbrecht, D
Cell separation columns MS, LS	Miltenyi Biotec, Bergisch Gladbach, D
Cryo tubes	Nunc, Wiesbaden, D
DryEase Mini Cellophane	Thermo Fisher Scientific, Waltham, USA
Falcon tubes 15 ml, 50 ml	Sarstedt, Nümbrecht, D
Filter tips 10 μl, 100 μl, 200 μl, 1000 μl	Starlab, Ahrensburg, D
Filtropur S 0.45	Sarstedt, Nümbrecht, D
Membranes 5 μm pores	Neuroprobe Inc, Gaithersburg, USA
Optical adhesive covers	Applied Biosystems, Foster City, USA
Pasteur pipettes	Sarstedt, Nümbrecht, D
Pipette tips (w/o filters) 20 μl, 100 μl, 1000 μl	Sarstedt, Nümbrecht, D
Reaction tubes 0.5 ml, 1.5 ml, 2 ml	Sarstedt, Nümbrecht, D
Serological pipettes 5 ml, 10 ml, 25 ml	Sarstedt, Nümbrecht, D
Sterling nitrile powder-free examination gloves	Kimberly-Clark, Zaventem, B
Syringe 5 ml, 10 ml, 50 ml	B. Braun Melsungen, Melsungen, D
Tissue culture dish 6 cm, 10 cm	Sarstedt, Nümbrecht, D
Tissue culture plates 6 well, 12 well, 24 well	Sarstedt, Nümbrecht, D
VueLife FEP cell culture bag 32 ml, 72 ml	CellGenix, Freiburg im Breisgau, D
Round bottom falcon tubes 5 ml	Becton Dickinson, Franklin Lakes, USA
Cryo box	Nunc, Wiesbaden, D

2.1.4   Buffers and media

Recipes of buffers and media used in this study are listed in Table 4. If not otherwise indicated all buffers and solutions are on water basis.

Table 4: Recipes of buffers and solutions

Buffer or solution	Recipe
Acid fuchsin solution	0.06 % (w/v) Ponceau S
	0.5 mM Acid fuchsin
	0,18 % (v/v) Acetic acid
Cell culture medium I (lymphoma cells and macrophages)	RPMI 1640 with L-glutamine
	10 % (v/v) FCS
	100 U/ml Penicillin
	100 μg/ml Streptomycin
Cell culture medium II (monocyte isolation)	RPMI 1640 no phenol red
	10 % (v/v) FCS
Collagen I solution (1 mg/ml, membrane coating)	DPBS
	0.89 mM Sodium bicarbonate
	1 mg/ml Collagen I
Crystal violet staining solution	25 % (v/v) Methanol
	0.5 % (w/v) Crystal violet
Destaining solution	40 % (v/v) Methanol
	10 % (v/v) Acetic acid
Development buffer	50 mM Tris Base
	0,15 mM Sodium chloride
	10 mM Calcium chloride
	7,7 mM Sodium azide
DPBS-EDTA	DPBS
	1 mM EDTA
FACS buffer	DPBS
	10 % (v/v) human AB serum
Fixation buffer	5 % (v/v) Glycerol
	30 % (v/v) Methanol
Freezing medium	90 % (v/v) FCS

Buffer or solution	Recipe
	10 % (v/v) DMSO
Iso-osmotic percoll solution	23.13 ml Percoll
	1.87 ml 10x DPBS
Lightgreen solution	0.135 % (w/v) Lightgreen SF
	0.18 % (v/v) Acetic acid
MACS buffer	DPBS
	0.5 % (w/v) BSA
	1 mM EDTA
Percoll separation solution	23 ml Iso-osmotic percoll solution
	27 ml RPMI-1640
Phosphotungstic acid + Orange G solution	3.6 % (w/v) Phosphotungstic acid
	1.8 % (w/v) Orange G
qRT PCR Mastermix	5.76 μl SYBRGreenMix
	5 μM forward primer
	5 μM reverse primer
	10 ng cDNA
	ad 8 μl H_2O
Renaturation buffer	2.5 % Triton-X-100
Running buffer	25 mM Tris-Base
	192 mM Glycin
	34.67 mM SDS
Sample buffer	62.5 mM Tris HCL pH 6,8
	4 % (w/v) SDS
	25 % (v/v) Glycerol
	0.01 % (w/v) Bromphenolblau
Separation Gel Mix	375 mM Tris-base, pH 8.8
	25 % (v/v) Acrylamide/Bis solution (40 %)
	0.0004 % (w/v) APS
	0.00125 % (v/v) TEMED
	2 mg/ml gelatin
Stacking Gel Mix	125 mM Tris Base pH 6.8

Buffer or solution	Recipe
	12.5 % (v/v) Acrylamide/Bis solution (30 %)
	0.0004 % (w/v) APS
	0.00125 % (v/v) TEMED
Staining solution	0.5 % (w/v) Coomassie-Blue
	40 % (v/v) Methanol
	10 % (v/v) Acetic acid
SYBRGreenMix	1 x PCR buffer
	3 mM MgCl2
	1:80.000 SYBRGreen
	0.2 mM dNTP each
	20 U/ml Hot FIREpol DNA polymerase
	0.25 % (v/v) TritonX-100
	0.5 mM Trehalose
TE buffer	10 mM Tris-base, pH 9
	1 mM EDTA
Weigert's iron hematoxylin solution (solution A)	Ethanol
	1 % (w/v) Hematoxylin
Weigert's iron hematoxylin solution (solution B)	17.9 mM Iron(III) chloride
	2.5 % (w/v) Hydrochloric acid
Weigert's iron hematoxylin solution (working solution)	50 % (v/v) Solution A
	50 % (v/v) Solution B

2.1.5 Equipment

The equipment used in this study is listed in Table 5.

Table 5: Equipment

Instrument	Manufacturer
ABI PRISM 7900HT Fast Real-time PCR System	Thermo Fisher Scientific, Waltham, USA
Accu-jet	Brand, Hamburg, D
Biofuge Pico, Primo R	Heraeus Instruments, Hanau, D

Instrument	Manufacturer
Boyden chamber 48-Well	Neuroprobe Inc, Gaithersburg, USA
Centrifuge 5451D	Eppendorf, Hamburg, D
Consort E734 Power Supply	Schütt Labortechnik, Göttingen, D
FACS Canto II	BD Biosciences, Franklin Lakes, USA
Filter wiper	Neuroprobe Inc, Gaithersburg, USA
Hera freeze -80°C freezer	Heraeus Instruments, Hanau, D
IKA KS 260 shaker	IKA, Staufen, D
IKAMAG RCT magnetic stirrer	IKA, Staufen, D
Incubator Cytoperm	Heraeus Instruments, Hanau, D
Incudrive incubator	Schütt Labortechnik, Göttingen, D
Leica DM 5000B with camera: DFC290	Leica Microsystems GmbH, Wetzlar, D
MACS MultiStand	Miltenyi Biotec, Bergisch Gladbach, D
Microcoolcentrifuge 1-15k	Sigma, Munich, D
Microflow Laminar Downflow Workstation: Telstar Bio-II-A	Azbil Telstar Technologies, Terrassa, E
MiniMACS Separator	Miltenyi Biotec, Bergisch Gladbach, D
Motic SMZ-161 with Moticam 3	Motic, Hong Kong, CHN
Multifuge 3 L-R	Heraeus Instruments, Hanau, D
ND-1000 UV/Vis-Spectrophotometer	Thermo Fisher Scientific, Waltham, USA
Neubauer Counting Chamber Improved	Lo Labor Optik, Friedrichsdorf, D
Power Pac 300 Power Supply	Bio-Rad, Munich, D
QuadroMACS Separator	Miltenyi Biotec, Bergisch Gladbach, D
Tecan Infinite F50 Reader	Tecan Group Ltd., Männedorf, CH
Thermocycler T3000	Biometra, Göttingen, D
Thermomixer Compact	Eppendorf, Hamburg, D
Vortex Genie 2	Schütt Labortechnik, Göttingen, D
Water bath	Köttermann Labortechnik, Hänigsen, D

2.1.6 Stimulants and inhibitors

Cells were stimulated with recombinant proteins and fluorescently labeled substances using the concentrations given in Table 6. Inhibitors used for this study with their respective working concentrations are listed in Table 7.

Table 6: Stimulants

Stimulant	Manufacturer	Final concentration
FITC-dextran, 10kDa, 70 kDa	Sigma-Aldrich, Munich, D	1 mg/ml
Gelatin, Oregon Green™ 488 Conjugate	Thermo Scientific, Waltham, USA	5 μg/ml
IFN-γ, recombinant human	Peprotech, Hamburg, D	10 ng/ml
IL-13, recombinant human	Peprotech, Hamburg, D	10 ng/ml
Latex beads, 1μm, Nile red, carboxylate modified	Thermo Scientific, Waltham, USA	5 beads per cells
LPS, *E. coli* O55:B5	Sigma-Aldrich, Munich, D	100 ng/ml
M-CSF, recombinant human	Immunotools, Friesoythe, D	2.5 ng/ml

Table 7: Inhibitors

Inhibitor	Target	Manufacturer	Final concentration
JAK inhibitor I (Pyridone-6)	JAK1/2/3, Tyk2	Merck, Darmstadt, D	1 μM
Ruxolitinib	JAK1/2	Selleck Chemicals, Houston, USA	1 μM

2.1.7 Antibodies

Antibodies used for flow cytometry are presented in Table 8. Antibodies used for immunohistochemical staining of CAM tumors are listed in Table 9.

Table 8: Antibodies for flow cytometry

Antibody	Label	Clone	Manufacturer
mouse anti CD1a	FITC	HI149	Immunotools, Friesoythe, D
mouse anti CD11b	FITC	LT11	Immunotools, Friesoythe, D
mouse anti CD11c	FITC	BU15	Immunotools, Friesoythe, D

Antibody	Label	Clone	Manufacturer
mouse anti CD14	FITC	M5E2	BD Biosciences, Franklin Lakes, USA
mouse anti CD163	APC	GHI/61	BioLegend, San Diego, USA
mouse anti CD206	APC	15-2	BioLegend, San Diego, USA
mouse anti CD31	FITC	MEM-05	Immunotools, Friesoythe, D
mouse anti CD33	FITC	HIM3-4	Immunotools, Friesoythe, D
mouse anti CD40	FITC	HI40a	Immunotools, Friesoythe, D
mouse anti CD44	FITC	MEM-85	Immunotools, Friesoythe, D
mouse anti CD54	FITC	1H4	Immunotools, Friesoythe, D
mouse anti CD68	PE	Y1/82A	BD Biosciences, Franklin Lakes, USA
mouse anti CD80	FITC	MEM-233	Immunotools, Friesoythe, D
mouse anti CD86	FITC	BU63	Immunotools, Friesoythe, D
mouse anti HLA-DR	FITC	G46-6	BD Biosciences, Franklin Lakes, USA
mouse anti PDL1	APC	29E.2A3	BioLegend, San Diego, USA
mouse IgG1	FITC	PPV-06	Immunotools, Friesoythe, D
mouse IgG1	PE	MOPC-21	BD Biosciences, Franklin Lakes, USA
mouse IgG2a	FITC	G155-178	BD Biosciences, Franklin Lakes, USA
mouse IgG2b	APC	MPC-11	BioLegend, San Diego, USA
mouse IgG2b	FITC	PLRV219	Immunotools, Friesoythe, D
mouse IgG2b	PE	27-35	BD Biosciences, Franklin Lakes, USA

Table 9: Antibodies used for immunohistochemical staining

Antibody	Clone	Manufacturer
mouse anti CD30	Ber-H2	Dako, Agilent, Santa Clara, USA
mouse anti CD68	KP1	Dako, Agilent, Santa Clara, USA
goat anti-mouse HRP	polyclonal	Dako, Agilent, Santa Clara, USA

2.1.8 Oligonucleotides

Oligonucleotides used as primers in quantitative Real Time PCR are listed in Table 10. Oligonucleotides were synthesized by IBA GmbH (Göttingen, D).

Table 10: Oligonucleotides

Gene (protein name)	Sequence
CCR7	fwd: GGC TGG TCG TGT TGA CCT ATA TCT
	rev: GGT ATC GGT CAT GGT CTT GAG C
CSF1 (M-CSF)	fwd: GGA GAC CTC GTG CCA AAT TA
	rev: CGC ATG GTG TCC TCC ATT AT
CSF2 (GM-CSF)	fwd: CGG AAA CTT CCT GTG CAA CC
	rev: TCT CAC TCC TGG ACT GGC TC
CXCL8 (IL-8)	fwd: GCA GAG GGT TGT GGA GAA GT
	rev: TTT GCT TGA AGT TTC ACT GGC AT
GAPDH	fwd: CAG CCT CAA GAT CAT CAG CA
	rev: CAT GAG TCC TTC CAC GAT ACC
IL10	fwd: AAC CTG CCT AAC ATG CTT CGA G
	rev: AAC AAG TTG TCC AGC TGA TCC TTC
IL13	fwd: GAT TCT GCC CGC ACA AGGT
	rev: GCC ACC TCG ATT TTG GTG TCT
IL1B (IL-1β)	fwd: CTC TGG GAT TCT CTT CAGC CAA
	rev: AAG TCA TCC TCA TTG CCA CTG T
IL32	fwd: CCT CTC TGA TGA CAT GAA GAA GCT G
	rev: CTC TGC CAG GCT CGA CAT CA
MRC1 (CD206)	fwd: TGG AGT AAT ATT CAC TGT TCA TCC T
	rev: AGG GTC CAT CTT CCT TGT GT
TNF (TNFα)	fwd: TCT CTA ATC AGC CCT CTG G
	rev: CTA CAA CAT GGG CTA CAG G

2.1.9 Ready to use reaction systems

Ready to use reaction systems and kits used for this study are presented in Table 11.

Table 11: Ready to use reaction systems

Ready to use reaction system	Manufacturer
CD14 microbeads	Miltenyi Biotec, Bergisch Gladbach, D
Cytofix/Cytoperm Kit	BD Biosciences, Franklin Lakes, USA
DAB High contrast kit	Nordic BioSite AB, Täby, S
Human M-CSF Quantikine ELISA Kit	R&D Systems, Minneapolis, USA
Nucleo Spin RNA II	Machery-Nagel, Düren, D

Ready to use reaction system	Manufacturer
SuperScript™ II Reverse Transcriptase	Thermo Scientific, Waltham, USA

2.1.10 Software

The software used in this study is listed in Table 12.

Table 12: Software

Software	Developer
ABI 7900HT Sequence Detection Systems Ver. 2.4	Thermo Fisher Scientific, Waltham, USA
Adobe Illustrator CS6 Ver 16.0.3	Adobe Systems Inc. San José, USA
FACSDiva™	BD Biosciences, Franklin Lakes, USA
GraphPad Prism 7.03	GraphPad Software Inc., La Jolla, USA
ImageJ software 1.45s	National Institutes of Health, Bethesda, USA
Leica Application Suite Ver 3.8.0	Leica Microsystems GmbH, Wetzlar, D
Magellan for F50 7.0	Tecan Group Ltd., Männedorf, CH
Mendeley Desktop Ver 1.15.2	Mendeley Ltd, London, UK
Microsoft Office (Word, Excel, PowerPoint)	Microsoft Corporation, Redmont, USA
ND-1000 V3.8.1	Thermo Fisher Scientific, Waltham, USA
RQ Manager Ver. 1.2.1	Thermo Fisher Scientific, Waltham, USA
Servier Medical Art (licensed under a Creative Commons Attribution 3.0 Unported License)	Les Laboratoires Servier, Neuilly-sur-Seine, F

2.2 Cell biology

2.2.1 Cell culture

All cell lines used were cultivated in culture medium I and maintained at 37°C with 5 % CO_2. The cells were counted using a Neubauer chamber after mixing the cell suspension with 0.4 % Trypan blue solution and split every 2 – 3 d to maintain a cell density of 0.5-1.5 Mio/ml. Cells were kept in culture for up to five weeks.

For freezing cells were centrifuged 5 min at 121xg and the pellet was collected in freezing medium to yield a cell density of 5 Mio/ml. Each 1 ml was filled into Cryo tubes which were transferred to -80°C in a Cryobox ensuring constant cooling down with 1°C/min. After 24 h the Cryo tubes were placed in a -150°C freezer for long term storage.

For generation of conditioned media (CM) cells were seeded out at 0.5 Mio/ml. After 48 h the cell suspensions were centrifuged for 5 min at 121xg and the supernatant was filtered using a 0.45 μm sterile filter. The conditioned medium was kept at -20°C and thawed immediately before use.

For RNA isolation cells were counted and centrifuged 5 min at 121xg, washed with PBS and centrifuged again. The supernatant was removed and the cell pellet was stored at -80°C until RNA isolation. For RNA Sequencing one tenth *Drosophila melanogaster* cells were added to the cells for external Spike-In (Feist 2016).

2.2.2 Isolation of human monocytes via double gradient centrifugation

Monocytes from cell enriched fractions of whole blood, so called buffy coats, were isolated by double gradient centrifugation for further differentiation to macrophages in cell culture bags or Teflon dishes (Menck et al. 2014). In brief, each 25 ml of human blood cell suspension from one buffy coat was mixed with 25 ml DPBS EDTA and centrifuged for 10 min at 1350xg without brake. The interphase containing leukocytes was collected and DPBS-EDTA was added to a total volume of 30 ml. The cell suspension was then carefully layered on top of 15 ml Biocoll separating solution and centrifuged 30 min at 400xg without brake. Again the interphase containing mononuclear cells as well as platelets was collected and pooled into one tube. The cells were washed twice adding 40 ml DPBS-EDTA, centrifuged at 300xg for 10 min without brake and removing the supernatant containing platelets. The cell pellet was finally resuspended in 20 ml cell culture medium II and layered on top of 25 ml Percoll separating

27

solution. The gradient was centrifuged 30 min at 550xg without brake. Due to the colloidal silica particles coated with polyvinylpyrrolidone in the Percoll lymphocytes sedimentate at the bottom of the tube whereas monocytes remain in the interphase (Feige et al. 1982). The interphase was collected, diluted with DPBS-EDTA to give a total volume of 50 ml and centrifuged at 400xg for 10 min. The monocyte pellet was resuspended in 20 ml RPMI 1640 containing 10 % FCS and cells were counted in a Neubauer chamber mixing the cell suspension with 0.4 % Trypan blue solution.

2.2.3 Isolation of human monocytes via magnetic cell separation

Monocytes were isolated from buffy coats via magnetic cell separation (MACS) for stimulation and inhibition experiments and functional assays. In short, mononuclear cells from buffy coats were isolated by Biocoll gradient centrifugation as described in the previous section. The cells were counted and resuspended in MACS buffer according to the manufacturer's instructions. Cells were labelled with CD14 microbeads and washed following the manufacturer's instructions. Up to 70 Mio cells were applied on a MS column and up to 700 Mio cells on an LS column. The columns were prepared by placing them into the corresponding cell separator attached to a Multistand and rinsing them with MACS buffer as depicted in the instruction guidelines. The labeled cell suspension was applied onto the column. After complete passage the column was rinsed three times with MACS buffer and the cell were eluated in MACS buffer by pushing the plunger in the column as described in the instruction guidelines. To estimate the purity of CD14$^+$ cells in the resulting cell suspension 100 μl were stained with a FITC labeled CD14 antibody and data was collected on a FACS Canto II flow cytometer with FACSDiva software. Gating on CD14 positive events isolated cells were used for further experiments when the portion of CD14$^+$ monocytes was 95 % or higher. Cell numbers were determined using a Neubauer chamber mixing the cell suspension with 0.4 % Trypan blue solution.

2.2.4 Differentiation of human monocytes to macrophages

Monocytes isolated by double gradient centrifugation were differentiated into macrophages in fluorinated ethylene propylene (FEP) coated cell culture bags which allows the detachment of the cells after the differentiation period. Cell were differentiated for 7 d at 37°C and 5 % CO2 either in cell culture medium I containing 2.5 ng/ml Macrophage colony-stimulating factor (M-CSF) or in lymphoma CM mixed in equal amounts with cell culture medium I.

$1x10^6$ cells/ml were filled into FEP coated cell culture bags, adequate volumes for each bag are listed in Table 3. After 7 d cell culture bags were removed from the incubator and placed on ice for 1 h. Cell were resuspended by pulling the bag with minimal pressure 5 times over the edge of a desk or board. The cell suspension was removed from the bag using a syringe and centrifuged at 400xg for 10 min. Cells were resuspended in 10 ml medium, counted and seeded according to the experimental set-up. After adherence of the cells, macrophages were washed twice with DPBS to remove non-differentiated cell and debris and immediately used for further experiments.

For differentiation with IL-13 cells were added to a cell culture bag in cell culture medium I containing 10 ng/ml IL-13, 2.5 ng/ml M-CSF or both and maintained for 7 d. After 1 d and 7 d an aliquot was removed and used for flow cytometric analysis.

For RNA sequencing (RNA-Seq) macrophages were differentiated as described above using L-428 and HBL-1 CM mixed in equal amounts with cell culture medium I or cell culture medium I containing 2.5 ng/ml M-CSF. After 7 d macrophages were extracted from the cell culture bag and plated on cell culture dishes. After 3 h the cells were washed and lysed. Lysates were stored at -80°C until RNA isolation. The experiment was performed with macrophages from three donors and in duplicates for each condition (L-428 CM, HBL-1 CM, M-CSF).

2.2.5 Stimulation and inhibitor treatment of human monocytes

Monocytes isolated by MACS were used for stimulation and inhibitor treatment. 2 Mio cells were seeded in 2 ml cell culture medium I in a 12-well plate or in 1 ml cell culture medium I and 1 ml CM was added. Stimulants were added according to Table 6. For inhibitor treatment 2 Mio monocytes were seeded in 1 ml cell culture medium in a 12-well plate. Inhibitors were added at two-fold of the final concentration as given in Table 7, equal amount of DMSO were added to control cells. After 1 h 1 ml cell culture medium I and IL-13 or CM was added.

After the indicated time points cells were harvested by transferring the suspension to a 2 ml reaction tube followed by centrifugation at 1000xg for 5 min. The supernatant was removed and cells were washed once with ice cold DPBS. After another centrifugation step the supernatant was removed and the collected cell pellet was kept at -80°C until RNA extraction.

2.2.6 Stimulation of macrophages

Macrophages were extracted from cell culture bags and plated in 6-well plates with 0.5 Mio cells/well. Cells were allowed to adhere for 3 h, washed twice with DPBS and 1 ml cell culture medium I was added. 1 ml cell culture medium or 1 ml cell culture medium containing 5 ng/ml M-CSF or lymphoma CM was added und macrophages were incubated for 24 h. Afterwards cells were washed with DPBS and immediately lysed. Lysates were stored at -80°C until RNA extraction.

2.2.7 Flow cytometry

Expression of cell surface proteins was examined using flow cytometry. Monocytes were analyzed directly after MACS, macrophages were analyzed directly taken from cell culture bags. Cells were centrifuged and taken up in FACS buffer at a density of 10 Mio/ml. Each 250,000 – 500,000 cells were given in round bottom tubes and antibodies or isotype controls given in Table 8 were added in appropriate amounts. For intracellular staining of CD68 cells were fixed and permeabilized using Cytofix/Cytoperm Kit according to the manufacturer instructions before adding CD68 or the isotype control. Cells were stained for 20 min on ice and then washed by adding 500 μl 2 % BSA in DPBS and removing the supernatant after centrifugation for 5 min at 400xg. Following another washing step using DPBS cells were resuspended in 300 μl DPBS. Data was collected on a FACS Canto II flow cytometer using FACSDiva software. After gating on living cells doublets were excluded by plotting the width against the area of the side scatter. Unstained cells were used to adjust the laser powers. For each sample data from 5,000 – 10,000 single cells were collected. Mean fluorescence intensities were calculated by FACSDiva software. Mean fluorescence intensity ratios were obtained dividing the mean fluorescence intensity of each antibody by their corresponding isotype control.

2.2.8 Endocytosis assays

Endocytosis assays were performed to estimate the uptake of particles, sugars and collagen by macrophages. 1 Mio macrophages were seeded in 6 cm cell culture dishes and allowed to sit over night. The next day cells were washed twice with DPBS and covered with 1 ml Medium. For each condition tested two dishes were prepare. 20 min before adding a labeled substance one dish was placed on ice as control for surface binding. Carboxylate modified beads were added as 5 Mio beads in 20 μl aqueous solution, FITC-dextran was added to give a final

concentration of 1 mg/ml and OG-gelatin was used in a final concentration of 5 μg/ml. For blocking of dextran uptake with mannose, mannose was added at 3 mg/ml 10 min before addition of dextran. For bead and dextran uptake macrophages were incubated 2 h, for OG-gelatin uptake 30 min. Afterwards cells were washed twice with DPBS and harvested with trypsin/EDTA solution. Cells were transferred to round bottom tubes and centrifuged at 400xg for 5 min. The supernatant was removed and cells were fixed in 2 % PFA in DPBS for 10 min on ice. Cells were centrifuged again to remove the PFA solution and taken up in 300 μl DPBS. Fluorescence intensities were measured on a FACS Canto II flow cytometer using FACSDiva software as described in the previous section. Mean fluorescence intensities of 37°C samples were normalized to their corresponding control incubated on ice.

2.2.9 Migration and invasion assay

The chemotactic potential of lymphoma CM for monocytes and macrophages was determined using a Boyden chamber with a 5 μm porous membrane.

In short, monocytes were isolated via magnetic cell separation and resuspended in RPMI 1640. The chamber was prepared filling the lower wells with RPMI 1640 containing 1 % or 10 % FCS or lymphoma conditioned medium. The 5 μm membrane was applied covering the wells and the upper chamber was attached to the lower chamber. 50,000 monocytes were filled in each upper well and allowed to migrate for 2 h. Afterward the upper chamber and the membrane was removed from the lower part and 22 μl of each lower well was mixed with 10 μl 0.4 % Trypan blue solution. Cells were counted using Neubauer chamber slide chips. Six wells per condition were used in each experiment.

For invasion assays with macrophages 5 μm membranes were coated using 1 mg/ml collagen I solution. Macrophages were washed and harvested using Accutase solution. Cells were resuspended in RPMI 1640 and cell viability was determined by counting in a Neubauer chamber using 0.4 % Trypan blue solution. Cells with viability higher than 85 % were used for invasion assays. The lower wells of the Boyden chamber were filled with RPMI 1640 without additives or containing 10 % FCS or lymphoma CM. 50,000 macrophages were applied to the upper wells. After 4 h the chamber was disassembled and cells from the top of the membrane were removed using a filter wiper. Cells attached to the bottom of the membrane were fixed in ice cold methanol and stained in Crystal violet staining solution. Stained membranes were applied on microscope slides, covered with mounting medium and a coverslip. Three pictures

per well were taken using a Leica DM 5000B microscope with camera and cells were counted using ImageJ software. Numbers of migrated cells are given as mean of three pictures per well. Four to six wells per condition were used in each experiment.

2.2.10 Chick chorion allantois membrane assay

Chick chorion allantois membrane (CAM) assays were performed by Frederike von Bonin including sawing of the egg shells, cultivation of L-428 cells, cell inoculation, tumor harvest, fixation, trichrome and peroxidase staining. Generation of macrophages and the later evaluation including scoring of hemorrhages, measurement of the tumor area, assessment of the results, microscoping of stained slices and statistics have been performed by me.

In brief, eggs were bred for 4 d at 37°C and 80 % humidity with regular movement every 40 min. At day 4 of egg development a 0.75 cm^2 squared window was cut into the egg shell above the embryo using a saw and sealed with adhesive tape. After incubation for additional 7 d, at day 11 of embryonic development, the egg was removed from the incubator. The window was cut open and 2 Mio L-428 cells, 2 Mio L-428 cells and 1 Mio L-428 CM derived macrophages or 1 Mio L-428 CM derived macrophages in 20 μl Matrigel were applied on the CAM. The window was again closed with adhesive tape and the inoculated eggs were incubated another 4 d. At day 15 of embryonic development the tumors were harvested. The window was cut open and the tumor with surrounding CAM was cut out and transferred to DPBS. The tumors were photographed using a Motic SMZ-161 stereomicroscope with camera and fixed over night in 4 % PFA in DPBS. Afterwards the tumors were dehydrated following the steps given in Table 13. The tumors were embedded in paraffin and finally cut into 4 μm thick slices on a microtome and placed on microscopic slides for subsequent staining.

Table 13: Dehydration of CAM tumors

Number of repeats	Time	Solvent
1	1.5 h	60 % Ethanol
2	1.5 h	75 % Ethanol
2	1.5 h	96 % Ethanol
2	1.5 h	100 % Ethanol
2	1.5 h	Xylol
1	1.5 h	Paraffin
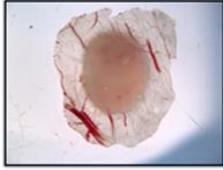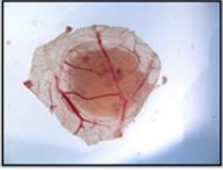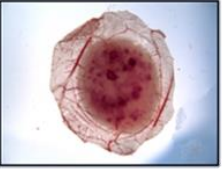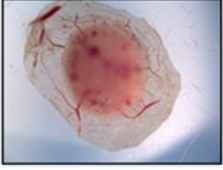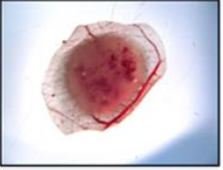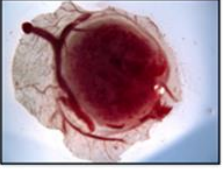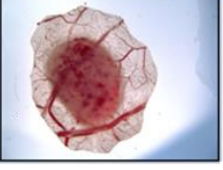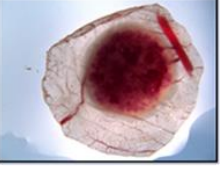
2.2.10.1 Measurement of CAM tumor areas

The area of CAM tumors was measured using ImageJ software by means of top side pictures of CAM tumors. The tumor area was defined using the polygon tool. Pictures of a defined distance were used to set the scale and consequently the area of the encircled region was calculated.

2.2.10.2 Scoring hemorrhages in CAM tumors

Hemorrhages were scored based on appearance, intensity and relative area covered as proposed by Linke 2016. In each criterion zero to three points were given leading to a maximum of nine points per tumor (Table 14).

Table 14: Hemorrhage score for CAM tumors

Criteria	Example			
I Appearance of hemorrhages 0: none 1: small, sporadic 2: big, sporadic 3: big, converging	0	1	2	3
II Intensity of hemorrhages 0: none 1: light 2: medium 3: dark	0	1	2	3
III Area covered by hemorrhages 0: none 1: <20 % 2: 20 – 50 % 3: >50 %	0	1	2	3

2.2.10.3 Trichrome staining of CAM tumor sections

Tumor sections placed on microscopic slides were dewaxed and stained as listed in Table 15 and Table 17, respectively. Stained section were dehydrated (Table 16) starting with 90 % ethanol and mounted with Roti-Histokitt II. After drying slides were ready for microscopy using a Leica DM 5000B microscope with camera.

Table 15: Dewaxing of CAM tumor sections

Number of repeats	Time	Solvent
3	3 min	Xylol
2	3 min	100 % Ethanol
1	3 min	96 % Ethanol
1	3 min	80 % Ethanol
1	3 min	70 % Ethanol
1	3 min	Distilled water

Table 16: Dehydration of stained CAM tumor sections

Number of repeats	Time	Solvent
1	3 min	50 % Ethanol
1	3 min	70 % Ethanol
1	3 min	90 % Ethanol
2	3 min	100 % Ethanol
3	3 min	Xylol

Table 17: Trichrome staining of CAM tumor sections

Time	Solution
2 min	Weigert's hematoxylin working solution
3 min	Tap water
9 min	Acid fuchsin solution
5 min	1 % Acetic acid in water
1 min	Phosphotungstic acid + Orange G solution
1 min	1 % Acetic acid in water
1 min	Lightgreen solution
5 min	1 % Acetic acid in water

2.2.10.4 Peroxidase staining of CAM tumor sections

Tumor sections were dewaxed following the procedure given in Table 15. The antigen was demasked by incubation for 20 min in vaporized TE buffer followed by staining according to Table 18. For development of the antibody labeled sections 100 μl DAB Chromogen and 1 ml DAB Substrate buffer were added on the slice for 1 min. The conversion of the substrate leads a brown color, which was controlled by microscopy of the slide during staining. When an intense brown color was visible the reaction was stopped by covering the slide in tap water.

Finally the nuclei were stained by placing the slide in Mayer's hemalum solution for 2 min followed by tap water for 10 min. The sections were dehydrated as described in Table 16 and mounted with Roti Histokitt II. After drying slides were ready for microscopy using a Leica DM 5000B microscope with camera.

Table 18: Peroxidase staining of CAM tumor sections

Time	Temperature	Solution
15 min	rt	1% Hydrogen peroxide in DPBS
5 min	rt	Distilled water
15 s	rt	DPBS
30 min	rt	2 % Goat serum in DPBS
15 s	rt	DPBS
16 h	4°C	CD30 or CD68 in 2 % goat serum in DPBS
15 s	rt	DPBS
1 h	rt	Goat anti-mouse HRP in 2 % goat serum in DPBS
15 s	rt	DPBS

2.3 Protein biochemistry

2.3.1 Detection of matrix metalloproteinase activity by zymography

The activity of matrix metalloproteinase (MMP)-9 and MMP-2 was determined in cell culture supernatants by gelatin zymography. First, proteins contained in the supernatant were separated by molecular weight by SDS-polyacrylamide gel electrophoresis (PAGE). Gel mixes listed in Table 4 were used to prepare 8 % separation gels containing 1 % gelatin and 5 % stacking gels. 15 μl cell culture supernatant were mixed with equal amount of loading buffer and loaded onto the gel. Electrophoresis was performed at 120 V for 2.5 h with constant cooling using freezer packs. Afterwards gels were incubated in wash buffer for 1 h. Gels were transferred to renaturation buffer and incubated 1 h. Afterwards gels were covered in 500 ml development buffer per gel and incubated over night at 37°C with soft agitation. To visualize the gel degradation by MMP activity, the gels were then stained in staining buffer for 1 h, followed by destaining in destaining buffer for 1.5 h. Gels were then fixed for 30 min in fixation buffer, placed between two cellophane membranes and dried over night. Fixed and dried gels were scanned for image processing.

2.3.2 Enzyme-linked immunosorbent assay of M-CSF

M-CSF concentrations in lymphoma CM were measured by enzyme-linked immunosorbent assay (ELISA) using Human M-CSF Quantikine ELISA Kit according to the manufacturer's instructions. Optical densities were detected at 450 nm with wavelength correction at 540 nm using the Tecan Infinite F50 microplate Reader.

2.4 Molecular biology

2.4.1 mRNA isolation

Total RNA from cell pellets was isolated using NucleoSpin RNA kit according to manufacturer's instructions. RNA was eluted using 20 μl RNase free water and concentrations were measured with ND-1000. RNA was stored at -80°C.

2.4.2 Reverse transcription

SuperScript™ II Reverse Transcriptase was used for cDNA synthesis from total RNA. In brief, 400 ng – 1 μg RNA was diluted with RNase free water to give a total volume of 10 μl. 2 μl Random Primer Hexamers were added and samples were denaturated for 10 min at 70°C and cooled on ice to allow primer annealing. 8 μl mastermix were added (Table 19) and reverse transcription was performed in a Thermocycler T3000 following the program given in Table 20.

Table 19: Reverse transcription mastermix

Amount	Substance
4 μl	5x First strand buffer
2 μl	0.1M DTT
1 μl	Super Script II RT
1 μl	dNTP mix (each 10mM)

Table 20: Reverse transcription cycler program

Temperature	Cycle length
25°C	10 min
42°C	60 min
65°C	10 min
4°C	pause

2.4.3 Quantitative real-time polymerase chain reaction

Gene expression was analyzed by SYBR green-based quantitative real-time polymerase chain reaction (qRT-PCR) using 7900HT Fast Real-Time PCR System in 384-well plates. Upon binding of SYBR green to DNA the resulting complex will absorb blue light (λ_{max} = 488 nm) and emit green light (λ_{max} = 522 nm), hence, fluorescence increases in the course of the PCR. cDNA samples generated as described in the previous section were diluted to give a solution of 5 ng/ml. 10 ng cDNA were added to 8 μl qRT-PCR mastermix. The PCR was performed following the program given in Table 21. Three qRT-PCRs were analyzed for each sample.

Table 21: qRT-PCR cycler program

Temperature	Cycle length	Number of cycles
95°C	15 min	
95°C	15 s	
60°C	1 min	40
95°C	15 s	
60°C	15 s	
95°C	15 s	

Gene expression was evaluated using the SDS 2.4 and RQ Manager 1.2.1. Target gene transcript abundance was calculated using the ΔΔCT method. CT values of genes of interest have been normalized to the CT of a housekeeper. In this study *GAPDH* was used as a housekeeper.

$$\Delta CT = CT_{geneofinterest} - CT_{GAPDH}$$

Further the changes between treated and untreated control samples were calculated as follows:

$$\Delta\Delta CT = \Delta CT_{treatment} - \Delta CT_{control}$$

The number of cycles exponentially correlates with amount of DNA in the sample, thus, relative n-fold changes can be calculated as

$$RQ = 2^{-\Delta\Delta CT}$$

2.4.4 RNA sequencing

RNA sequencing and normalization

RNA sequencing (RNA-Seq) was performed by GATC Biotech (Konstanz, Germany). Quality assessment, read mapping and normalization was performed by Paula Rubio-Perez. In brief, the data from all samples was filtered to generate healthy operational *fastq files. The criterions used to filter the data were: to remove RNA impurities a read was removed if it matched rRNA_CRUnit.fa exactly, the ends of all reads were inspected and trimmed until the base calling quality was above 27, the remaining part was only accepted if it contained less than 5 % low quality base callings and obtained the largest N free subsequence of the read (accepted if longer than 24 nucleotides). In order to align the data, genome, transcriptome, and annotation files were generated as a concatenation of the corresponding *Homo sapiens* (GRCh38, Ensembl release 87) and *Drosophila melanogaster* reference genomes (BDGP, Ensembl release 87). The data was aligned and a count table was created using Kallisto (Bray et al. 2016). The data were calibrated using the *Drosophila melanogaster* Spike-Ins for cell lines and *GAPDH* for macrophage samples where only genes whose count means exceeded 30 reads were taken into account.

Gene set enrichment

Gene set enrichments were calculated using genes that were differentially expressed in L-428 CM derived macrophages and M-CSF derived cells by Log2FC $\geq$ 1 and Log2FC $\leq$ -1 in all three donors. Annotation of enriched genes to GO terms in biological process, molecular function and cellular compartment and InterPro terms and functional annotation clustering was performed using online DAVID bioinformatics annotation tool (Huang et al., 2009). EASE scores were set to 0.1 and classification stringency to high. Clusters were taken into account if at least 5 genes were annotated.

2.5 Statistical analyses

Results are shown as mean $\pm$ standard deviation (mean $\pm$ SD). Statistical analyses have been performed using GraphPad Prism 7.03. The statistical significance of the values was determined using the Student's t-test. If applicable group results were compared using the One-way ANOVA-method with Bonferroni's post-hoc test to correct for multiple comparisons as indicated. Significance levels are indicated as *=$p<0.05$, **=$p<0.01$, ***=$p<0.001$.

3 Results

3.1 Monocytes migrate toward cHL secreted factors

TAMs are defined as macrophages within or in close proximity to the tumor. Several routes are possible for macrophages to occur in the TME: monocytes are recruited by tumor cell secreted factors and differentiated into macrophages, macrophages are recruited by tumor cell secreted factors, monocytes or macrophages are recruited indirectly by other recruited cell types or by cancer associated inflammations. To test for the first option migration of monocytes toward different lymphoma conditioned media (CM), five cHL cell lines and two diffuse large B cell (DLBCL) cell lines, was investigated in a Boyden chamber assay (Figure 3). Since lymphoma cells are cultivated in medium containing 10 % FCS 1 % and 10 % FCS containing medium was applied as controls for nutrient dependent migration. Notably, monocytes did not migrate in the given time frame of 2 h without any attractant. Offering FCS or lymphoma CM monocytes were found to migrate towards any of the given attractants. The migration can be enhanced with higher FCS contents, hence, a directed migration toward nutrition is existent. Migration is heightened toward L-428, L-1236, L-540, and KM-H2 CM in comparison to 10 % FCS. Especially L-428 and L-1236 CM are strong chemoattractants for monocytes. Migration toward HDLM-2 as well as HBL-1 and OCI-LY3 CM, both DLBCL CMs, are not increased compared to 10 % FCS. Thus, cHL CMs with the exception of HDLM-2 CM seem to contain factors that are highly attractive for monocytes. The tested DLBCL CMs and HDLM-2 CM, however, contain less factors attracting monocytes or in lower concentrations. Since the conditioned medium was used pure and lymphoma cells also consume FCS over culture time it is not probable that the conditioned medium still contained the originally applied 10 % FCS. Thus, it can be suspected that other factors than FCS in the medium of HDLM-2, HBL-1 and OCI-LY3 lead to the migration toward these CM which is still significantly higher than toward no attractant or 1 % FCS. However, FCS content in the exhausted medium was not measured.

In conclusion, we found that different lymphoma cell lines secret factors to attract monocytes to a different extent. All used cHL CMs except HDLM-2 CM were able to attract monocytes, of which highest migration was toward L-428 and L-1236 CM. Both tested DLBCL CMs and HDLM-2 CM attracted monocytes to a weaker extent comparable to the migration toward 10 % FCS.
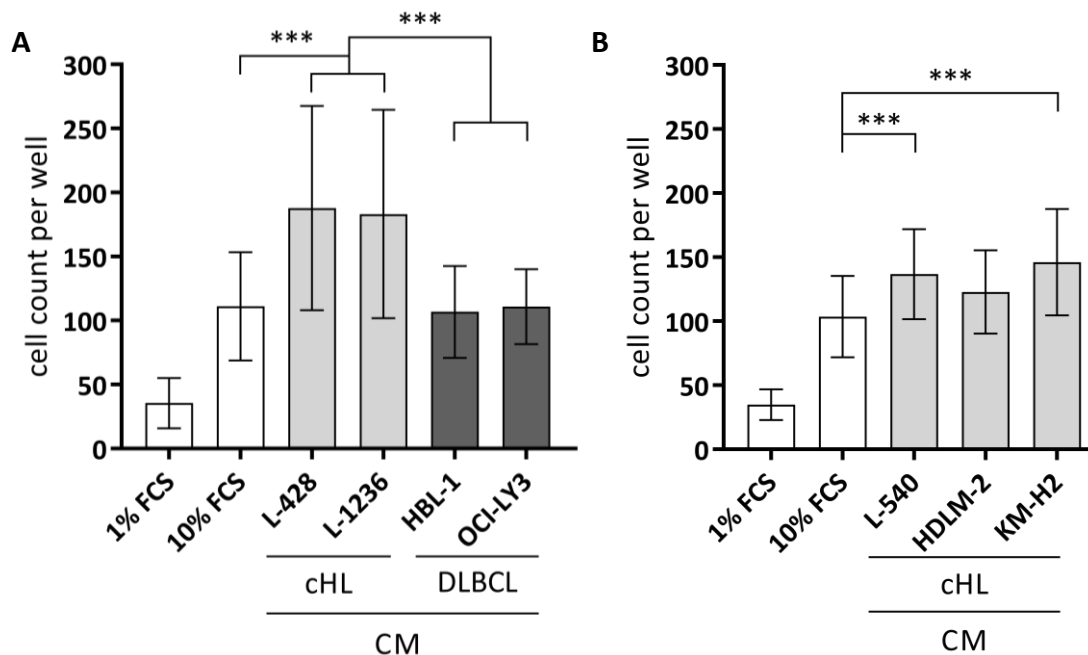
Figure 3: Monocytes migrate toward cHL CM.

A+B: Monocyte migration toward different lymphoma CMs was measured in a Boyden chamber assay with 5 μm porous membranes for 2 h (means ± SD, n = 10, one-way ANOVA with Bonferroni's post-test).

3.2 Monocytes differentiate into macrophages in the presence of lymphoma CM

The previous finding that monocytes migrate toward lymphoma CMs raised the question whether after recruitment monocytes are further differentiated by lymphoma secreted factors. To investigate if lymphoma cells can secret factors that influence the differentiation of monocytes into macrophages CM of the cell lines used in the migration assays were applied on freshly isolated primary human monocytes and after 7 d the resulting macrophages were counted (Figure 4). As suspected cHL CM does not only attract monocytes but also supports the differentiation into macrophages. Namely, differentiation with L-428, L-540, HDML-2 and L-1236 CM led to high macrophage numbers whereas KM-H2, HBL-1 and OCI-LY3 CM as well as differentiation with recombinant M-CSF led to lower cell numbers. Interestingly, though KM-H2 CM was attractive for monocytes in the Boyden chamber assay, differentiation resulted in lower macrophage outcome than HDLM-2 CM toward less monocytes migrated. Thus, secreted factor that attract or differentiate monocytes might not overlap.
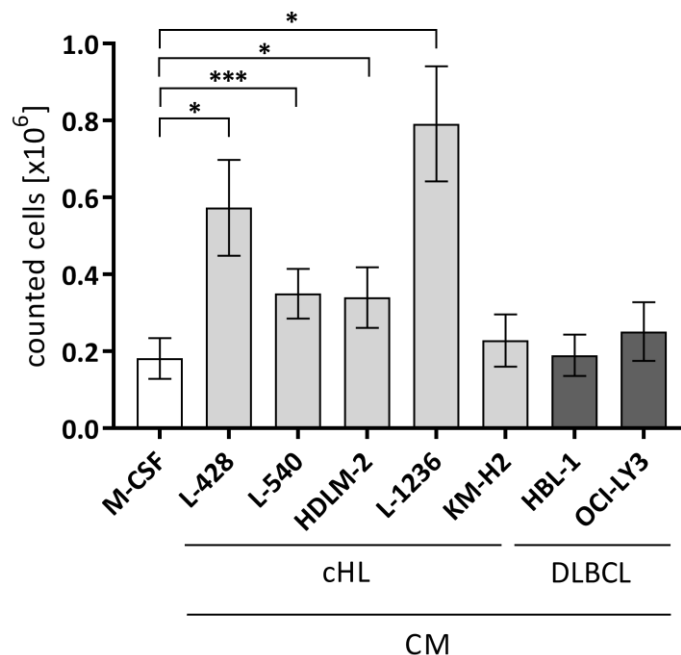
Figure 4: Differentiation of monocytes with various lymphoma CMs leads to differential outcome in cell numbers.

Monocytes were isolated via double gradient centrifugation and each 2 Mio cells were given into a 6-well Teflon culture dish either in medium containing 2.5 ng/ml M-CSF or with lymphoma CM mixed in equal parts with fresh medium. Cells were incubated for 7 d and afterwards macrophages were counted based on appearance and size (mean ± SD, n = 6, paired one-way ANOVA with Bonferroni's post-test).

We tested the lymphoma cell lines for the expression of growth factors that mediate macrophage differentiation. Mainly two endogenous growth factors are described to induce the differentiation of monocytes into macrophages, i.e. M-CSF and granulocyte macrophage-colony stimulating factor (GM-CSF) (Metcalf 2013). We analyzed the cell lines for the gene expression of both growth factors (Figure 5A+C). *CSF1* (M-CSF) was found in all cell lines except for OCI-LY3 whereas *CSF2* (GM-CSF) expression was only found in L-428, L-540 and L-1236. We additionally performed an ELISA to determine the concentrations of secreted M-CSF in the lymphoma CMs (Figure 5B). In general, the gene expression pattern is reflected in the measured M-CSF content of the CMs with highest expression/secretion in L-428 and lowest in L-540. An exception are HBL-1 cells which at low level expressed *CSF1*, however, but M-CSF in the CM was not detected, which could be because it was below the detection limit of the ELISA (78 pg/ml).
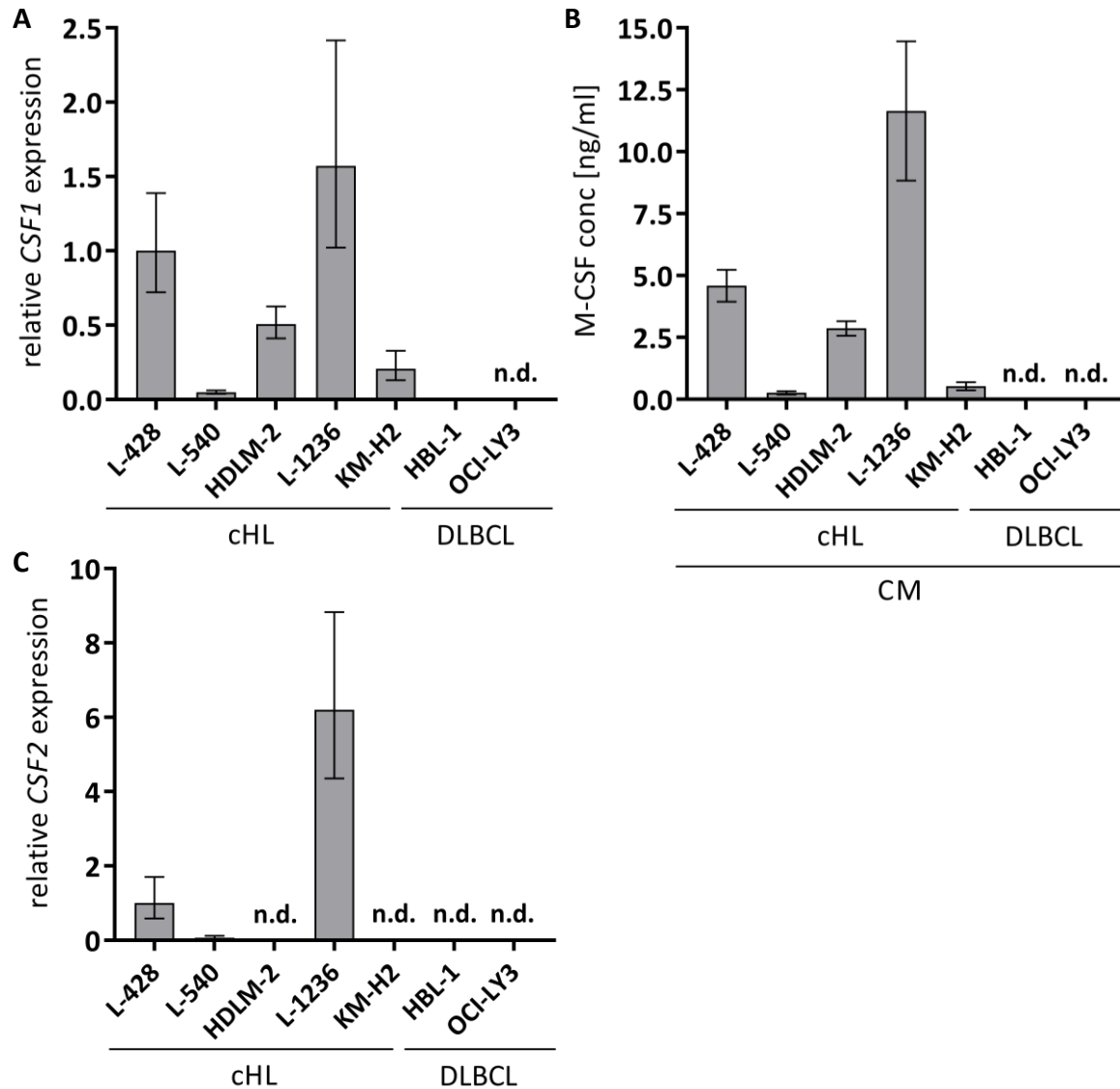
Figure 5: Gene expression of *CSF1* and *CSF2* and M-CSF secretion is most prominent in cHL cell lines.

(A+C) Gene expression of *CSF1* and *CSF2* in lymphoma cell lines was measured by qRT-PCR. Expression was calculated relative to *GAPDH* and L-428 cells (mean ± SD, n = 3). (B) M-CSF concentrations in lymphoma CM were measured by ELISA (mean ± SD, n = 3).

M-CSF could be one factor to explain the macrophage numbers as the expression patterns is loosely reflected in the macrophage count after stimulation. However, it is important to note that recombinant M-CSF was used at a final concentration of 2.5 ng/ml which equals the amount of M-CSF on monocytes differentiated in the presence of L-428 CM. Yet the differentiation with L-428 CM resulted in three times more cells than with M-CSF alone. Hence, there are likely other factors in the CM that contribute to the differentiation process.

One factor could be GM-CSF which is on gene expression level only expressed in L-428, L-540 and L-1236. In this context, the amount of M-CSF in L-540 is relatively low, however it yielded similar macrophage numbers like the differentiation with HDLM-2 CM. A reason for this might also be the GM-CSF production since the gene is expressed in L-540 cells but not by HDLM-2 cells. Additionally, there are more macrophages when differentiated with L-540 CM than with KM-H2 CM though KM-H2 CM contains twice as much M-CSF. Furthermore, 1.4 ng/ml M-CSF and no GM-CSF are applied on monocytes differentiated in the presence of HDLM-2 CM, which results in twice as many cells compared to M-CSF alone. In HBL-1 and OCI-LY3 neither M-CSF in the CM nor GM-CSF on gene expression level were detected, however, it still resulted in notable macrophage amounts. Altogether this shows that the macrophage outcome cannot be explained by M-CSF and GM-CSF expression alone. Numerous chemokines and cytokines were additionally identified by RNA-Seq to be expressed in L-428 and HBL-1 cells (Figure A-19). Among these are factors known to promote macrophage differentiation such as *VEGFA* by both cell lines, *IL13* by L-428 cells and *IL6* by HBL-1 cells which supports the view that several factors in the CMs might contribute to macrophage differentiation.

In conclusion, monocytes can be differentiated into macrophages in the presence of lymphoma CM. Especially differentiation with L-428, L-540, HDLM-2 and L-1236 CM resulted in high macrophage numbers. We measured the gene expression of M-CSF and GM-CSF in the lymphoma cells as well as the M-CSF content in the CMs. Notable expression was found in the cells and CMs that lead to high macrophages numbers. However, the macrophage outcome cannot sufficiently be explained by presence of these two growth factors concluding there are other factors in the CM also involved in the differentiation process. Accordingly, we found multiple factors to be expressed on RNA level in L-428 and HBL-1 cells that could promote the macrophage differentiation.

3.3   L-428 CM derived macrophages strongly resemble an M2 phenotype

3.3.1   Analysis of cell surface markers on M-CSF and L-428 CM differentiated macrophages and monocytes

With the previous experiments we found that cHL cells recruit macrophages to a large extent indicating that these cells fulfill functions in the TME. Next we aimed to characterize the cHL

differentiated cells in greater detail to identify specific features that account for their functions in context of cHL. Monocytes from the same donor were differentiated using M-CSF or L-428 CM. Differentiation of monocytes with M-CSF leads to an M2 phenotype in the resulting macrophages. TAMs are often referred to expose an M2 phenotype as well (see section 1.1.3). First, we determined the morphological properties of the macrophages via flow cytometric analysis using the forward scatter (FSC) and sideward scatter (SSC) and microscopy of plated cells (Figure 6).
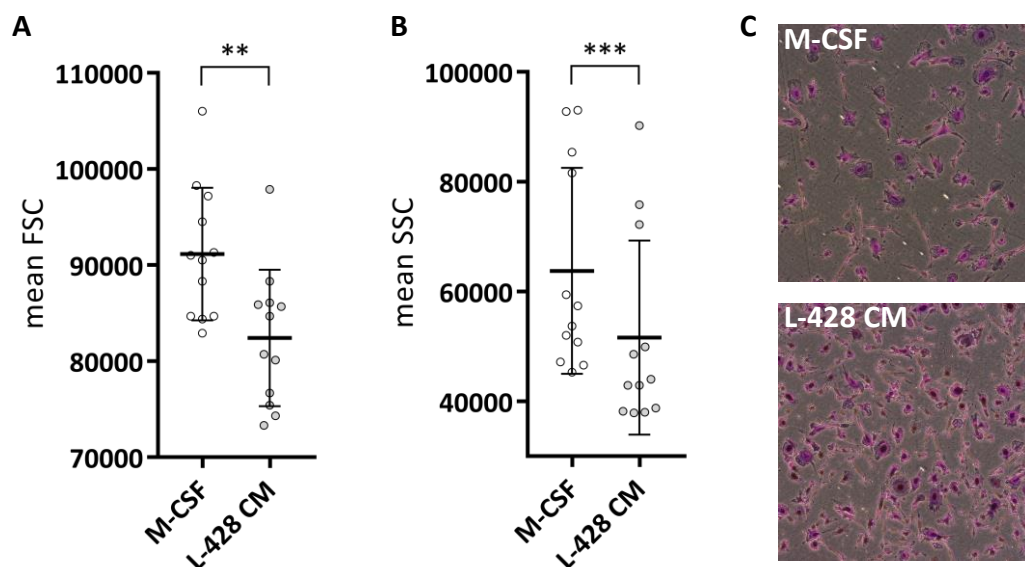
Figure 6: L-428 CM differentiated macrophages are smaller in forward and sideward scatter compared to M-CSF cells.

(A+B) Macrophages were differentiated either with 2.5 ng/ml M-CSF or L-428 CM mixed in equal parts with fresh medium for 7 d in Teflon coated cell culture bags and analyzed by flow cytometry concerning appearance in forward and sideward scatter (mean ± SD, n = 12, paired t-test, two-tailed). (C) Equal volumes of cell suspensions were removed from the cell culture bags and plated on cell culture dishes. Cell were allowed to adhere for 3 h. Afterwards cells were washed, fixed and stained with Crystal violet. Representative images are shown.

Macrophages differentiated with L-428 CM appear to be smaller and less granulated by means of FSC and SSC than M-CSF derived cells. However, differences in size cannot be seen in plated cells.

Next we analyzed the cells concerning their protein surface expression, intracellular CD68 expression and gene expression. Figure 7 shows the relative protein expressions of M-CSF and L-428 CM derived macrophages as well as of freshly isolated monocytes.

Figure 7: Surface expression of selected proteins in M-CSF or L-428 CM derived macrophages and freshly isolated monocytes.

Monocytes were isolated by MACS, immediately stained and protein expression was measured by flow cytometry. Macrophages were differentiated in Teflon coated cell culture bags with either 2.5 ng/ml M-CSF or L-428 CM mixed in equal parts with fresh medium. Macrophages were extracted from the cell culture bags after 7 d and immediately stained for flow cytometric analysis (mean ± SD, n = 12, paired t-test, two-tailed).

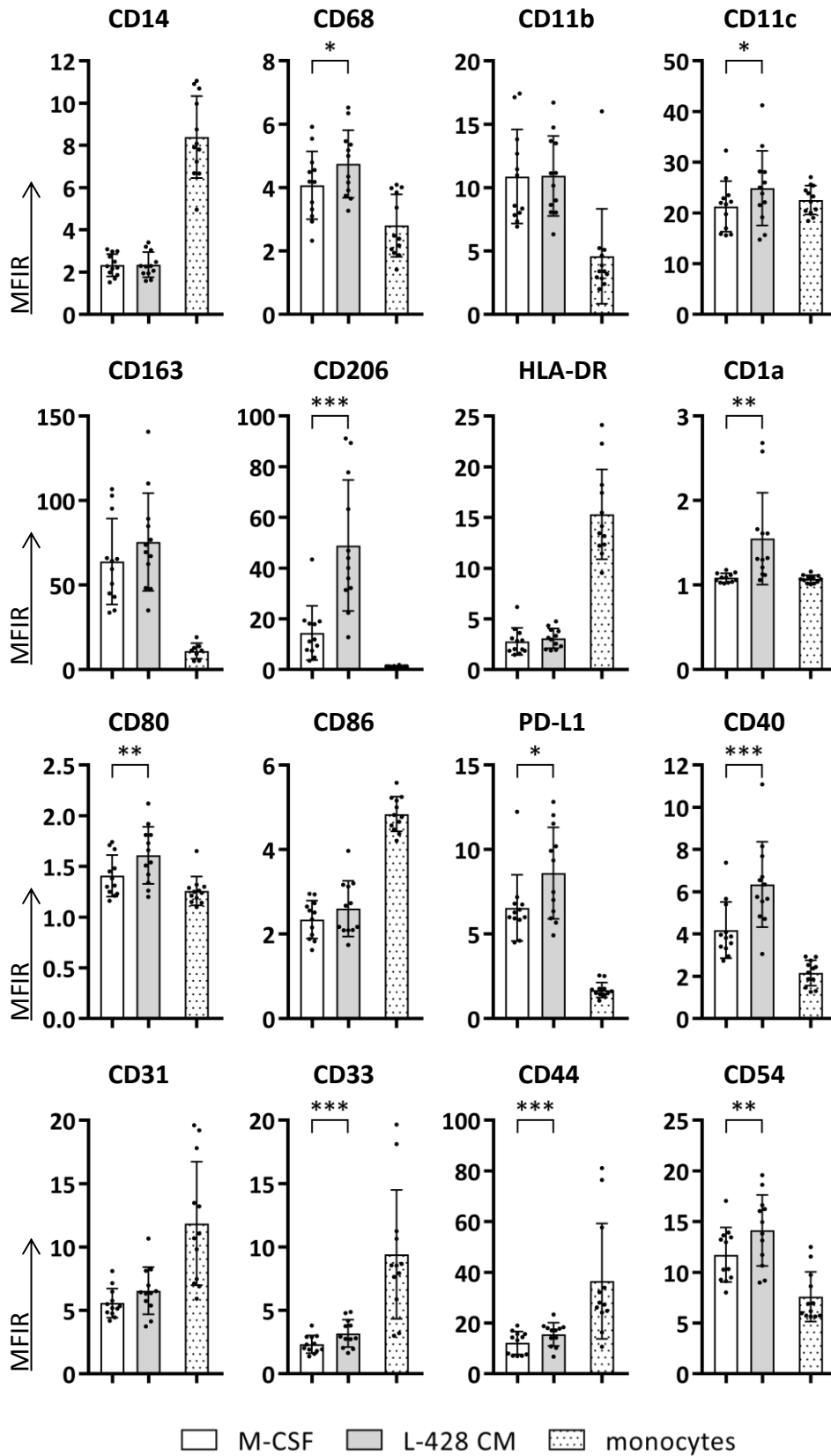Expression of maturation markers

CD14, CD11b, CD11c and CD68 were markers selected to monitor the differentiation state of the two macrophages types and monocytes. Naturally, the CD14 expression in monocytes is notably higher than in the macrophages as this marker decreases during the differentiation process. The resulting macrophages, however, show no differential expression. Additionally, CD11b is known to behave conversely and is upregulated during the differentiation process in macrophages which we also observed. CD11c another maturation marker shows no major changes after differentiation but a small significant increase in L-428 CM derived macrophages compared to M-CSF derived cells. CD68, a pan macrophage marker, is at low level also expressed in monocytes and as anticipated upregulated in mature macrophage. Also here a higher expression in L-428 CM derived compared to M-CSF derived can be detected.

M2 marker expression

Two commonly used surface markers to detect the M2 activation state of macrophages are CD163 and CD206. Both markers are strongly upregulated upon differentiation from monocytes to macrophages. Of note, CD163 is the highest expressed marker in this panel. Importantly, CD206 is about three fold higher expressed on L-428 CM macrophages than on M-CSF derived macrophages and shows the strongest differential expression in this panel. It is not detected on monocytes.

Expression of antigen presenting and co-stimulatory/-inhibitory molecules

The markers human leukocyte antigen (HLA)-DR, CD1a, CD40, CD80, CD86 and PD-L1 are involved in communication of macrophages with T cells by antigen presentation or as co-stimulatory/-inhibitory molecules. Interestingly, we see an increased expression in CD1a, CD80, PD-L1 and CD40 in L-428 CM differentiated cells compared to M-CSF derived cell and monocytes suggesting enhanced interactions with T cell which are a dominant factor in the cHL microenvironment. Notably, CD40 a co-stimulatory molecule is also upregulated which is

a marker for M1 activation of macrophages. Furthermore, CD1a commonly used as a DC marker is not expressed on monocytes and M-CSF derived macrophages but was detectable on L-428 CM derived cells.

Expression of adhesion markers

In order to further evaluate functional properties, especially those connected to cell adhesion, four adhesion markers were tested in this experiment namely CD31, CD33, CD44 and CD54. Strikingly all these markers are increased in L-428 CM macrophages compared to M-CSF macrophages. However, all markers except CD54 are decreased compared to monocytes which means a downregulation overall in the differentiation process. Still the consequent upregulation comparing the two macrophages types suggests a functional distinction of these cell types and a special requirement of L-428 cells to educate macrophage with advanced properties in cell-cell or cell-matrix interactions.

In summary, application of L-428 CM or M-CSF on monocytes led to the expected changes in the expression of surface markers commonly used to monitor macrophages differentiation. This shows that after 7 d mature macrophages are derived. These cells are M2 activated as seen by high expression of CD163 and CD206. Comparing M-CSF and L-428 CM differentiated macrophages a number of proteins are upregulated in L-428 CM derived cells. The higher expression of CD1a, CD80, CD40 and PD-L1 hints toward functions of the macrophages in T cell interaction, the expression of CD11c, CD206, CD33, CD44 and CD54 toward functions that require improved cell-matrix or cell-cell interactions. The other markers analyzed were not differentially expressed, notably, there was no lower expression in any protein on L-428 CM derived cells compared to M-CSF cells.

3.3.2 Gene expression of M1 and M2 markers in M-CSF and L-428 CM derived macrophages

To further estimate the activation state of M-CSF and L-428 CM macrophages gene expression analysis of markers, which could not be detected by flow cytometry, was performed. TNF-α, IL1-β, IL-8 (gene name *CXCL8*) and CCR7 characterize the M1 activation status. No differential expression was found in the respective genes, only *CCR7* seems to be lower expressed in L-428 CM macrophages compared to M-CSF cells. *IL10* and *VEGFA* further define the M2 state

47

of macrophages. No differences in the expression of *VEGFA* were found. *IL10* is highly expressed in M2 activated macrophages, here, was lower expressed in L-428 CM than in M-CSF cells. Overall, the gene expression analysis of the selected markers confirms the M2 activational state of L-428 CM derived macrophages.
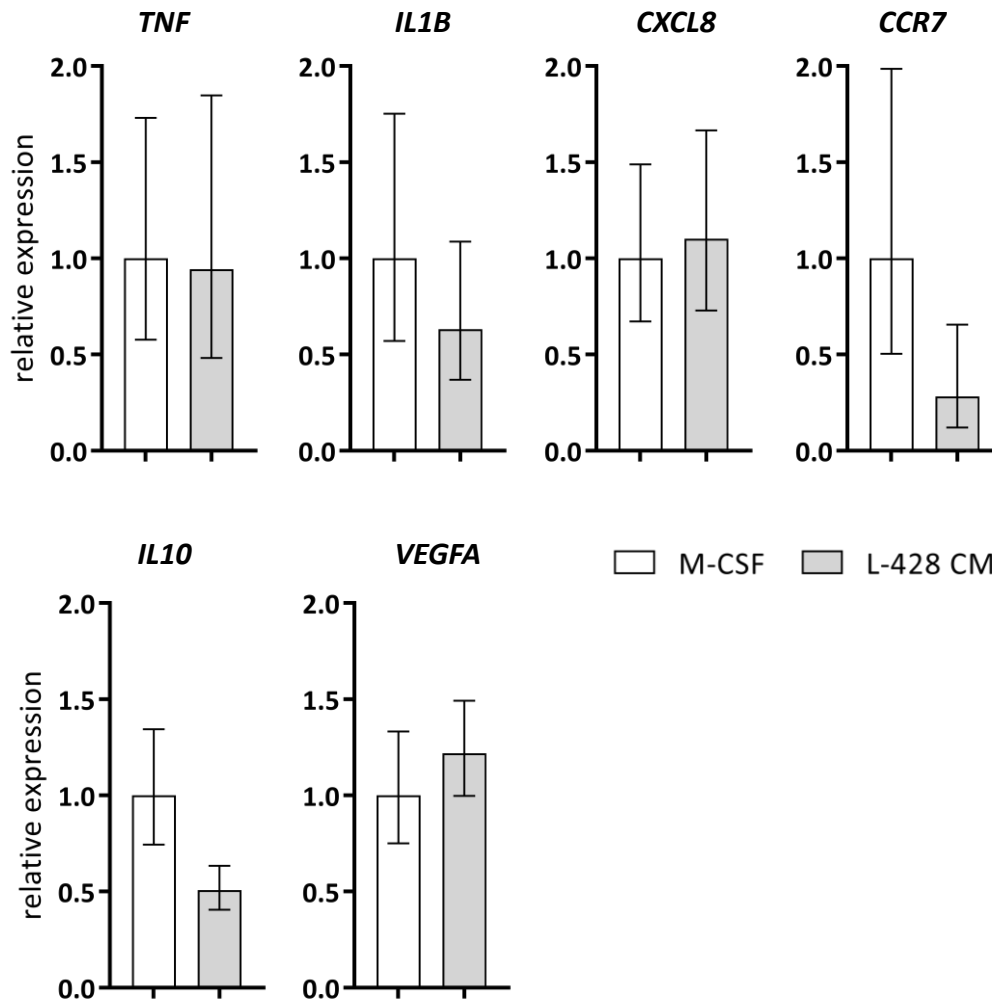
Figure 8: Gene expression of selected markers shows no differences between M-CSF and L-428 CM derived macrophages.

Macrophages were differentiated in Teflon coated cell culture bags with either 2.5 ng/ml M-CSF or L-428 CM. Macrophages were extracted from the cell culture bags after 7 d and plated on cell culture dishes. After 3 h non-adherent cells were washed off the dish and adherent were immediately lysed for RNA extraction and gene expression analysis by qRT-PCR. Expression is relative to *GAPDH* and M-CSF macrophages (mean ± SD, n = 12).

3.3.3 Transcriptional changes in L-428 CM derived macrophages compared to M-CSF and HBL-1 CM derived cells

We used a second approach to characterize differentiated macrophages in detail by detecting genome wide gene expression changes. Monocytes from three different donors were differentiated with L-428 CM, M-CSF and HBL-1 CM and gene expression was measured by RNA-Seq. In order to define which genes are altered in their expression the top differentially expressed genes were extracted based on their Log_2FC being ≥ 1 and ≤ -1 in all three donors. In total we found 276 genes to be differentially expressed in L-428 CM compared to M-CSF derived macrophages in the three donors of which the majority, 249 genes, were upregulated and 27 genes were downregulated (Figure 9A).

To gain more insight into the functions of the altered transcripts we performed a gene enrichment analysis and functional annotation clustering using DAVID to identify enriched gene ontology terms and InterPro domains (Figure 9B). We found that the top enriched GO terms and InterPro domains are mainly concerned with leukocyte interactions, antigen processing and presentation, peptidase activity and enrichment in MHC, C-type lectin and peptidase domains. This supports the hypothesis based on the protein expression analysis that L-428 CM derived cells are primed to mediate leukocyte interaction, specifically T cell interactions, indicated by GO terms assigned to biological processes (see full cluster in Figure A-21). Furthermore, several terms are connected to MHC complex and antigen presentation. Among the top terms we also find enrichment in genes whose products are connected to intracellular membranes and enriched domains belong aside from the MHC complex, to C-type lectins and peptidase. This hints toward endocytic processes, that could either serve antigen presentation or matrix degradation.
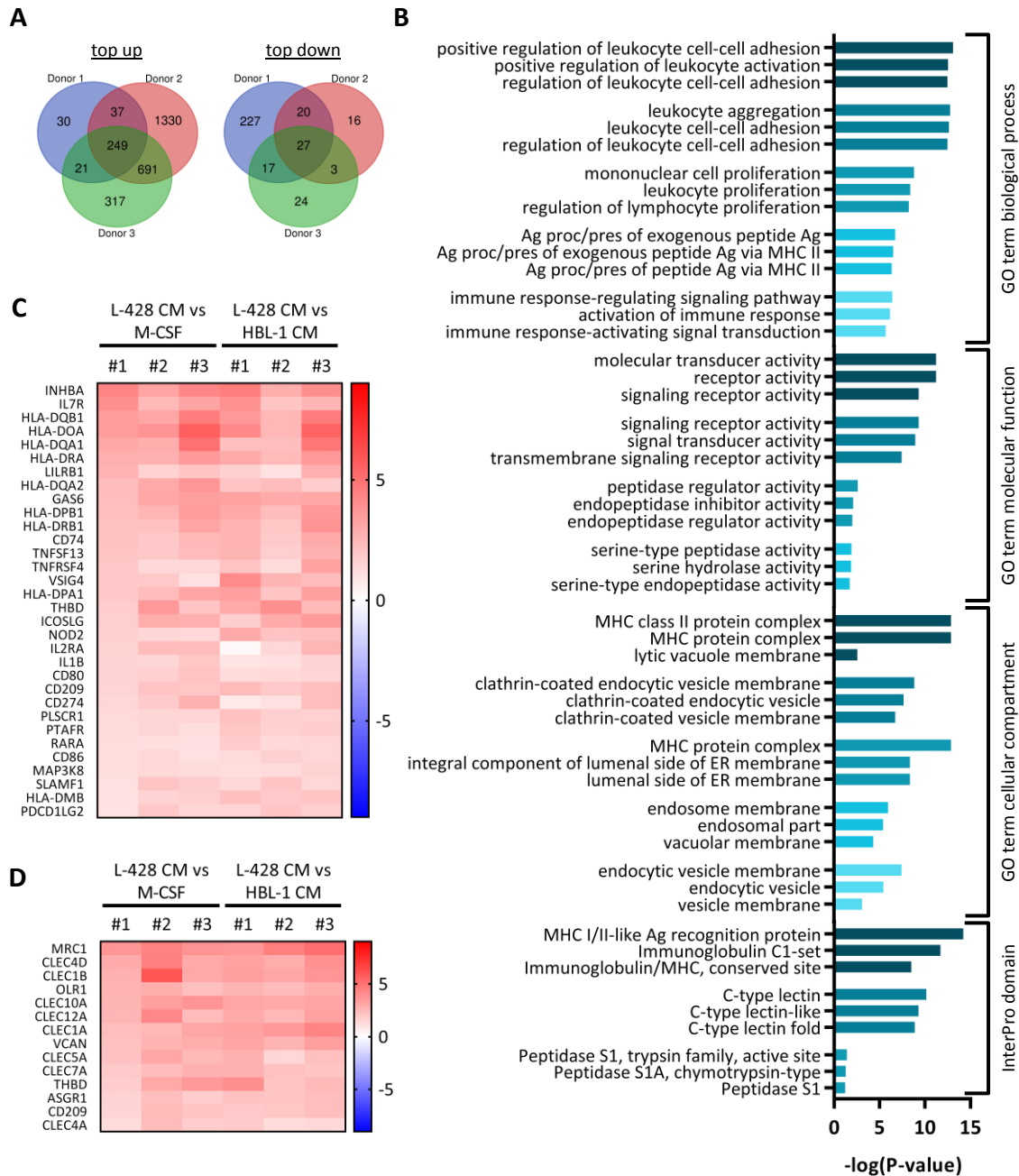
Figure 9: Global gene expression analysis reveals upregulation of genes in L-428 CM derived macrophages involved in leukocyte activation, antigen presentation and endocytosis.

(A) Venn diagrams of upregulated and downregulated genes in L-428 CM derived macrophages compared to M-CSF derived cells from three donors. (B) GO term and InterPro enrichment analysis calculated by DAVID online annotation tool for the overlap in (A) is shown. The top five clusters by enrichment score and their three top terms by P-value are depicted. Complete clusters are shown in the appendix Figure A-21 and Figure A-22. (C) Heatmap of differentially expressed genes in L-428 CM derived macrophages compared to M-CSF and HBL-1 CM derived cells from three donors (#1, #2, #3) assigned to the first GO term biological process cluster (D) Heatmap of differentially expressed genes assigned to the InterPro C-type lectin cluster.

Figure 9C shows the heatmap of genes annotated to the leukocyte activation cluster. Among them we find a striking number of HLA genes and additionally a number of co-stimulatory and -inhibitory molecules such as *CD80*, *CD86* and *CD274* (PD-L1). It has to be argued though that some of these were analyzed for their surface expression such as HLA-DR, CD80, CD86 and PD-L1 and we found only CD80 and PD-L1 to be increased on L-428 CM derived macrophages compared to M-CSF derived cells. This means the identification of upregulated genes by RNA-Seq does not per se correlate with enhanced protein expression. However, the number of upregulated genes that have been identified to be involved in leukocyte interaction and antigen presentation strongly indicates the functional relevance of L-428 CM derived macrophages in leukocyte and T cell communication.

Figure 9D depicts the genes annotated to the C-type lectin cluster. Here we find as the top upregulated gene *MRC1* which is in accordance with the strong induction of CD206 on the surface of L-428 CM educated macrophages compared to M-CSF cells. Additionally, several C-type lectin-like domain-containing proteins (CLEC) are upregulated in L-428 CM derived macrophages. This suggests enhanced carbohydrate binding and uptake of the cells.

Interestingly, we find most genes differentially expressed in L-428 CM differentiated macrophages compared to M-CSF derived cells are up- and downregulated the same way compared to HBL-1 CM derived cells. Thus, the proposed functions might be a specific feature of cHL educated macrophages.

Overall, the global analysis of transcriptional changes supports the view that L-428 CM derived macrophages have been primed to fulfill function in leukocytes, especially T cell interactions, and have altered endocytic behavior accounting for antigen uptake or matrix degradation.

3.4 Functional properties of L-428 CM and M-CSF derived macrophages

3.4.1 L-428 CM and M-CSF differentiated macrophages can be repolarized toward the M1 type

Macrophages are known to expose a high plasticity reacting to various stimuli leading to changes in their phenotype and behavior. However, there is still some controversy about whether switching from any phenotype to another is possible under any given circumstance or

if fully activated cells rather undergo apoptosis. In order to test whether L-428 CM derived macrophages can still react toward danger signals and switch to an M1 phenotype LPS and interferon-γ (IFN-γ) were applied on L-428 CM and M-CSF differentiated cells. Stimulation led to the upregulation of all classical M1 markers in both macrophage types and almost to the same extent (Figure 10). This indicates that the cells possess the plasticity to switch into other phenotypes here namely toward M1 activation.
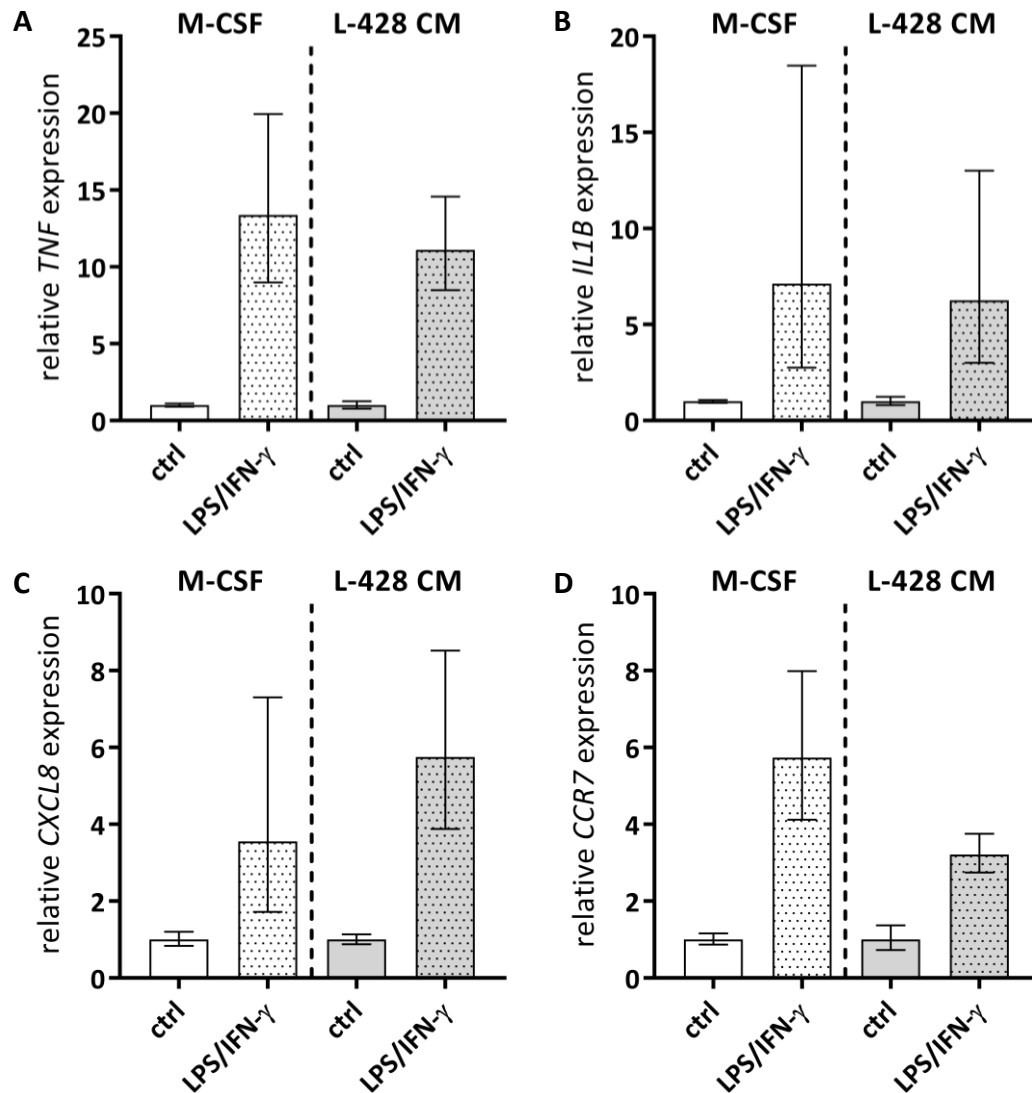
Figure 10: M-CSF and L-428 CM differentiated macrophages can be activated toward the M1 type.

Macrophages were differentiated in Teflon coated cell culture bags with either 2.5 ng/ml M-CSF or L-428 CM mixed with equal volumes of fresh medium. Macrophages were extracted from the cell culture bag after 7 d and plated on cell culture dishes. After 3 h non-adherent cells were washed off the dish and adherent cells were stimulated with 100 ng/ml LPS and 10 ng/ml IFN-γ for 24 h. Gene expression analysis was measured by qRT-PCR. Expression is relative to *GAPDH* and untreated control cells (mean ± SD, n = 12).

3.4.2 Endocytosis of specific targets is enhanced in L-428 CM macrophages

Several markers were shown to be upregulated in L-428 CM derived macrophages compared to M-CSF derived cells (section 3.3.1). This includes CD11c, that belongs to the integrin family regulating matrix cell interactions, and the tested adhesion markers, CD33, CD44 and CD54. The highest differential expression was observed for the mannose receptor CD206 which is binds to various substrates leading to their ingestion. Analysis of global gene expression changes between L-428 CM derived macrophages and M-CSF cells, additionally showed an enrichment of genes that are involved in antigen processing, localized in the endocytic compartment and an enrichment of C-type lectin domains. Taken together this hints toward an altered endocytic capacity of L-428 CM derived macrophages.
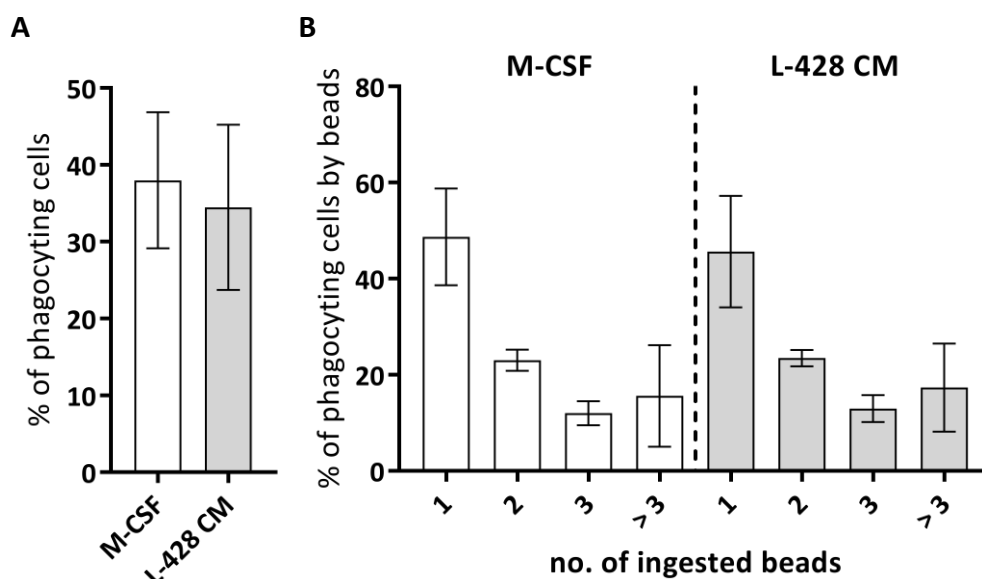
Figure 11: No differences in the uptake of polar beads between M-CSF and L-428 CM derived macrophages.

Macrophages were differentiated in Teflon coated cell culture bags with either 2.5 ng/ml M-CSF or L-428 CM mixed with equal volumes of fresh medium. Macrophages were extracted from the cell culture bag after 7 d and plated on cell culture dishes. After 3 h non-adherent cells were washed off the dish and adherent cells were incubated with 5 Latex beads per cell for 2 h at 37°C or on ice. Fluorescence was measured by flow cytometry. Amounts of phagocyting cells and distribution of ingested beads were calculated by subtracting percentages of cells kept on ice from cells incubated at 37°C (mean ± SD, n = 12).

To test whether L-428 CM educated macrophages are characterized by different endocytic capacities compared to M-CSF differentiated cells different endocytosis assays were applied. First carboxylate modified fluorescently labeled latex beads were used to monitor the phagocytic activity. The weak negative charge on the surface of the beads leads to binding of

positively charged proteins of the surrounding medium and the accumulation of water molecules. Therefore several pathways for detection and ingestion can be triggered by these beads. Figure 11 shows the uptake of beads by L-428 CM and M-CSF derived macrophages. There are no differences in the percentage of cells taking up latex beads. The distinct size of the beads furthermore allows the discrimination of how many beads have been taken up as the increasing fluorescence intensity with each bead is resolved in distinct peaks. However, also the numbers of beads ingested does not differ between L-428 CM and M-CSF derived macrophages suggesting that overall the ability for the uptake of particles is not altered.
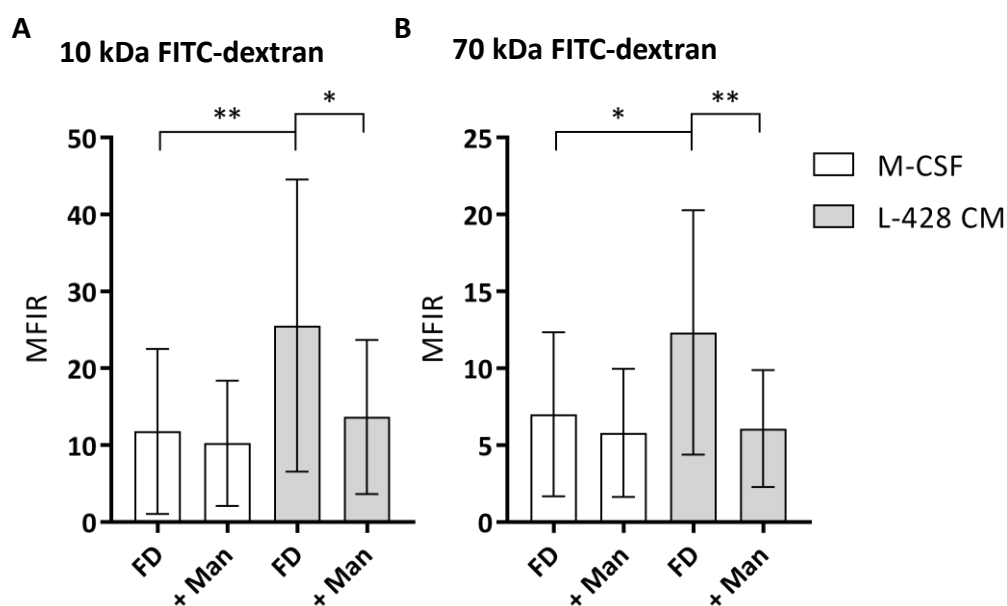
Figure 12: Uptake of FITC-dextran is enhanced in L-428 CM derived macrophages compared to M-CSF cells.

Macrophages were differentiated in Teflon coated cell culture bags with either 2.5 ng/ml M-CSF or L-428 CM mixed with equal volumes of fresh medium. Macrophages were extracted from the cell culture bag after 7 d and plated on cell culture dishes. After 3 h non-adherent cells were washed off the dish and adherent cells were incubated with 1 mg/ml 10 kDa or 70 kDa FITC-dextran for 2 h at 37°C or on ice. For blocking mannose was given 10 min prior to dextran. Fluorescence was measured by flow cytometry. Mean fluorescence intensity ratios (MFIR) were calculated dividing the MFI of a 37°C sample by the MFI of the corresponding sample kept on ice (mean ± SD, n = 12, paired one-way ANOVA with Bonferroni's post-test).

Since L-428 CM cells showed a strong induction in CD206 we hypothesized that the uptake of sugars could be increased in these cells because of enhanced target binding. CD206 is a mannose receptor but has been described to bind other sugars as well. In DCs an increased uptake of dextran was connected to CD206 expression on these cells (Kato et al. 2000). Therefore, we applied labeled 10 and 70 kDa size dextran on macrophages and measured the

uptake by flow cytometry. As mannose still has a higher binding affinity to CD206 in parallel unlabeled mannose was added prior to dextran to test whether it blocks the dextran uptake. Macrophages differentiated with L-428 CM ingested significantly more dextran than M-CSF derived cells (Figure 12). Additionally, the uptake could be partially blocked in the presence of mannose indicating that indeed the higher dextran ingestion is mediated by CD206. Different dextran weights were used for this assay suggesting that several endogenous molecules can be affected as tested here within a range of 10 kDa to 70 kDa.

In conclusion, M-CSF and L-428 CM derived cells possess similar properties concerning the uptake of particles as seen by the ingestion of beads with non-specific surface labeling. The uptake of CD206 specific targets, however, is enhanced in L-428 CM derived cells, which is in accordance with their high surface expression.

3.4.3 Collagen uptake is enhanced in L-428 CM derived macrophages and macrophages secret high amounts of MMP-9

Beside the uptake of sugars CD206 was described to contribute to the collagen uptake in murine bone marrow derived macrophages (section 1.2.2). Thus, we used labeled gelatin to investigate if the uptake of collagen differs between M-CSF and L-428 CM differentiated macrophages. As expected the collagen uptake was significantly higher in L-428 CM derived cells than in M-CSF cells (Figure 13A). The enhanced uptake of collagen suggests that the upregulation of CD206 in macrophages by L-428 CM could be an important aspect of matrix remodeling in cHL. Hence, we analyzed the secretion of matrix metalloproteinase (MMP)-9 and MMP-2 by zymography using gelatin containing gels. MMP-2 was not detected. MMP-9 was detected and is secreted by macrophages, but there was no differential expression between M-CSF and L-428 CM educated cells (Figure 13B). However noteworthy is that in comparison to L-428 cells itself macrophages secret very high amounts of MMP-9. Both findings indicate that L-428 CM associated macrophages could play a role in tissue reorganization.
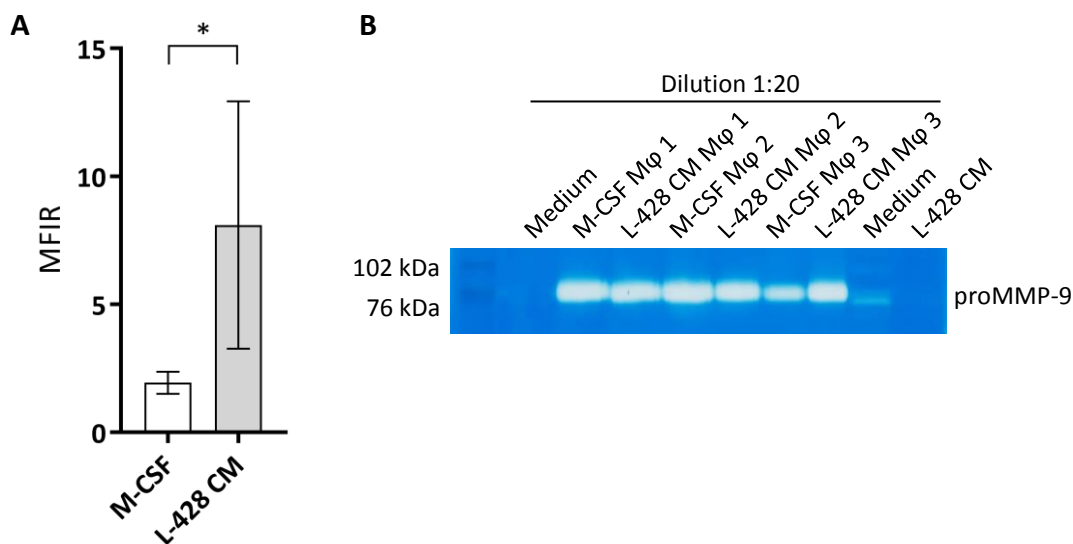
Figure 13: Collagen uptake is enhanced in L-428 CM derived macrophages and macrophages secret high amounts of MMP-9.

(A) Macrophages were differentiated in Teflon coated cell culture bags with either 2.5 ng/ml M-CSF or L-428 CM mixed with equal volumes of fresh medium. Macrophages were extracted from the cell culture bag after 7 d and plated on cell culture dishes. After 3 h non-adherent cells were washed off the dish and adherent cells were incubated with 5 μg/ml gelatin OG-488 conjugate for 30 min at 37°C or on ice. Fluorescence was measured by flow cytometry. Mean fluorescence intensity ratios (MFIR) were calculated dividing the MFI of a 37°C sample by the MFI of the corresponding sample kept on ice (mean ± SD, n = 5, paired t-test, two-tailed) (B) MMP-9 levels in macrophage and lymphoma CM were analyzed by zymography.

3.4.4 Co-culture of L-428 cells and macrophages in an *in vivo* chorion allantois membrane assay leads to altered tumor formation

A direct co-culture of cHL cells and macrophages was applied to investigate the tumor formation in a CAM assay. L-428 cells alone or with macrophages were suspended in a collagen gel and applied on the CAM of chicken eggs. After four days by macroscopic examination tumor size and vascularization can be determined. Histological processing and immunohistochemical staining of tumors show the intratumoral structure and organization of cells. Figure 14A shows representative images of tumors formed on the CAM and trichrome stained tumor sections. By visual inspection the co-culture tumors appear to be smaller with less hemorrhages. In the stained tumor sections we found that the co-culture tumors are furthermore less densely packed with cells than the L-428 tumors. We measured the tumor areas and scored the hemorrhages which confirmed these observations (Figure 14B+C).

Peroxidase staining of CD30 and CD68 on tumor sections show a compartmentalization of the tumor (Figure 14D). CD30 positive L-428 cells are located in the upper and lower parts of the tumor but are almost absent in the central area. CD68 positive macrophages dominate the upper and central part and are mainly present in the remaining collagen gel and in close proximity to it. In the L-428 tumor the cells are evenly distributed throughout the tumor.
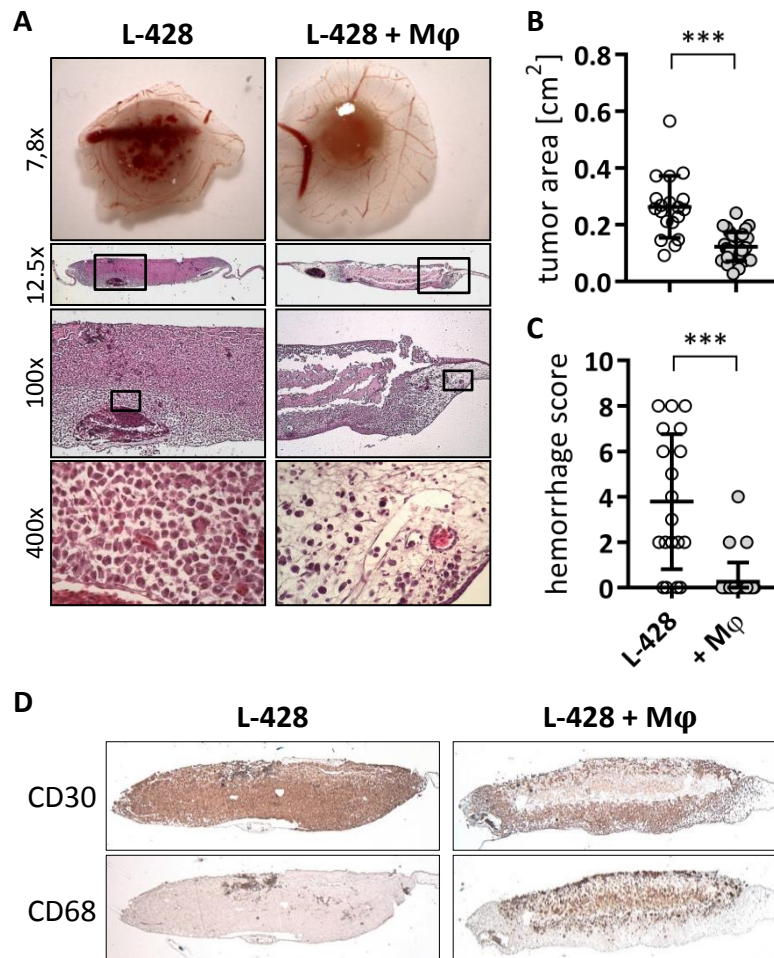
Figure 14: Addition of macrophages alters tumor formation of L-428 cells in an *in vivo* CAM assay.

(A) Representative stereomicroscopic (7.8x magnification) and trichrome stained pictures of L-428 and L-428 CM derived macrophages (Mφ). Rectangles indicate the magnified area of the image. (B+C) Tumor area and hemorrhage score were quantified from stereomicroscopic images (mean ± SD, L-428: n = 19, L-428 + Mφ: n = 31, B: two-tailed t-test with Welsh's correction, C: Mann-Whitney test). (D) Representative CD30 and CD68 peroxidase stained images of L-428 tumor with and without macrophages (12.5x magnification).

In conclusion, we found an altered tumor formation when adding macrophages to L-428 cells in a CAM assay but contrary to the expectation we found the co-culture tumors to be smaller with less bleedings and less cells in the tumor mass. The structural differences in the tumors

indicate a mutual interaction of L-428 cells with macrophages and support the proposed function of macrophages in tissue remodeling processes. However, the significance is unclear, since macrophages are not beneficial for the tumor growth in this CAM assay by means of the tumor size.

3.5   CD206 expression on L-428 CM derived macrophages

In the previous section we described a high expression of CD206 on L-428 CM derived macrophages compared to M-CSF derived cells. Additionally, we observed enhanced endocytic activity connected to this increased expression. Therefore we aimed to identify potential factors in cHL CM that can induce CD206 expression on macrophages.

3.5.1   IL-13 induces gene and cell surface expression of CD206

A characteristic and distinguished feature of cHL is the secretion IL-13 (Skinnider et al. 2002). Additionally, macrophages are known to be polarized toward an M2 phenotype by IL-13 which includes an upregulation of CD206. Hence, we questioned if high CD206 expression is a direct result of IL-13 stimulation which is produced by cHL cells. We isolated and stimulated monocytes with M-CSF and IL-13 or a combination in direct comparison to L-428 CM stimulated cells. Figure 15A shows the result for *MRC1* (CD206) gene expression after 6 h, 24 h and 7 d of stimulation. As already seen in section 3.3.1 CD206 is not expressed on the cell surface of monocytes. There is also no detectable gene expression in unstimulated and M-CSF stimulated monocytes after 6 h. Interestingly, gene expression of CD206 can be found after 24 h in these cells suggesting there is an endogenous factor that can trigger the expression. IL-13 stimulation results in an induction of *MRC1* expression leading to its detection after 6 h, expression is further enhanced after 24 h and downregulated after 7 d. Notably, addition of M-CSF does affect CD206 expression neither alone nor in combination with IL-13. L-428 CM shows the same pattern like IL-13 stimulation, however, CD206 expression is about ten times higher after 6 h and two times higher after 24 h. Since the used concentrations of IL-13 is with 10 ng/ml higher than published concentrations measured in L-428 CM it is most likely that the induction in CD206 gene expression is not solely due to secreted IL-13 but other factors in the CM also activate CD206 gene expression (Kapp et al. 1999).
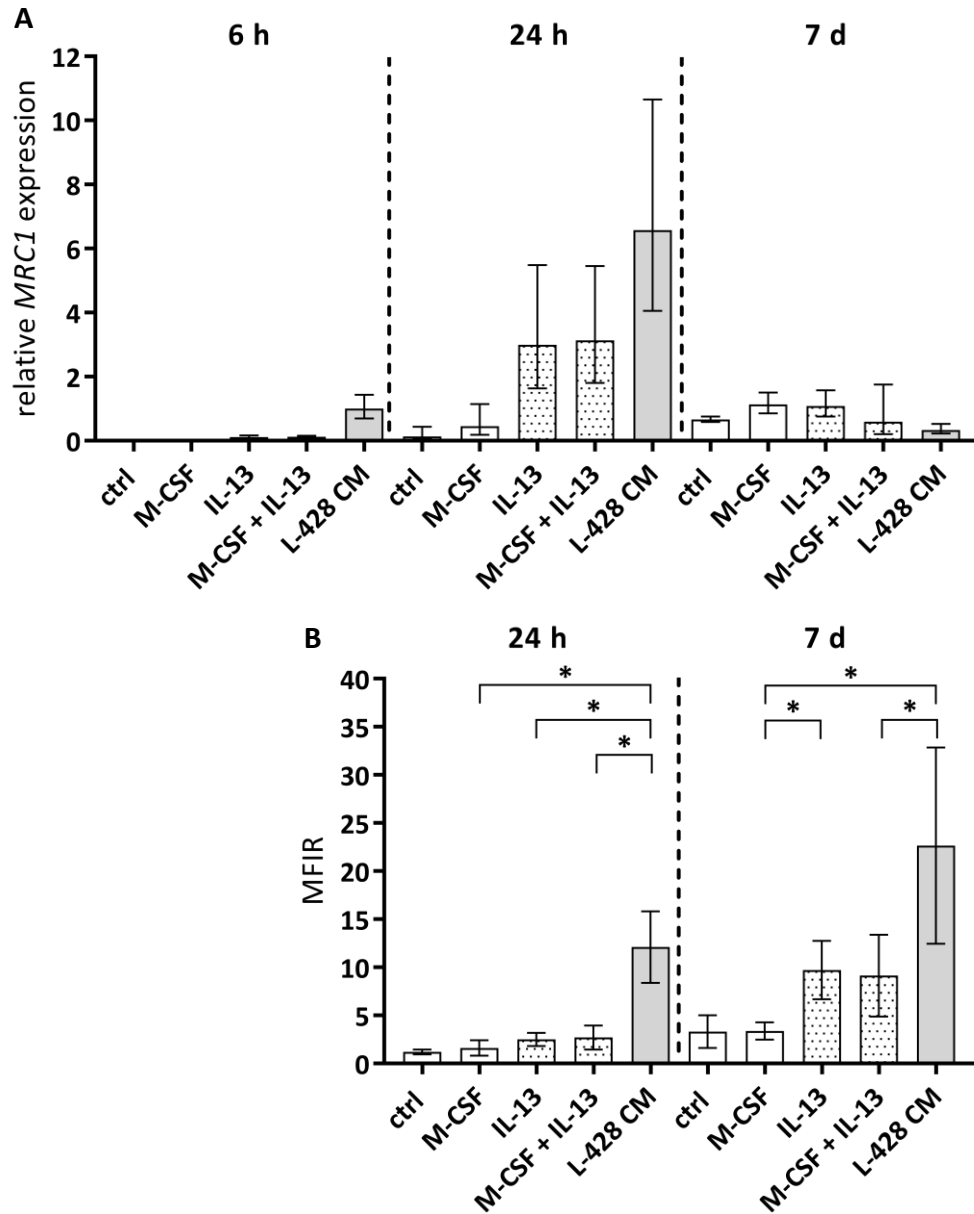
Figure 15: CD206 gene and surface expression is induced by IL-13 and L-428 CM.

(A) Monocytes were stimulated with 2.5 ng/ml M-CSF, 10 ng/ml IL-13 or both or L-428 CM for the indicated time. Gene expression of *MRC1* was analyzed by qRT-PCR. Expression is relative to *GAPDH* and L-428 CM treated cells (mean ± SD, n = 5). (B) Monocytes were seeded in Teflon coated cell culture bags with 2.5 ng/ml M-CSF, 10 ng/ml IL-13 or both or L-428 CM mixed with equal volumes of fresh medium. Aliquots were taken at the indicated time points and stained for CD206 expression. MFIRs were calculated by dividing the MFI of CD206 by the MFI of the isotype control (mean ± SD, n = 6, paired one-way ANOVA with Bonferroni's post-test).

CD206 surface expression was also measured after 24 h and 7 d (Figure 15B). In concordance with the findings of *MRC1* gene expression levels surface expression is increased in IL-13 and

L-428 CM treated cells after 24 h but not in untreated controls or M-CSF stimulated cells. Again in L-428 CM treated cells the CD206 expression is higher than in IL-13 treated cells by about four times. The expression is further increased after 7 d and at that time point also measurable in unstimulated and M-CSF treated cells. In general the expression pattern seen after 24 h is repeated with low expression on untreated and M-CSF treated monocytes, higher expression on IL-13 treated cells and highest expression on L-428 CM treated cells. In combination with the measured gene expression this suggests that CD206 accumulates on the cells surface while the transcription is down regulated.

To conclude, IL-13 but nor M-CSF activates CD206 gene expression in monocytes within 6 h which is otherwise absent in these cells. L-428 CM does the same, however, to a much greater extent. The expression increases further within 24 h and is at that time point also measurable in unstimulated and M-CSF treated cells. The CD206 surface expression largely resembles this gene expression pattern at 24h with increasing expression from day 1 to day 7. These findings indicate that IL-13 indeed might be a factor in L-428 CM that up-regulates CD206 expression, however, other factor must be involved in this process leading to a higher expression of CD206 in L-428 CM treated compared to IL-13 treated monocytes.

3.5.2 *MRC1* expression is abolished in monocytes treated with JAK inhibitors

IL-13 is known to bind to a heterodimer of IL-4 receptor α (IL4Rα) and IL-13 receptor α (IL13Rα) which is associated intracellularly with Janus kinase (JAK)1, JAK2 and tyrosine kinase 2 (TYK2) (Bhattacharjee et al. 2013). Therefore we used two JAK inhibitors namely Pyridone-6 which inhibits JAK1, JAK2, JAK3 and TYK2 and Ruxolitinib which inhibits JAK1 and JAK2 to test whether *MRC1* expression can be blocked in IL-13 and L-428 CM treated cells. Clearly, *MRC1* expression is present after 6 h only in IL-13 and L-428 CM treated cells and remains absent in cells treated with a JAK inhibitor (Figure 16). As mentioned in the previous section other factors than IL-13 in L-428 CM are likely to be involved in CD206 induction. However, also in L-428 CM treated cells *MRC1* expression is blocked after JAK inhibition. Hence, JAK1 and JAK2 activity is essential for induction of *MRC1* gene expression and additional factors in L-428 CM induce the expression in an JAK1 or JAK2 dependent manner.
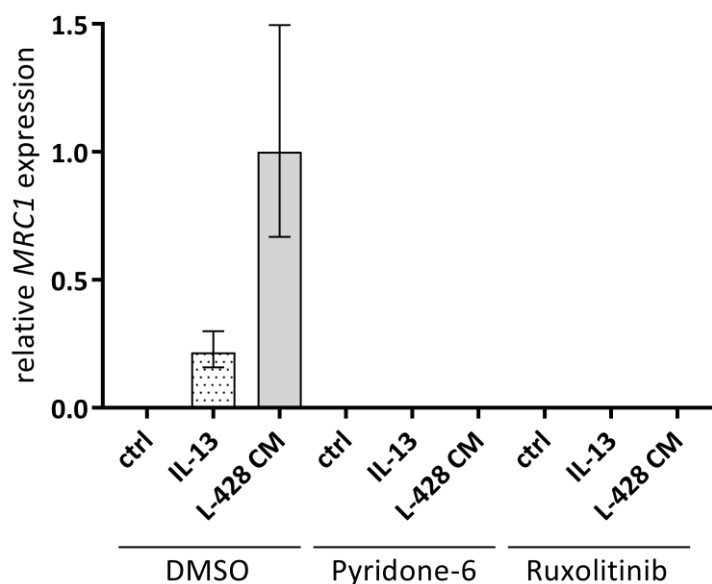
Figure 16: Inhibition of JAKs prohibits *MRC1* expression in monocytes.

Monocytes were preincubated with DMSO or inhibitors for 1 h before 10 ng/ml IL-13 or L-428 CM was added for 6 h. Gene expression of *MRC1* was analyzed by qRT-PCR. Expression is relative to *GAPDH* and L-428 CM treated cells (mean ± SD, n = 6).

3.5.3   CD206 expression after stimulation with cHL and DLBCL CMs

We further tested the five cHL and two DLBCL cell lines used in section 3.1 and 3.2 if an induction of CD206 expression can be observed (Figure 17A). The CMs derived from L-428, L-540, HDLM-2 and L-1236 could all induce *MRC1* expression in monocytes after 6 h. Strongest effects on *MRC1* expression occurred after L-428 and L-1236 CM stimulation whereas cells stimulated with L-540 and HDLM-2 CM expressed about one fifth to one tenth less *MRC1*. However, also in these cells the *MRC1* expression is detectable while it is absent in unstimulated cells as well as in cells stimulated with KM-H2, HBL-1 or OCI-LY3 CM.
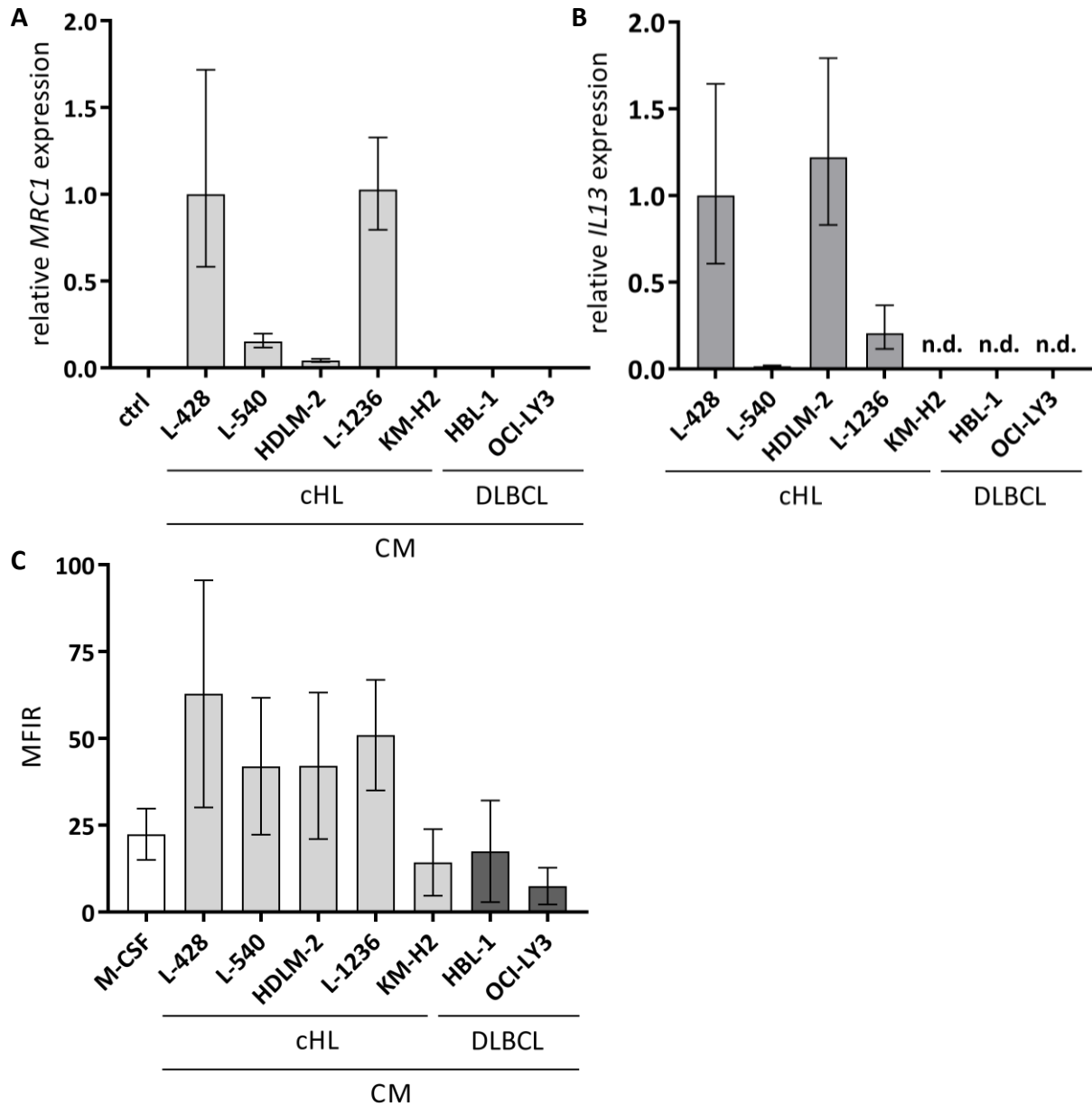
Figure 17: Monocytes increase CD206 gene and surface expression after stimulation with cHL CM.

(A) Monocytes were stimulated with cHL CM for 6 h. Gene expression of *MRC1* was analyzed by qRT-PCR. Expression is relative to *GAPDH* and L-428 CM treated cells (mean ± SD, n = 6). (B) Gene expression of *IL13* was analyzed in lymphoma cell lines by qRT-PCR. Expression is relative to *GAPDH* and L-428 cells (mean ± SD, n = 3). (C) Monocytes were stimulated with cHL CM for 7 d. CD206 surface expression was analyzed by flow cytometry. MFIRs were calculated dividing the MFI of CD206 by the MFI of the isotype control (mean ± SD, n = 6, paired one-way ANOVA with Bonferroni's post-test).

We next analyzed the gene expression of IL-13 in the cell lines (Figure 17B). Interestingly, in accordance with the induction of *MRC1* expression in monocytes IL-13 expression was only detected in L-428, L-540, HDLM-2 and L-1236 cells but was not detectable in KM-H2, HBL-1

and OCI-LY3 cells. Notably, IL-13 gene expression is highest in HDML-2 while in L-1236 the expression is about 80 % lower though they have opposite effects on the *MRC1* expression in monocytes. The amount of secreted protein does not necessarily reflect the gene expression that means concentrations might still be lower in the HDLM-2 CM than in L-1236 or L-428 CM. However, as stated in the previous section other factors might be involved in the induction of *MRC1* expression. One factor in this context might be GM-CSF which was reported to increase CD206 expression on human monocytes (Däbritz et al. 2015). Interestingly, gene expression of *CSF2* (GM-CSF) was only found in L-428, L-540 and L-1236 but none of the other cell lines and was highest in L-1236 which also showed the strongest induction of *MRC1* expression in monocytes (Figure 5).

Finally, we screened the CM treated monocytes for CD206 expression on the cell surface after 7 d. Figure 17C shows the results of the flow cytometric analysis. As already observed after 7 d all differentiated macrophages express CD206 on the cell surface. A higher expression of CD206 is seen on cell treated with the four cHL CMs that also induced the gene expression after 6 h compared to M-CSF treated cells and the remaining three CM that induced no CD206 expression initially. However the differences in the CD206 gene expression after 6 h, namely high induction in L-428 and L-1236 CM stimulated cells compared to lower induction L-540 and HDLM-2 CM stimulated cells, is not further reflected. There is only a tendency for HDLM-2 and L-540 treated cells to express less CD206.

In conclusion, we showed that four out of five cHL CMs can induce CD206 gene expression in monocytes. Notably, these four cell lines were expressing *IL13*. Additionally, three of these cell lines also express *CSF2* which has been described to induce CD206 gene expression. Finally, macrophages that were derived from CM of these four cHL cell lines express more CD206 on their cell surface.

3.6 Recruitment of macrophages and repolarization by lymphoma secreted factors

As mentioned in section 3.1 several mechanisms of how macrophages reach the TME are proposed and we showed that monocyte recruitment might be one possible way. We also tested whether macrophages could be attracted by lymphoma secreted factors as well.

Therefore we differentiated macrophages using M-CSF and assessed the migration toward lymphoma CM in Boyden chamber assays (Figure 18A). First, there is a measurable migration of cells without addition of chemoattractants which was absent in monocytes. Additionally, the migration toward 10 % FCS is relatively low, hence, FCS is not as attractive for macrophages as for monocytes and directed movement rather requires specific chemoattractants. Movement toward L-428 and L-1236 CM was again highest as it was seen for monocyte whereas movement toward HBL-1 and OCI-LY3 CM is lower, however, it is still higher than toward FCS indicating that DLBCL cells secret chemoattractants as well.
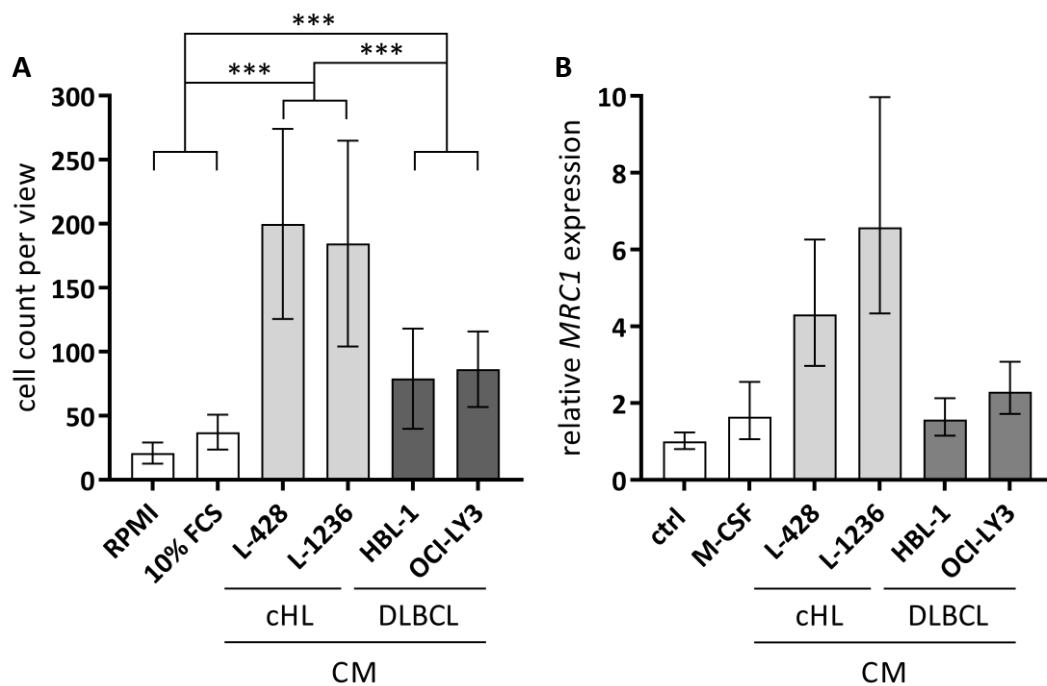
Figure 18: Macrophages migrate toward lymphoma CM and increase CD206 gene expression after stimulation with cHL CM.

(A) Macrophage migration toward different lymphoma CMs was measured in a Boyden chamber assay with collagen coated 5 μm porous membranes for 2 h (means ± SD, n = 6, one-way ANOVA with Bonferroni's post-test). (B) Macrophages were stimulated with lymphoma CM for 24 h. Gene expression of *MRC1* was analyzed by qRT-PCR. Expression is relative to *GAPDH* and L-428 CM treated cells (mean ± SD, n = 4).

Since we saw a strong induction of CD206 with cHL CM we tested if macrophages also increase the *MRC1* expression in the presence of cHL CM meaning if they can be repolarized after recruitment by HL cells (Figure 18B). We observed an increased expression of *MRC1* in

macrophages after stimulation with cHL CM and an unaltered gene expression with DLBCL CM.

Taken together, both findings hint toward an attraction and repolarization of fully differentiated macrophages by cHL cells resulting in an increased CD206 expression in these cells. Besides also DLBCL cells secret factors that attract macrophages.

4   Discussion

The aim of this study was to investigate the recruitment and activation of macrophages by lymphoma derived factors. We found that cHL cells attract and differentiate monocytes in high numbers. Additionally, macrophages were attracted and repolarized by cHL CM. A distinguished feature of cHL derived macrophages was a high CD206 expression accompanied by high endocytic uptake of CD206 substrates. Furthermore, we found that IL-13 contained in cHL CM could be one factor that leads to high CD206 expression. The impact of these findings for cHL development and progression will be discussed below.

4.1   Recruitment and differentiation of macrophages by lymphoma secreted factors

4.1.1   Recruitment of monocytes and macrophages by chemoattractants in lymphoma CM

In this study we found that monocytes as well as macrophages actively move toward lymphoma CM in Boyden chamber assays. This is in concordance with previous findings indicating active recruitment of monocytes or macrophages into the tumor by tumor cell secreted factors (Estko et al. 2015; Gazzaniga et al. 2007; Wang et al. 2014; Tripathi et al. 2014). Whether the main source for TAMs *in vivo* is recruitment of circulating monocyte or tissue resident macrophages is still discussed. Several studies carried out in mice proposed that mainly monocytes are recruited by tumor cell derived CCL2 (Tymoszuk et al. 2014; Alonso-Nocelo et al. 2018; Franklin et al. 2014). Interestingly, L-428 and HBL-1 cells analyzed by RNA-Seq showed no expression of *CCL2* and no *CCR2* expression was detectable in CM or M-CSF derived macrophages. Loss of CCR2 on *in vitro* M-CSF differentiated human macrophages was reported before and here also occurred after CM treatment though HBL-1

65

cells had no detectable M-CSF (Sierra-Filardi et al. 2014). There is currently no evidence for the presence of CCR2^{+} tissue resident macrophages in humans but their occurrence was demonstrated in mice (Li et al. 2016; Conrad et al. 2007; Wei et al. 2016). In tumor sections of cHL *CCL2* mRNA was detected and human primary monocytes express CCR2 on their surface (Luciani et al. 1998; Appleby et al. 2013). Thus, recruitment of monocytes via CCL2-CCR2 interactions might still play a role *in vivo*, but in these experiments cannot explain their attraction by L-428 and HBL-1 CM and in general the attraction of macrophages. Other chemokines that are expressed by these cell lines and could attract monocytes or macrophages include chemokine (C-X3-C motif) ligand 1 (*CX3CL1*) by both cell lines and *CCL5* by L-428 cells. CX3CL1 has been found to be expressed in several cancers such as neuroblastoma, colorectal cancer and chronic lymphocytic leukemia (Ferretti et al. 2014). Its receptor chemokine (C-X3-C motif) receptor 1 (CX3CR1) is expressed on CD14^{+} monocytes and CX3CL1 has been shown to attract monocytes to inflammatory sites (D'Haese et al. 2010). Its role in the recruitment of monocytes to the tumor site, however, remains unclear. Importantly, CX3CL1 can exist in a membrane-bound and a soluble form. Expression of the membrane-bound form on tumor cells mediates direct cell-cell interactions with the microenvironment (Ferretti et al. 2011). In order to be chemotactic the ligand must be released from the cell surface. Shedding of CX3CL1 from the membrane is mediated by ADAM10 and ADAM17, both genes are also expressed by L-428 and HBL-1 cells (data not shown). Therefore the occurrence of the soluble form in lymphoma CM can be assumed which would lead to an attraction of monocytes. CCL5 has been previously found to be expressed in cHL cell lines as well as in tumor sections of cHL and was proposed to attract mast cells to the tumor (Maggio et al. 2002; Fischer et al. 2003). It is also known to attract monocytes, notably, Met-RANTES, a chemokine receptor antagonist, was found to suppress the CCL5 dependent recruitment of monocytes in transplant mice models (Gröne et al. 1999; Stojanovic et al. 2002). As CCL5 secretion was already shown in several Hodgkin cell lines it can be proposed that it led to the attraction of monocytes in our experiment which could be further tested by the introduction of Met-RANTES into the experimental setup. It could also play a role in *in vivo* recruitment of monocytes in cHL as it was detected in patient samples. Beside chemokines other factors have been shown to be chemoattractants for monocytes or macrophages. Notably, M-CSF which is expressed by all cHL cell lines were shown to be chemotactic for monocytes and macrophages (Pixley 2012). Additionally, TNF-α and VEGF-A were found to

attract monocytes or macrophages and are also expressed by L-428 and HBL-1 cells (Ming et al. 1987; Barleon et al. 1996; Yang et al. 2004).

Taken together, our results show that cHL cells and also DLBCL cells produce factors to attract monocytes and macrophages into their environment. Potentially a mixture of various factors account for the attraction of monocytes and macrophages in these experiments. The widely proposed CCL2-CCR2 axis does not play a role in this context for the attraction of macrophages or attraction of monocytes by L-428 CM. Since we observed migration of both cell types toward lymphoma secreted factors, whether the occurrence of TAMs *in vivo* results from attraction of circulating monocytes or tissue macrophages cannot be concluded, both mechanisms are possible.

4.1.2   Differentiation of monocytes into macrophages by lymphoma derived factors

A key finding of this study is that differentiation of monocytes into macrophages can occur in the presence of lymphoma CM and is especially promoted by cHL CM. The differentiation of macrophages by lymphoma secreted factors is in concordance with *in vitro* studies of other entities such as small cell lung cancer and pancreatic cancer where the malignant cells likewise secret factors that promote differentiation (Kuen et al. 2017; Hamilton et al. 2016). Additionally, a number of mouse studies found circulating monocytes to infiltrate the tumor thereby differentiating into macrophages (Afik et al. 2016; Madsen et al. 2017; Franklin et al. 2014). In our experiments strikingly high macrophage amounts were found after differentiation with cHL CMs. We showed that M-CSF a growth factor known to promote macrophage differentiation is highly expressed by cHL cells. Increased M-CSF expression is a feature in several cancers (El-Gamal et al. 2018). Likewise elevated M-CSF serum levels in cHL patients have been reported and HRS cells were found to be M-CSF positive in immunostained tumor sections (Kowalska et al. 2012; Zheng et al. 1999). However, the measured M-CSF amounts in the lymphoma CM and the resulting macrophage numbers also indicated the involvement of other factors to support the differentiation. GM-CSF was expressed by three cHL cell lines in this study and is known to contribute to macrophage differentiation. However, *in vivo* expression was not found on cHL tumor sections (Merz et al. 1991). Another factor known to support macrophage differentiation is VEGF-A (Sato et al. 2008; Yan et al. 2017). VEGF-A was previously reported to be expressed in immunostained cHL patient samples (Doussis-Anagnostopoulou et al. 2002). We also detected *VEGFA* in L-428 and HBL-1 cells. Hence, VEGF-A might account *in vitro* as well as *in vivo* for macrophage differentiation.

Besides promoting the developmental changes and polarization of monocytes toward macrophages factors in the CM might lead to improved survival or proliferation of monocytes. In this context, M-CSF again plays a role as it was shown to induce the proliferation of macrophages (Tymoszuk et al. 2014). IL-6, which is expressed on RNA level by L-428 and HBL-1 cells, was found to improve the survival of cultured monocytes (Roca et al. 2009). Since we also found a certain number of macrophages after differentiation with HBL-1 CM despite the fact that M-CSF was undetectable other factors such IL-6 or VEGF-A could account for these effects. A characteristic cytokine expressed in cHL cells is IL-13 that is also known to promote monocytes survival (McKenzie et al. 1993). Likewise an inhibited apoptosis can lead to high macrophage numbers after differentiation. A study showed that stimulation of monocytes with tumor derived exosomes resulted in impaired caspase activation (Song et al. 2016).

In conclusion, lymphoma cells secret numerous factors to support macrophage differentiation, notably, the expression of M-CSF and *IL13* was found in cHL cells. Besides other factors were found to be expressed by L-428 but also HBL-1 cells that can contribute to differentiation and survival of monocytes. However, the high macrophage numbers yielding from differentiation with cHL CM show that specifically HRS cells secret a strong mixture of factors to support macrophage differentiation indicating a special requirement of these cells in the context of cHL.

4.2 Phenotype and functions of cHL recruited macrophages

4.2.1 Expression of cell surface markers and functional implications

In this study we found that L-428 CM derived macrophages resemble M2 activated mature macrophages by analyses of the expression of several cell surface markers, CD68 and selected genes. This finding is in accordance with published data that widely proposes an M2-state of TAMs (see section 1.1.3). We identified several molecules to be higher expressed on L-428 CM derived macrophages compared to M-CSF derived cells these included CD11c, CD68, CD206, CD1a, CD80, CD40, PD-L1, CD33, CD44 and CD54. Notably, we found the highest differential expression between L-428 CM and M-CSF derived macrophages in CD206. Among the proteins analyzed were several involved in T cell interactions by antigen presentation and co-stimulation/-inhibition, i.e. HLA-DR, CD1a, CD80, CD86, CD40 and PD-L1, of which four were strongly expressed on L-428 CM derived cells. The inhibitory potential of macrophages

on T cell proliferation is a feature of M2 macrophages and was also found in tumor cell educated macrophages (Oishi et al. 2016; Huber et al. 2010; Yue et al. 2015; Lievense et al. 2016; Duluc et al. 2007). The induction of PD-L1 may account for inhibition of cytotoxic T cell activity. Staining of cHL patient samples showed that the majority of tissue PD-L1 was expressed by macrophages and that these cells were surrounded by PD1^{+} T cells which presumably accounted for inhibitory interactions (Carey et al. 2017). Importantly, in our study CD40 a known co-stimulatory molecule was also upregulated in L-428 CM derived cells which rather suggests T cell activating properties. Of note CD40 is a common M1 marker for macrophages. We found L-428 CM derived macrophages to resemble M2 activated cells by the expression of several markers this suggests that M1 features were also acquired and that the cells have a distinct phenotype apart from those conventionally described for M1 or M2 activated cells. Other receptors that interact with ligands on the T cell surface are CD80 and CD86. CD80 was upregulated and CD86 downregulated compared to monocytes. So far these receptors are described to expose redundant functions, whether these are stimulatory or inhibitory depend on the ligands on the T cell surface (Jonker et al. 2002). Thus, the significance of CD80/CD86 expression remains unclear. Interestingly, L-428 CM derived macrophages also expressed CD1a a molecule predominantly present on dendritic cells, but its expression on macrophages has also been described (Coventry & Heinzel 2004; Henkel et al. 2004). It is proposed that CD1a^{+} DCs in the tumor present tumor glycolipids to T cells. Increased antigen presentation usually accounts for T cell activation. Consistent with this clinical studies found the presence of CD1a^{+} DCs to be associated with better prognosis (Coventry & Heinzel 2004). In cHL the presence of CD1a^{+} cells has also been described in one study and the cells have been assigned as DCs without staining of additional lineage markers (Tudor et al. 2014). Thus, so far nothing is known about the occurrence of CD1a^{+} macrophages in tumors.

The notion that L-428 CM derived macrophages are involved in T cell interactions is strongly supported by the global gene expression analysis. Among the genes upregulated in this context were several HLA genes and genes encoding for co-stimulator and -inhibitory molecules such as CD80, CD86 and PD-L1. Again the set of genes found to be upregulated does not allow concluding the definite T cell response. Enhanced antigen presentation accompanied by co-stimulatory as well as -inhibitory signal could account for T cell activation as well as inhibition. Additionally, the differences in gene expression have to be validated whether they

translate into differences in protein expression. This does not necessarily have to be the case as seen e.g. in CD86 which was upregulated on gene expression level in L-428 CM derived cells compared to M-CSF macrophages but this difference was not seen in its surface expression.

Taken together, our data strongly indicates a function of L-428 CM derived macrophages in T cell interaction. This would be in concordance with the observation that T cells are the predominant cellular fraction in the cHL TME. Clinical studies also suggest suppression of T cell function by macrophages. However, from our data the result of their interaction cannot be definitely predicted. Further investigations have to determine the effect of L-428 CM derived macrophages on T cells by applying direct interaction experiments with both cell types.

4.2.2   CD206 expression and endocytic activity of cHL CM derived macrophages

A principal finding of this study is the induction of CD206 expression and the corresponding changes in endocytic activities of cHL CM derived macrophages. Namely, we found the uptake of dextran and collagen was increased in L-428 CM derived cells compared to M-CSF cells which expressed less CD206 on their cell surface. As stated when introducing the mannose receptor family the sugar and collagen binding is mediated by different domains and the bent conformation of the receptor might account for specific binding of glycosylated collagens (see section 1.2.1). Thus, the enhanced endocytic activity could under physiological conditions account for binding and uptake of specific glycosylated collagens. Additionally, on L-428 CM derived macrophages we found a higher expression of adhesion molecules, i.e. CD11c, CD33, CD44 and CD54 compared to M-CSF derived cells. This further indicates that L-428 CM macrophages might expose functions in matrix interaction and organization. Matrix remodeling is a common process in tumor development and the tumor stroma is characterized by profound proteolytic degradation (Luciani et al. 1998). In a mouse model of lung cancer it was shown that matrix degradation and subsequent collagen uptake by macrophages was partly dependent on CD206 (Madsen et al. 2017). In addition to the high uptake of CD206 substrates in cHL CM derived cells we found high MMP-9 secretion, yet not increased compared to M-CSF derived cells. These findings suggest that matrix remodeling by macrophages might also be functionally relevant in cHL. Altered matrix composition has been shown to account for tumor growth and metastasis. A study found that matrix stiffness can modulate cancer cell proliferation in an *in vitro* 3D model (Alonso-Nocelo et al. 2018). Additionally, degradation of the basal membrane by macrophages is an important step in

cancer cell extravasion as seen in a mouse model of mammary tumors (Wang et al. 2002). Using direct co-culture of L-428 cells with macrophages in a CAM assay we found tumors to be smaller. Stained sections revealed that co-culture tumors contained fewer cells. This argues against improved proliferation of the cells and benefits in tumor progression by macrophage addition. However, reduced cell numbers could be the result of cells disseminating from the application spot. A study using pancreatic cancer cells in a CAM assay found an accumulation of disseminating cells in the chicken embryo lung and liver (Zijlstra et al. 2008). Hence, further investigation on the cause of the reduction of the tumor mass should include the detection of tumor cells at distant sites in the egg.

Another potential function of enhanced uptake of CD206 targets is the presentation of the corresponding antigens to T cells. Thus far this was shown to occur in CD206^{+} DCs (Burgdorf et al. 2006). Macrophages are also antigen presenting cells able to activate T cells (Hilhorst et al. 2014). Improved antigen presentation as a result of increased CD206 expression is therefore possible. Noteworthy in this context is that CD206 also binds to glycolipids which can be presented by CD1a, a protein we also found to be upregulated on L-428 CM derived macrophages (Rawlings et al. 2004). Antigen presentation to T cells usually results in T cell activation arguing against immune suppressive functions that are proposed for TAMs. However, in combination with co-inhibitory signals it might lead to T cell exhaustion impairing the anti-tumor defense of T cells (Wherry 2011). Further investigations have to assess whether the increased CD206 expression leads to enhanced antigen presentation. The T cell response in this case still depends on the co-stimulatory and -inhibitory repertoire of the cells as already depicted in the previous section. Further studies of these effects would again require direct interaction experiments of macrophages and T cells and additionally cytotoxic killing assays of stimulated CD8^{+} T cells.

4.3 Factors inducing CD206 expression on cHL derived macrophages

We hypothesized that IL-13 expressed by cHL cells is responsible for increased CD206 expression on macrophages. The M2 activation of macrophages *in vitro* is usually achieved by stimulation with IL-4, IL-13 or a combination which leads to CD206 expression (Doyle et al. 1994). Here we could show that IL-13 leads to an induction of *MRC1* gene expression within 6 h and increased expression on the cell surface within 24 h on monocytes which was otherwise absent. This indicates that IL-13 in the cHL CM is a critical factor to increase *MRC1*

expression in CM generated macrophages. Strikingly, only cell lines that expressed *IL13* were found to induce *MRC1* expression in monocytes within 6 h. However, since the *MRC1* expression after L-428 CM stimulation was stronger increased than with IL-13 alone it is reasonable to propose that additional factors secreted by cHL cells are involved in *MRC1* induction. Notably, it was found that GM-CSF can induce *MRC1* expression in human monocytes (Däbritz et al. 2015). We detected *CSF2* gene expression in three cHL cell lines suggesting GM-CSF could also be involved in the *MRC1* induction in these experiments. Another factor widely known to induce *MRC1* expression is IL-4 (Martinez et al. 2006). However, no gene expression was found by RNA-Seq in L-428 and HBL-1 cells. Thus, in L-428 CM which highly induced *MRC1* expression this factor does not play a role. Additionally, we observed that after inhibition of JAK1 and JAK2 *MRC1* expression in monocytes was abolished. IL-13 binds to an IL4Rα-IL13Rα heterodimer which intracellularly binds to JAK1, JAK2 and TYK2. The absence of *MRC1* expression after Ruxolitinib treatment indicates JAK1 or JAK2 rather than TYK2 are essential for the induction of gene expression. Likewise this is the case in L-428 CM stimulated cells since also here *MRC1* expression was absent after Ruxolitinib treatment. Activated JAKs subsequently phosphorylate STAT proteins which upon phosphorylation enter the nucleus and regulate gene transcription (Rawlings et al. 2004). Little is known about the transcriptional regulation of *MRC1* including whether it is regulated by STATs. A described mechanism for the induction of *MRC1* expression after IL-13 stimulation is via phosphorylation of phospholipase A2 (PLA2) which leads to enhanced production of prostaglandins and activation of peroxisome proliferator-activated receptor γ (PPARγ)(Coste et al. 2003). This suggests that rather than STATs PPARγ mediates the transcriptional control of *MRC1*. Further investigation on the activation of STATs or PLA2 and consequently PPARγ as well as their binding to the *MRC1* promoter region have to clarify the specific mechanism of *MRC1* induction by IL-13 stimulation. Additionally, blocking of the IL-13 receptor or IL-13 depletion from the lymphoma CM could reveal the specific impact of IL-13 in the CM on *MRC1* expression in monocytes.

5 Summary and Conclusion

A rich and vast TME is a characteristic of cHL and interactions between bystander cells and malignant HRS cells are essential for tumor progression. In the presented study we showed that HRS cells secret factors to attract monocytes and macrophages. The recruited cells are either differentiated or repolarized, respectively. Recruitment of macrophages and differentiation of monocytes was also found with DLBCL CM, however, to a lesser extent. Further investigations on the phenotype of cHL derived cells showed their M2-like activation state and upregulation of several cell surface markers which indicates functions in T cell communication and tissue remodeling. This supports the view of an active recruitment of myeloid cells into the tumor and their manipulation to exhibit specific functions. Studies on functional properties revealed an enhanced endocytic activity that was in accordance with a high CD206 expression on these cells. The high MMP-9 secretion and the changes in the tumor formation of L-428 cells by addition of macrophages provided further evidence that cHL derived macrophages are involved in tissue remodeling. Ongoing analyses have to evaluate the role of this in tumor progression especially an improved dissemination and metastasis is suggested. Another indicated function of cHL CM derived macrophages is their interplay with T cells. Further analyses are necessary to confirm this proposed function in T cell interaction and whether it is inhibitory or stimulatory. Among the factors produced by cHL cells we found that IL-13 can induce CD206 expression. Identification of the mediating factors that leads to the observed phenotype of cHL derived macrophages could further improve the understanding of macrophage recruitment into the TME.

Analyses of interactions of malignant cells with their TME have proven valuable to dissect new therapeutic targets and to develop anti-cancer therapies. This study has provided evidence on interactions of HRS cells with macrophages focusing on the manipulation of macrophages by HRS cell secreted factors. Additional work has to be done to fully understand the mutual interplay of these two cell types, to define the molecular mediators and whether a disruption of this communication is beneficial in order to induce anti-tumor actions of macrophages.

References

Afik, R. et al., 2016. Tumor macrophages are pivotal constructors of tumor collagenous matrix. *The Journal of Experimental Medicine*, 213(11), pp.2315–2331.

Ajami, B. et al., 2007. Local self-renewal can sustain CNS microglia maintenance and function throughout adult life. *Nature Neuroscience*, 10(12), pp.1538–1543.

Albini, A. et al., 2015. Cancer stem cells and the tumor microenvironment: interplay in tumor heterogeneity. *Connective tissue research*, 56(5), pp.414–25.

Aldinucci, D. et al., 2008. Expression of CCR5 receptors on Reed–Sternberg cells and Hodgkin lymphoma cell lines: Involvement of CCL5/Rantes in tumor cell growth and microenvironmental interactions. *International Journal of Cancer*, 122(4), pp.769–776.

Aldinucci, D., Celegato, M. & Casagrande, N., 2016. Microenvironmental interactions in classical Hodgkin lymphoma and their role in promoting tumor growth, immune escape and drug resistance. *Cancer Letters*, 380(1), pp.243–252.

Alonso-Álvarez, S. et al., 2017. The number of tumor infiltrating T-cell subsets in lymph nodes from patients with Hodgkin lymphoma is associated with the outcome after first line ABVD therapy. *Leukemia & Lymphoma*, 58(5), pp.1144–1152.

Alonso-Nocelo, M. et al., 2018. Matrix stiffness and tumor-associated macrophages modulate epithelial to mesenchymal transition of human adenocarcinoma cells. *Biofabrication*, 10(3), p.35004.

Andreu, P. et al., 2010. FcRgamma activation regulates inflammation-associated squamous carcinogenesis. *Cancer Cell*, 17(2), pp.121–34.

Appleby, L.J. et al., 2013. Sources of heterogeneity in human monocyte subsets. *Immunology Letters*, 152(1), pp.32–41.

Atanasov, G. et al., 2015. Prognostic significance of macrophage invasion in hilar cholangiocarcinoma. *BMC Cancer*, 15(1), p.790.

Aziz, A. et al., 2009. MafB/c-Maf deficiency enables self-renewal of differentiated functional macrophages. *Science*, 326(5954), pp.867–71.

Badawi, M.A. et al., 2015. Tumor-Associated Macrophage (TAM) and Angiogenesis in Human Colon Carcinoma. *Open access Macedonian journal of medical sciences*, 3(2), pp.209–14.

Barleon, B. et al., 1996. Migration of human monocytes in response to vascular endothelial growth factor (VEGF) is mediated via the VEGF receptor flt-1. *Blood*, 87(8), pp.3336–43.

Barros, M.H.M. et al., 2013. Macrophage Polarisation: an Immunohistochemical Approach for Identifying M1 and M2 Macrophages. *PloS one*, 8(11), p.e80908.

Barros, M.H.M. et al., 2015. Macrophage polarization reflects T cell composition of tumor microenvironment in pediatric classical Hodgkin lymphoma and has impact on survival. *PloS one*, 10(5), p.e0124531.

Barros, M.H.M., Hassan, R. & Niedobitek, G., 2012. Tumor-associated macrophages in pediatric classical Hodgkin lymphoma: association with Epstein-Barr virus, lymphocyte subsets, and prognostic impact. *Clinical Cancer Research*, 18(14), pp.3762–71.

Beatty, G.L. et al., 2011. CD40 Agonists Alter Tumor Stroma and Show Efficacy Against Pancreatic Carcinoma in Mice and Humans. *Science*, 331(6024), pp.1612–1616.

Bhattacharjee, A. et al., 2013. IL-4 and IL-13 employ discrete signaling pathways for target gene expression in alternatively activated monocytes/macrophages. *Free Radical Biology and Medicine*, 54, pp.1–16.

Bianchetti, L. et al., 2012. Extracellular matrix remodelling properties of human fibrocytes. *Journal of Cellular and Molecular Medicine*, 16(3), pp.483–495.

Bigley, V. et al., 2011. The human syndrome of dendritic cell, monocyte, B and NK lymphoid deficiency. *The Journal of Experimental Medicine*, 208(2), pp.227–34.

Boskovic, J. et al., 2006. Structural model for the mannose receptor family uncovered by electron microscopy of Endo180 and the mannose receptor. *The Journal of Biological Chemistry*, 281(13), pp.8780–7.

Bray, N.L. et al., 2016. Near-optimal probabilistic RNA-seq quantification. *Nature Biotechnology*, 34(5), pp.525–527.

Burgdorf, S., Lukacs-Kornek, V. & Kurts, C., 2006. The mannose receptor mediates uptake of

soluble but not of cell-associated antigen for cross-presentation. *The Journal of Immunology*, 176(11), pp.6770–6.

Canioni, D. et al., 2009. Prognostic Significance of New Immunohistochemical Markers in Refractory Classical Hodgkin Lymphoma: A Study of 59 Cases. *PloS one*, 4(7), p.e6341.

Carey, C.D. et al., 2017. Topological analysis reveals a PD-L1-associated microenvironmental niche for Reed-Sternberg cells in Hodgkin lymphoma. *Blood*, 130(22), pp.2420–2430.

Cavaillon, J.-M., 2011. The historical milestones in the understanding of leukocyte biology initiated by Elie Metchnikoff. *Journal of Leukocyte Biology*, 90(3), pp.413–424.

Chevrier, S. et al., 2017. An Immune Atlas of Clear Cell Renal Cell Carcinoma. *Cell*, 169(4), p.736–749.e18.

Chiu, J., Ernst, D.M. & Keating, A., 2018. Acquired Natural Killer Cell Dysfunction in the Tumor Microenvironment of Classic Hodgkin Lymphoma. *Frontiers in Immunology*, 9, p.267.

Clynes, R.A. et al., 2000. Inhibitory Fc receptors modulate in vivo cytoxicity against tumortargets. *Nature Medicine*, 6(4), pp.443–446.

Conrad, S.M. et al., 2007. Leishmania-derived murine monocyte chemoattractant protein 1 enhances the recruitment of a restrictive population of CC chemokine receptor 2-positive macrophages. *Infection and immunity*, 75(2), pp.653–65.

Coste, A. et al., 2003. PPARγ Promotes Mannose Receptor Gene Expression in Murine Macrophages and Contributes to the Induction of This Receptor by IL-13. *Immunity*, 19(3), pp.329–339.

Coussens, L.M. et al., 2000. MMP-9 supplied by bone marrow-derived cells contributes to skin carcinogenesis. *Cell*, 103(3), pp.481–90.

Coventry, B. & Heinzel, S., 2004. CD1a in human cancers: a new role for an old molecule. *Trends in Immunology*, 25(5), pp.242–248.

D'Haese, J.G. et al., 2010. Fractalkine/CX3CR1: why a single chemokine-receptor duo bears a major and unique therapeutic potential. *Expert Opinion on Therapeutic Targets*, 14(2),

pp.207–219.

Däbritz, J. et al., 2015. Reprogramming of monocytes by GM-CSF contributes to regulatory immune functions during intestinal inflammation. *The Journal of Immunology*, 194(5), pp.2424–38.

De Palma, M. & Lewis, C.E., 2013. Macrophage Regulation of Tumor Responses to Anticancer Therapies. *Cancer Cell*, 23(3), pp.277–286.

Deau, B. et al., 2013. Macrophage, mast cell and T lymphocyte infiltrations are independent predictive biomarkers of primary refractoriness or early relapse in classical Hodgkin lymphoma. *Leukemia & Lymphoma*, 54(1), pp.41–45.

DeNardo, D.G. et al., 2011. Leukocyte complexity predicts breast cancer survival and functionally regulates response to chemotherapy. *Cancer Discovery,* 1(1), pp.54–67.

Doussis-Anagnostopoulou, I.A. et al., 2002. Vascular endothelial growth factor (VEGF) is expressed by neoplastic Hodgkin-Reed-Sternberg cells in Hodgkin's disease. *The Journal of Pathology*, 197(5), pp.677–683.

Doyle, A.G. et al., 1994. Interleukin-13 alters the activation state of murine macrophagesin vitro: Comparison with interleukin-4 and interferon-γ. *European Journal of Immunology*, 24(6), pp.1441–1445.

Duluc, D. et al., 2007. Tumor-associated leukemia inhibitory factor and IL-6 skew monocyte differentiation into tumor-associated macrophage-like cells. *Blood*, 110(13), pp.4319–30.

Egeblad, M., Nakasone, E.S. & Werb, Z., 2010. Tumors as organs: complex tissues that interface with the entire organism. *Developmental cell*, 18(6), pp.884–901.

El-Gamal, M.I. et al., 2018. Recent Advances of Colony-Stimulating Factor-1 Receptor (CSF-1R) Kinase and Its Inhibitors. *Journal of Medicinal Chemistry*, epub ahead.

Engert, A., 2016. ABVD or BEACOPP for Advanced Hodgkin Lymphoma. *Journal of clinical oncology : official journal of the American Society of Clinical Oncology*, 34(11), pp.1167–9.

Estko, M. et al., 2015. Tumour cell derived effects on monocyte/macrophage polarization and function and modulatory potential of Viscum album lipophilic extract in vitro. *BMC*

complementary and alternative medicine, 15, p.130.

Feige, U., Overwien, B. & Sorg, C., 1982. Purification of human blood monocytes by hypotonic density gradient centrifugation in Percoll. *Journal of immunological methods*, 54(3), pp.309–15.

Feist, M., 2016. Synergism of IL10R and TLR9 signaling affects gene expression, proliferation and metabolism in B cells: A comparative study of STAT3/NF-kB and c-Myc mediated effects. *Doctoral thesis*.

Ferretti, E. et al., 2011. A novel role of the CX3CR1/CX3CL1 system in the cross-talk between chronic lymphocytic leukemia cells and tumor microenvironment. *Leukemia*, 25(8), pp.1268–1277.

Ferretti, E., Pistoia, V. & Corcione, A., 2014. Role of fractalkine/CX3CL1 and its receptor in the pathogenesis of inflammatory and malignant diseases with emphasis on B cell malignancies. *Mediators of inflammation*, 2014, p.480941.

Fiete, D.J., Beranek, M.C. & Baenziger, J.U., 1998. A cysteine-rich domain of the "mannose" receptor mediates GalNAc-4-SO4 binding. *Proceedings of the National Academy of Sciences of the United States of America*, 95(5), pp.2089–93.

Fischer, M. et al., 2003. Expression of CCL5/RANTES by Hodgkin and Reed-Sternberg cells and its possible role in the recruitment of mast cells into lymphomatous tissue. *International Journal of Cancer*, 107(2), pp.197–201.

Franklin, R.A. et al., 2014. The cellular and molecular origin of tumor-associated macrophages. *Science*, 344(6186), pp.921–5.

Gao, D. et al., 2012. Microenvironmental regulation of epithelial-mesenchymal transitions in cancer. *Cancer Research*, 72(19), pp.4883–9.

Gazzaniga, S. et al., 2007. Targeting Tumor-Associated Macrophages and Inhibition of MCP-1 Reduce Angiogenesis and Tumor Growth in a Human Melanoma Xenograft. *Journal of Investigative Dermatology*, 127(8), pp.2031–2041.

Gentles, A.J. et al., 2015. The prognostic landscape of genes and infiltrating immune cells across human cancers. *Nature Medicine*, 21(8), pp.938–945.

Glimelius, I. et al., 2005. Angiogenesis and mast cells in Hodgkin lymphoma. *Leukemia*, 19(12), pp.2360–2362.

Gordon, S., 2003. Alternative activation of macrophages. *Nature Reviews Immunology*, 3(1), pp.23–35.

Green, M.R. et al., 2010. Integrative analysis reveals selective 9p24.1 amplification, increased PD-1 ligand expression, and further induction via JAK2 in nodular sclerosing Hodgkin lymphoma and primary mediastinal large B-cell lymphoma. *Blood*, 116(17), pp.3268–77.

Gröne, H.J. et al., 1999. Met-RANTES reduces vascular and tubular damage during acute renal transplant rejection: blocking monocyte arrest and recruitment. *FASEB journal : official publication of the Federation of American Societies for Experimental Biology*, 13(11), pp.1371–83.

Grugan, K.D. et al., 2012. Tumor-associated macrophages promote invasion while retaining Fc-dependent anti-tumor function. *The Journal of Immunology*, 189(11), pp.5457–66.

Guo, B. et al., 2016. Meta-analysis of the prognostic and clinical value of tumor-associated macrophages in adult classical Hodgkin lymphoma. *BMC Medicine*, 14(1), p.159.

Hamilton, G. et al., 2016. Small cell lung cancer: Recruitment of macrophages by circulating tumor cells. *Oncoimmunology*, 5(3), p.e1093277.

Henkel, J.S. et al., 2004. Presence of dendritic cells, MCP-1, and activated microglia/macrophages in amyotrophic lateral sclerosis spinal cord tissue. *Annals of Neurology*, 55(2), pp.221–35.

Heusinkveld, M. & van der Burg, S.H., 2011. Identification and manipulation of tumor associated macrophages in human cancers. *Journal of Translational Medicine*, 9(1), p.216.

Hildenbrand, R. et al., 1999. Urokinase plasminogen activator receptor (CD87) expression of tumor-associated macrophages in ductal carcinoma in situ, breast cancer, and resident macrophages of normal breast tissue. *Journal of Leukocyte Biology*, 66(1), pp.40–9.

Hilhorst, M. et al., 2014. T cell-macrophage interactions and granuloma formation in vasculitis. *Frontiers in Immunology*, 5, p.432.

Hoeffel, G. et al., 2012. Adult Langerhans cells derive predominantly from embryonic fetal liver monocytes with a minor contribution of yolk sac-derived macrophages. *The Journal of Experimental Medicine*, 209(6), pp.1167–81.

Hollander, P. et al., 2018. An anergic immune signature in the tumor microenvironment of classical Hodgkin lymphoma is associated with inferior outcome. *European Journal of Haematology*, 100(1), pp.88–97.

Hoppe, R.T. et al., 2017. Hodgkin Lymphoma Version 1.2017, NCCN Clinical Practice Guidelines in Oncology. *Journal of the National Comprehensive Cancer Network*, 15(5), pp.608–638.

Howard, M.J. & Isacke, C.M., 2002. The C-type lectin receptor Endo180 displays internalization and recycling properties distinct from other members of the mannose receptor family. *The Journal of Biological Chemistry*, 277(35), pp.32320–31.

Huber, S. et al., 2010. Alternatively activated macrophages inhibit T-cell proliferation by Stat6-dependent expression of PD-L2. *Blood*, 116(17), pp.3311–20.

Jonker, M., Ossevoort, M.A. & Vierboom, M., 2002. Blocking the CD80 and CD86 costimulation molecules: Lessons to be learned from animal models. *Transplantation*, 73(1), pp.23–26.

Kanzler, H. et al., 1996. Hodgkin and Reed-Sternberg cells in Hodgkin's disease represent the outgrowth of a dominant tumor clone derived from (crippled) germinal center B cells. *The Journal of Experimental Medicine*, 184(4), pp.1495–505.

Kapp, U. et al., 1999. Interleukin 13 is secreted by and stimulates the growth of Hodgkin and Reed-Sternberg cells. *The Journal of Experimental Medicine*, 189(12), pp.1939–46.

Kato, M. et al., 2000. Expression of multilectin receptors and comparative FITC-dextran uptake by human dendritic cells. *International Immunology*, 12(11), pp.1511–1519.

Kerkar, S.P. & Restifo, N.P., 2012. Cellular constituents of immune escape within the tumor microenvironment. *Cancer Research*, 72(13), pp.3125–3130.

Kiss, M. et al., 2018. Myeloid cell heterogeneity in cancer: not a single cell alike. *Cellular Immunology*, epub ahead.

Koreishi, A.F. et al., 2010. The role of cytotoxic and regulatory T cells in relapsed/refractory Hodgkin lymphoma. *Applied immunohistochemistry & molecular morphology : AIMM*, 18(3), pp.206–11.

Kowalska, M. et al., 2012. Serum macrophage colony-stimulating factor (M-CSF) in patients with Hodgkin lymphoma. *Medical Oncology*, 29(3), pp.2143–2147.

Kridel, R., Steidl, C. & Gascoyne, R.D., 2015. Tumor-associated macrophages in diffuse large B-cell lymphoma. *Haematologica*, 100(2), pp.143–5.

Kryczek, I. et al., 2006. B7-H4 expression identifies a novel suppressive macrophage population in human ovarian carcinoma. *The Journal of Experimental Medicine*, 203(4), pp.871–81.

Kuen, J. et al., 2017. Pancreatic cancer cell/fibroblast co-culture induces M2 like macrophages that influence therapeutic response in a 3D model. *PloS one*, 12(7), p.e0182039.

Kumar, V. et al., 2017. Cancer-Associated Fibroblasts Neutralize the Anti-tumor Effect of CSF1 Receptor Blockade by Inducing PMN-MDSC Infiltration of Tumors. *Cancer Cell*, 32(5), p.654–668.e5.

Küppers, R. et al., 1994. Hodgkin disease: Hodgkin and Reed-Sternberg cells picked from histological sections show clonal immunoglobulin gene rearrangements and appear to be derived from B cells at various stages of development. *Proceedings of the National Academy of Sciences of the United States of America*, 91(23), pp.10962–6.

Lavin, Y. et al., 2017. Innate Immune Landscape in Early Lung Adenocarcinoma by Paired Single-Cell Analyses. *Cell*, 169(4), p.750–765.e17.

Lee, S.J. et al., 2002. Mannose receptor-mediated regulation of serum glycoprotein homeostasis. *Science*, 295(5561), pp.1898–901.

Lee, S.J. et al., 2003. Normal host defense during systemic candidiasis in mannose receptor-deficient mice. *Infection and immunity*, 71(1), pp.437–45.

Lepique, A.P. et al., 2009. HPV16 tumor associated macrophages suppress antitumor T cell responses. *Clinical Cancer Research*, 15(13), pp.4391–400.

Leteux, C. et al., 2000. The Cysteine-Rich Domain of the Macrophage Mannose Receptor Is a Multispecific Lectin That Recognizes Chondroitin Sulfates a and B and Sulfated Oligosaccharides of Blood Group Lewis [a] and Lewis [x] Types in Addition to the Sulfated *N* -Glycans of Lutropin. *The Journal of Experimental Medicine,* 191(7), pp.1117–1126.

Li, W. et al., 2016. Heart-resident CCR2+ macrophages promote neutrophil extravasation through TLR9/MyD88/CXCL5 signaling. *JCI insight*, 1(12), p.e87315.

Lievense, L.A. et al., 2016. Pleural Effusion of Patients with Malignant Mesothelioma Induces Macrophage-Mediated T Cell Suppression. *Journal of Thoracic Oncology*, 11(10), pp.1755–64.

Liguori, M. et al., 2011. Tumor-associated macrophages as incessant builders and destroyers of the cancer stroma. *Cancers*, 3(4), pp.3740–61.

Linke, F., 2016. WNT signalling affects cell migration, invasion and the lymphoma-endothelial interplay in Hodgkin Lymphoma. *Doctoral thesis*.

Llorca, O., 2008. Extended and bent conformations of the mannose receptor family. *Cellular and Molecular Life Sciences*, 65(9), pp.1302–1310.

Luciani, M.G. et al., 1998. The monocyte chemotactic protein a (MCP-1) and interleukin 8 (IL-8) in Hodgkin's disease and in solid tumours. *Molecular Pathology*, 51(5), pp.273–6.

Luo, Y. & Knudson, M.J., 2010. Mycobacterium bovis bacillus Calmette-Guérin-induced macrophage cytotoxicity against bladder cancer cells. *Clinical & developmental immunology*, 2010, p.357591.

Madsen, D.H. et al., 2017. Tumor-Associated Macrophages Derived from Circulating Inflammatory Monocytes Degrade Collagen through Cellular Uptake. *Cell reports*, 21(13), pp.3662–3671.

Maggio, E.M. et al., 2002. Common and differential chemokine expression patterns in rs cells of NLP, EBV positive and negative classical hodgkin lymphomas. *International Journal of Cancer*, 99(5), pp.665–672.

Mantovani, A. et al., 2002. Macrophage polarization: tumor-associated macrophages as a paradigm for polarized M2 mononuclear phagocytes. *Trends in Immunology*, 23(11),

pp.549–555.

Marafioti, T. et al., 2000. Hodgkin and reed-sternberg cells represent an expansion of a single clone originating from a germinal center B-cell with functional immunoglobulin gene rearrangements but defective immunoglobulin transcription. *Blood*, 95(4), pp.1443–50.

Martinez-Pomares, L. et al., 2006. Carbohydrate-independent recognition of collagens by the macrophage mannose receptor. *European Journal of Immunology*, 36(5), pp.1074–1082.

Martinez-Pomares, L., 2012. The mannose receptor. *Journal of Leukocyte Biology*, 92(6), pp.1177–86.

Martinez, F.O. et al., 2006. Transcriptional Profiling of the Human Monocyte-to-Macrophage Differentiation and Polarization: New Molecules and Patterns of Gene Expression. *The Journal of Immunology*, 177, pp.7303–7311.

Mason, S.D. & Joyce, J.A., 2011. Proteolytic networks in cancer. *Trends in Cell Biology*, 21(4), pp.228–37.

McKenzie, A.N. et al., 1993. Interleukin 13, a T-cell-derived cytokine that regulates human monocyte and B-cell function. *Proceedings of the National Academy of Sciences of the United States of America*, 90(8), pp.3735–9.

Menck, K. et al., 2014. Isolation of human monocytes by double gradient centrifugation and their differentiation to macrophages in teflon-coated cell culture bags. *Journal of visualized experiments*, (91), p.e51554.

Merz, H. et al., 1991. Cytokine expression in T-cell lymphomas and Hodgkin's disease. Its possible implication in autocrine or paracrine production as a potential basis for neoplastic growth. *The American Journal of Pathology*, 139(5), pp.1173–80.

Metcalf, D., 2013. The colony-stimulating factors and cancer. *Cancer immunology research*, 1(6), pp.351–6.

Mills, C.D. et al., 2000. M-1/M-2 macrophages and the Th1/Th2 paradigm. *The Journal of Immunology*, 164(12), pp.6166–73.

Mills, C.D. & Ley, K., 2014. M1 and M2 macrophages: the chicken and the egg of immunity.

Journal of Innate Immunity, 6(6), pp.716–26.

Minard-Colin, V. et al., 2008. Lymphoma depletion during CD20 immunotherapy in mice is mediated by macrophage FcgammaRI, FcgammaRIII, and FcgammaRIV. *Blood*, 112(4), pp.1205–13.

Ming, W.J., Bersani, L. & Mantovani, A., 1987. Tumor necrosis factor is chemotactic for monocytes and polymorphonuclear leukocytes. *The Journal of Immunology*, 138(5), pp.1469–74.

Mosser, D.M. & Edwards, J.P., 2008. Exploring the full spectrum of macrophage activation. *Nature Reviews Immunology*, 8(12), pp.958–969.

Murray, P.J. et al., 2014. Macrophage Activation and Polarization: Nomenclature and Experimental Guidelines. *Immunity*, 41(1), pp.14–20.

Naito, M., Takahashi, K. & Nishikawa, S., 1990. Development, differentiation, and maturation of macrophages in the fetal mouse liver. *Journal of Leukocyte Biology*, 48(1), pp.27–37.

Napper, C.E., Dyson, M.H. & Taylor, M.E., 2001. An extended conformation of the macrophage mannose receptor. *The Journal of Biological Chemistry*, 276(18), pp.14759–66.

Niens, M. et al., 2008. Serum chemokine levels in Hodgkin lymphoma patients: highly increased levels of CCL17 and CCL22. *British Journal of Haematology*, 140(5), pp.527–536.

Oishi, S. et al., 2016. M2 polarization of murine peritoneal macrophages induces regulatory cytokine production and suppresses T-cell proliferation. *Immunology*, 149(3), pp.320–328.

Pagès, F. et al., 2010. Immune infiltration in human tumors: a prognostic factor that should not be ignored. *Oncogene*, 29(8), pp.1093–1102.

Palis, J. et al., 1999. Development of erythroid and myeloid progenitors in the yolk sac and embryo proper of the mouse. *Development*, 126(22), pp.5073–84.

Pander, J. et al., 2011. Activation of tumor-promoting type 2 macrophages by EGFR-targeting

antibody cetuximab. *Clinical Cancer Research*, 17(17), pp.5668–73.

Pauken, K.E. & Wherry, E.J., 2015. Overcoming T cell exhaustion in infection and cancer. *Trends in Immunology*, 36(4), pp.265–276.

Peinado, H. et al., 2012. Melanoma exosomes educate bone marrow progenitor cells toward a pro-metastatic phenotype through MET. *Nature Medicine*, 18(6), pp.883–891.

Pixley, F.J., 2012. Macrophage Migration and Its Regulation by CSF-1. *International Journal of Cell Biology*, 2012, p.501962.

Prigozy, T.I. et al., 1997. The mannose receptor delivers lipoglycan antigens to endosomes for presentation to T cells by CD1b molecules. *Immunity*, 6(2), pp.187–97.

Qian, B. et al., 2009. A Distinct Macrophage Population Mediates Metastatic Breast Cancer Cell Extravasation, Establishment and Growth. *PloS one*, 4(8), p.e6562.

Raes, G. et al., 2005. Macrophage galactose-type C-type lectins as novel markers for alternatively activated macrophages elicited by parasitic infections and allergic airway inflammation. *Journal of Leukocyte Biology*, 77(3), pp.321–327.

Rawlings, J.S., Rosler, K.M. & Harrison, D.A., 2004. The JAK/STAT signaling pathway. *Journal of cell science*, 117(Pt 8), pp.1281–3.

Reichel, J. et al., 2015. Flow sorting and exome sequencing reveal the oncogenome of primary Hodgkin and Reed-Sternberg cells. *Blood*, 125(7), pp.1061–72.

Robert Koch-Institut und die Gesellschaft der epidemiologischen Krebsregister in Deutschland, e. V., 2017. Krebs in Deutschland für 2013/2014. , 11th Editi.

Roca, H. et al., 2009. CCL2 and interleukin-6 promote survival of human CD11b+ peripheral blood mononuclear cells and induce M2-type macrophage polarization. *The Journal of Biological Chemistry*, 284(49), pp.34342–54.

Roemer, M.G.M., Advani, R.H., Redd, R.A., et al., 2016. Classical Hodgkin Lymphoma with Reduced β2M/MHC Class I Expression Is Associated with Inferior Outcome Independent of 9p24.1 Status. *Cancer immunology research*, 4(11), pp.910–916.

Roemer, M.G.M., Advani, R.H., Ligon, A.H., et al., 2016. PD-L1 and PD-L2 Genetic Alterations

Define Classical Hodgkin Lymphoma and Predict Outcome. *Journal of clinical oncology : official journal of the American Society of Clinical Oncology*, 34(23), pp.2690–7.

Ruffell, B. et al., 2014. Macrophage IL-10 Blocks CD8+ T Cell-Dependent Responses to Chemotherapy by Suppressing IL-12 Expression in Intratumoral Dendritic Cells. *Cancer Cell*, 26(5), pp.623–637.

Sato, W. et al., 2008. The pivotal role of VEGF on glomerular macrophage infiltration in advanced diabetic nephropathy. *Laboratory Investigation*, 88(9), pp.949–961.

Schmitz, R. et al., 2009. Pathogenesis of Classical and Lymphocyte-Predominant Hodgkin Lymphoma. *Annual Review of Pathology: Mechanisms of Disease*, 4(1), pp.151–174.

Schuette, V. et al., 2016. Mannose receptor induces T-cell tolerance via inhibition of CD45 and up-regulation of CTLA-4. *Proceedings of the National Academy of Sciences of the United States of America*, 113(38), pp.10649–54.

Schulz, C. et al., 2012. A Lineage of Myeloid Cells Independent of Myb and Hematopoietic Stem Cells. *Science*, 336(6077), pp.86–90.

Shabo, I. et al., 2008. Breast cancer expression of CD163, a macrophage scavenger receptor, is related to early distant recurrence and reduced patient survival. *International Journal of Cancer*, 123(4), pp.780–786.

Shree, T. et al., 2011. Macrophages and cathepsin proteases blunt chemotherapeutic response in breast cancer. *Genes & Development*, 25(23), pp.2465–79.

Sierra-Filardi, E. et al., 2014. CCL2 shapes macrophage polarization by GM-CSF and M-CSF: identification of CCL2/CCR2-dependent gene expression profile. *The Journal of Immunology*, 192(8), pp.3858–67.

Skinnider, B.F. et al., 2002. The role of cytokines in classical Hodgkin lymphoma. *Blood*, 99(12), pp.4283–97.

Skinnider, B.F., Kapp, U. & Mak, T.W., 2002. The Role of Interleukin 13 in Classical Hodgkin Lymphoma. *Leukemia & Lymphoma*, 43(6), pp.1203–1210.

Song, X. et al., 2016. Cancer Cell-derived Exosomes Induce Mitogen-activated Protein Kinase-

dependent Monocyte Survival by Transport of Functional Receptor Tyrosine Kinases. *The Journal of Biological Chemistry*, 291(16), pp.8453–64.

Steidl, C. et al., 2010. Tumor-Associated Macrophages and Survival in Classic Hodgkin's Lymphoma. *New England Journal of Medicine*, 362(10), pp.875–885.

Stojanovic, T. et al., 2002. Met-RANTES Inhibition of Mucosal Perfusion Failure in Acute Intestinal Transplant Rejection – Role of Endothelial Cell-Leukocyte Interaction. *Journal of Vascular Research*, 39(1), pp.51–58.

Swain, S.D. et al., 2003. Absence of the Macrophage Mannose Receptor in Mice Does Not Increase Susceptibility to Pneumocystis carinii Infection In Vivo. *Infection and immunity*, 71(11), pp.6213–6221.

Tan, M.C. et al., 1997. Mannose receptor-mediated uptake of antigens strongly enhances HLA class II-restricted antigen presentation by cultured dendritic cells. *European Journal of Immunology*, 27(9), pp.2426–35.

Taylor, P.R., Gordon, S. & Martinez-Pomares, L., 2005. The mannose receptor: linking homeostasis and immunity through sugar recognition. *Trends in Immunology*, 26(2), pp.104–110.

Tomita, T. et al., 2011. Imbalance of Clara cell-mediated homeostatic inflammation is involved in lung metastasis. *Oncogene*, 30(31), pp.3429–3439.

Tripathi, C. et al., 2014. Macrophages are recruited to hypoxic tumor areas and acquire a Pro-Angiogenic M2-Polarized phenotype via hypoxic cancer cell derived cytokines Oncostatin M and Eotaxin. *Oncotarget*, 5(14), pp.5350–5368.

Tudor, C.S. et al., 2014. Macrophages and Dendritic Cells as Actors in the Immune Reaction of Classical Hodgkin Lymphoma. *PloS one*, 9(12), p.e114345.

Tymoszuk, P. et al., 2014. In situ proliferation contributes to accumulation of tumor-associated macrophages in spontaneous mammary tumors. *European Journal of Immunology*, 44(8), pp.2247–2262.

Varol, C., Mildner, A. & Jung, S., 2015. *Macrophages: development and tissue specialization,*

Varol, C., Yona, S. & Jung, S., 2009. Origins and tissue-context-dependent fates of blood monocytes. *Immunology and Cell Biology*, 87(1), pp.30–38.

Wang, M. et al., 2017. Role of tumor microenvironment in tumorigenesis. *Journal of Cancer*, 8(5), pp.761–773.

Wang, T. et al., 2014. SECTM1 produced by tumor cells attracts human monocytes via CD7-mediated activation of the PI3K pathway. *The Journal of Investigative Dermatology*, 134(4), pp.1108–1118.

Wang, W. et al., 2002. Single cell behavior in metastatic primary mammary tumors correlated with gene expression patterns revealed by molecular profiling. *Cancer Research*, 62(21), pp.6278–88.

Wei, L. et al., 2016. Interleukin-17 potently increases non-small cell lung cancer growth. *Molecular Medicine Reports*, 13(2), pp.1673–80.

Weinberg, J.B. et al., 1995. Human mononuclear phagocyte inducible nitric oxide synthase (iNOS): analysis of iNOS mRNA, iNOS protein, biopterin, and nitric oxide production by blood monocytes and peritoneal macrophages. *Blood*, 86(3), pp.1184–95.

Wherry, E.J., 2011. T cell exhaustion. *Nature Immunology*, 12(6), pp.492–499.

Xu, J. et al., 2013. CSF1R signaling blockade stanches tumor-infiltrating myeloid cells and improves the efficacy of radiotherapy in prostate cancer. *Cancer Research*, 73(9), pp.2782–94.

Xue, J. et al., 2014. Transcriptome-Based Network Analysis Reveals a Spectrum Model of Human Macrophage Activation. *Immunity*, 40(2), pp.274–288.

Yan, D. et al., 2017. Vascular endothelial growth factor modified macrophages transdifferentiate into endothelial-like cells and decrease foam cell formation. *Bioscience reports*, 37(3).

Yang, Z.F. et al., 2004. Up-regulation of vascular endothelial growth factor (VEGF) in small-for-size liver grafts enhances macrophage activities through VEGF receptor 2-dependent pathway. *The Journal of Immunology*, 173(4), pp.2507–15.

Yue, Y. et al., 2015. IL4I1 Is a Novel Regulator of M2 Macrophage Polarization That Can Inhibit T Cell Activation via L-Tryptophan and Arginine Depletion and IL-10 Production. *PloS one*, 10(11), p.e0142979.

Zhang, B. et al., 2011. M2-polarized tumor-associated macrophages are associated with poor prognoses resulting from accelerated lymphangiogenesis in lung adenocarcinoma. *Clinics*, 66(11), pp.1879–86.

Zhang, Q. et al., 2012. Prognostic significance of tumor-associated macrophages in solid tumor: a meta-analysis of the literature. *PloS one*, 7(12), p.e50946.

Zheng, G.-G. et al., 1999. Expression of Membrane-Associated Macrophage Colony-Stimulating Factor (M-CSF) in Hodgkin's Disease and Other Hematologic Malignancies. *Leukemia & Lymphoma*, 32(3–4), pp.339–344.

Zijlstra, A. et al., 2008. The inhibition of tumor cell intravasation and subsequent metastasis via regulation of in vivo tumor cell motility by the tetraspanin CD151. *Cancer Cell*, 13(3), pp.221–34.
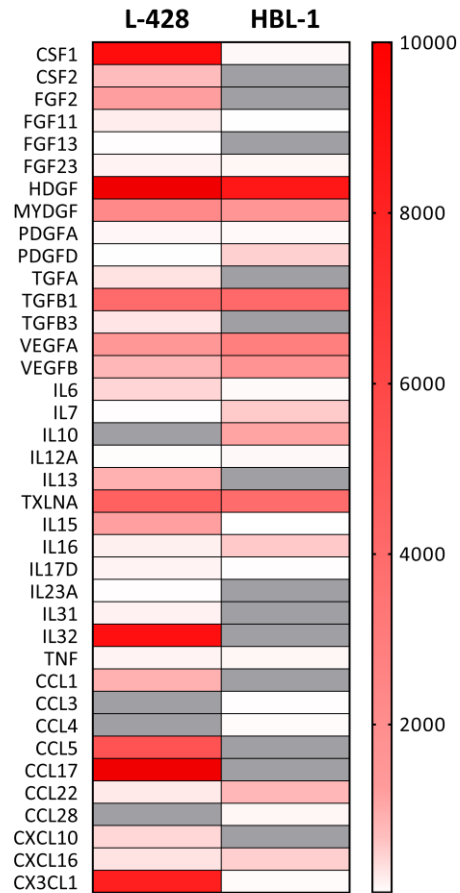
Appendix

Figure A-19: Expression of selected cytokines and chemokines in L-428 and HBL-1 cells by RNA-seq.

Presentation of normalized reads of selected cytokines and chemokines detected by RNA-Seq in L-428 and HBL-1 cells (mean, n = 2).
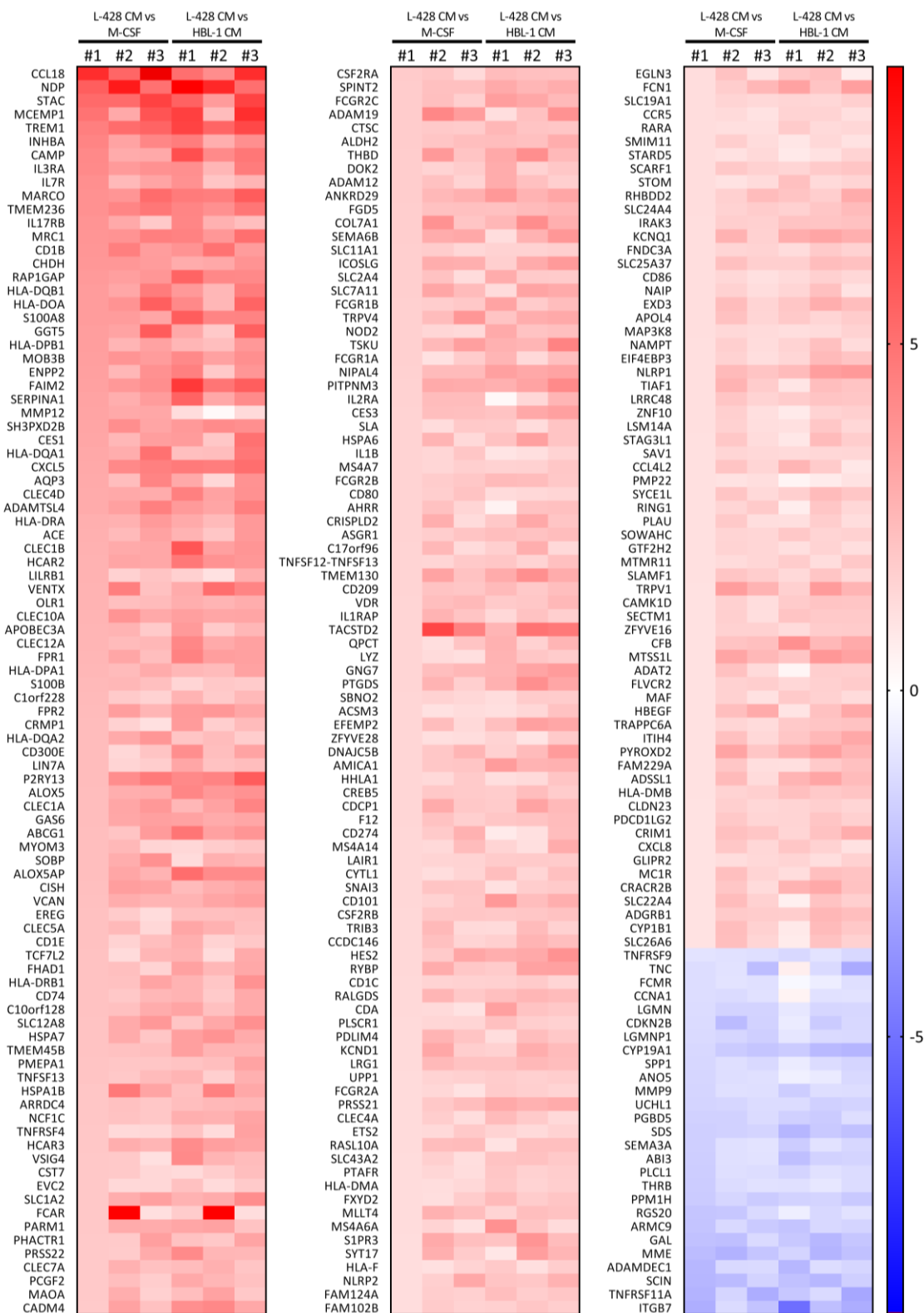
Figure A-20: Heatmap of differentially expressed genes between L-428 CM, M-CSF and HBL-1 CM derived macrophages.

Heatmap of all genes that were differentially expressed in L-428 CM derived macrophages compared to M-CSF cells by Log2FC ≥ 1 and Log2FC ≤ -1 in all three donors (#1, #2, #3) and compared to HBL-1 CM derived cells.
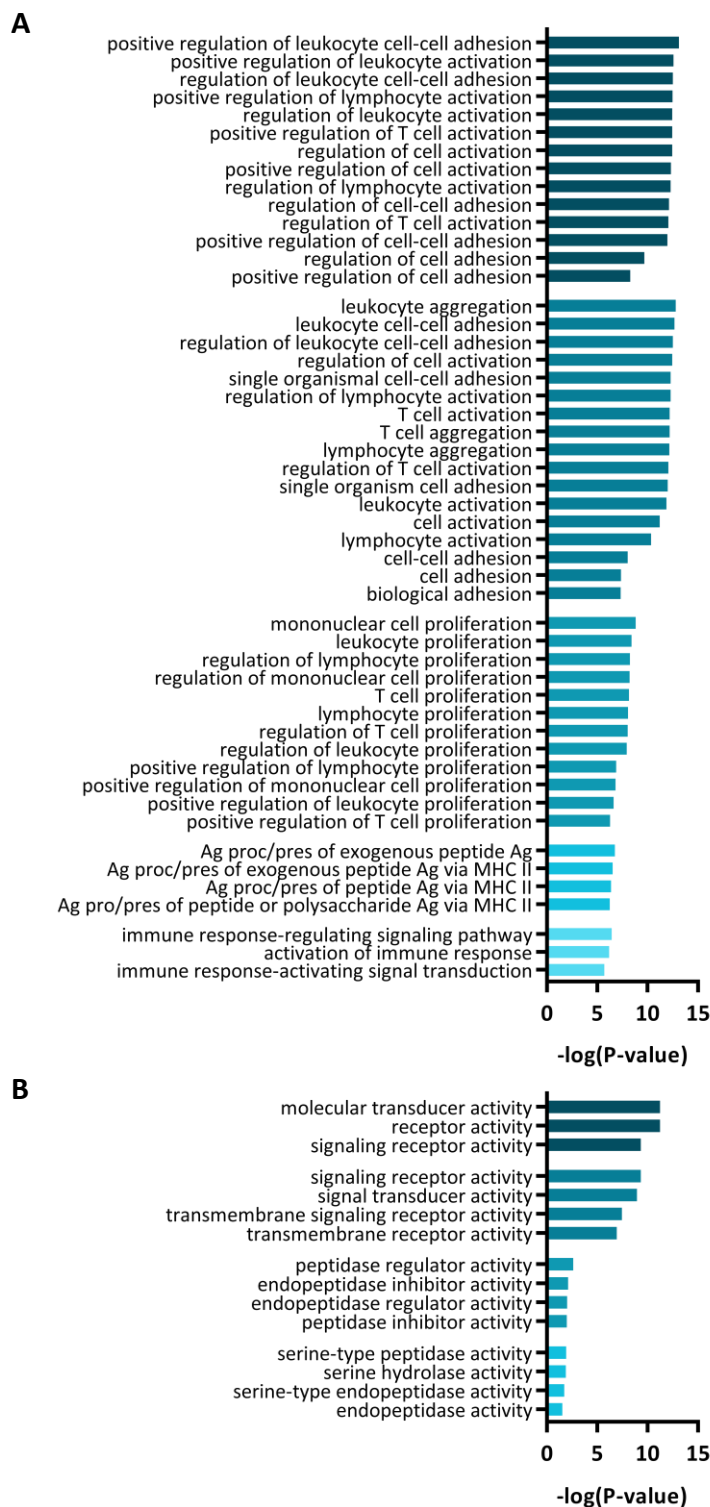
A

B

Figure A-21: GO term enrichment clusters calculated by DAVID for differentially expressed genes between L-428 CM and M-CSF derived macrophages.

Top five GO term enrichment clusters for differentially expressed genes between L-428 CM and M-CSF derived macrophages assigned to biological process (A) and molecular function (B) calculated by DAVID.
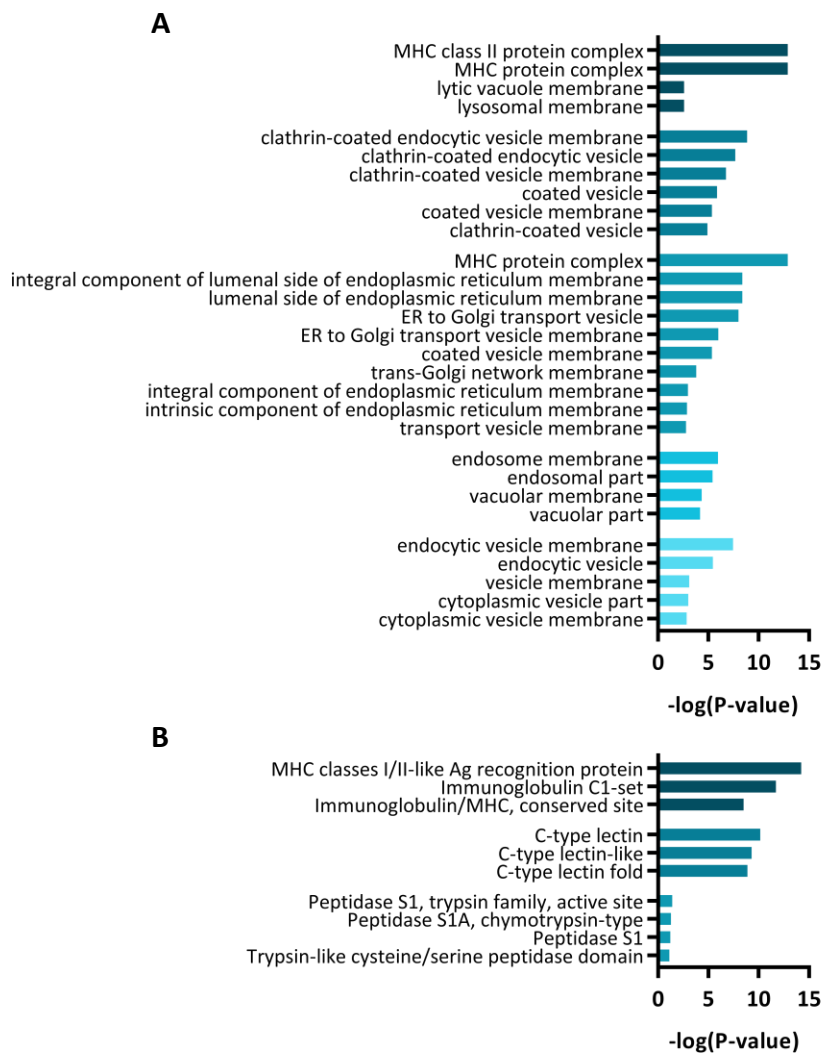
A

B

Figure A-22: GO term and InterPro enrichment clusters calculated by DAVID for differentially expressed genes between L-428 CM and M-CSF derived macrophages.

Top five GO term enrichment clusters for differentially expressed genes between L-428 CM and M-CSF derived macrophages assigned to cellular component (A) and InterPro enrichment clusters (B) calculated by DAVID.

Acknowledgements

First, I would like to express my sincere thanks to my supervisor Prof. Dieter Kube for the continuous support of my PhD study and related research. His guidance helped me in all the time of research and writing of this thesis.

In addition, I am very thankful to Prof. Lorenz Trümper for the opportunity to accomplish this thesis in his department.

Furthermore, I would like to thank the members of my thesis committee Prof. Jörg Wilting and Prof. Ralf Dressel for their support and valuable comments on this project.

I would also like to thank our cooperation partners from the MMML Demonstrators consortium. My special thanks go to Julia Engelmann and Paula Perez-Rubio for their bioinformatical and statistical support.

I am thankful to Frederike von Bonin for her assistance in the lab, especially the performance of countless qRTs and CAM assays. I thank Meike Schaffrinski for performing numerous monocyte isolations.

I would like to express my deep gratitude to my former colleagues Maren Feist and Franziska Linke. I am especially thankful to Franziska Linke for her ongoing interest and encouragement throughout the course of this research work. Lastly, my deepest thanks go to Isabel Rausch with whom I could share all the ups and downs of the last three years and whose patience and advice always kept me motivated.